NASA Contractor Report 179515

Flight Test Report of the NASA Icing Research Airplane

Performance, Stability, and Control After Flight Through Natural Icing Conditions

(NASA-CR-179515) FLIGHT TEST REPORT OF THE NASA ICING RESEARCH AIRPLANE: PERFORMANCE, STABILITY, AND CONTROL AFTER FLIGHT THROUGH NATURAL ICING CONDITIONS Final Report (Kohlman Systems Research, Inc.) 159 p N87-11797
G3/08 Unclas 44924

Jerry L. Jordan, Stewart J. Platz,
and William C. Schinstock

Kohlman Systems Research, Inc.
Lawrence, Kansas

October 1986

Prepared for
Lewis Research Center
Under Contract NAS3-24547

National Aeronautics and
Space Administration

REVISIONS

REV	DESCRIPTION	DATE	APPROVAL
	Original	14 MAR 1986	J.L.J.
	Revision A	7 July 1986	J.L.J.

THIS PAGE INTENTIONALLY LEFT BLANK

LIST OF ACTIVE PAGES

PAGE NUMBER	REV	ADDED PAGES: PAGE NUMBER	REV	ADDED PAGES: PAGE NUMBER	REV	PAGE NUMBER	REV	ADDED PAGES: PAGE NUMBER	REV	ADDED PAGES: PAGE NUMBER	REV
i	A					5.2.1	A				
ii						5.2.2					
iii	A					5.2.3					
iv	A					5.2.4					
v						5.2.5					
vi						5.2.6					
vii						5.3.1					
viii						5.3.2					
ix						5.3.3					
x						5.3.4					
1.1						6.1					
1.2						6.2					
2.1						6.3					
2.2						6.4					
2.3						7.1.1					
2.4						7.1.2	A				
2.5						7.1.3	A				
2.6						7.1.4					
3.1.1						7.1.5					
3.1.2						7.1.6					
3.1.3						7.2.1					
3.1.4						7.2.2					
3.2.1						7.2.3					
3.2.2						7.2.4					
3.3.1						7.2.5					
3.3.2						7.2.6					
3.3.3						7.3.1					
3.3.4						7.3.2	A				
3.3.5						7.3.3					
3.3.6						7.3.4					
3.3.7						7.3.5					
3.3.8						7.3.6					
3.3.9						7.3.7					
3.3.10						7.3.8					
3.3.11						7.3.9					
3.3.12						7.3.10					
3.3.13						8.1.1	A				
3.3.14						~~8.1.2~~	→	8.1.2a	A		
3.3.15						8.1.3	A	8.1.2b	A		
3.3.16						8.1.4		8.1.2c	A		
3.3.17						8.1.5					
3.3.18						8.1.6					
4.1						8.1.7					
4.2						8.1.8					
5.1.1						8.1.9					
5.1.2						8.1.10					
5.1.3						8.1.11					
5.1.4						8.1.12					
5.1.5						8.1.13					
5.1.6						8.1.14	A				

LIST OF ACTIVE PAGES

PAGE NUMBER	REV	ADDED PAGES PAGE NUMBER	REV	PAGE NUMBER	REV	PAGE NUMBER	REV	ADDED PAGES PAGE NUMBER	REV	PAGE NUMBER	R.
8.1.15	A					8.1.65	A				
8.1.16						8.1.66					
8.1.17						8.1.67					
8.1.18						8.1.68					
8.1.19						8.1.69					
8.1.20	A					8.1.70					
8.1.21	A					8.1.71					
8.1.22						8.1.72					
8.1.23						8.1.73					
8.1.24						8.1.74					
8.1.25						8.1.75					
8.1.26						9.1					
8.1.27						9.2					
8.1.28						A.1					
8.1.29						A.2					
8.1.30	A					A.3					
8.1.31						A.4					
8.1.32						A.5					
8.1.33						A.6					
8.1.34						A.7					
8.1.35						A.8					
8.1.36						A.9					
8.1.37						A.10					
8.1.38											
8.1.39											
8.1.40											
8.1.41											
8.1.42											
8.1.43											
8.1.44											
8.1.45											
8.1.46											
8.1.47											
8.1.48											
8.1.49											
8.1.50											
8.1.51											
8.1.52											
8.1.53											
8.1.54											
8.1.55											
8.1.56											
8.1.57											
8.1.58											
8.1.59	A										
8.1.60	A										
8.1.61	A										
8.1.62	A										
8.1.63	A										
8.1.64	A										

TABLE OF CONTENTS

PAGE #

THIS PAGE INTENTIONALLY LEFT BLANK

LIST OF FIGURES

De Havilland
Twin Otter

THIS PAGE INTENTIONALLY LEFT BLANK

1. INTRODUCTION

This report contains the results of flight tests of the NASA Lewis De Havilland Twin Otter, Serial Number 04. The first six sections contain information about the test airplane, the techniques used for data gathering, a list of symbols, and axes/sign conventions. A brief description of the flight test techniques used by KSR are presented in Section 7. The coefficients and derivatives for the longitudinal axis are contained in Section 8.

Due to contract and budgetary constraints, only a portion of the data acquired could be analyzed. Thus, priority was given to an analysis of aircraft performance, longitudinal stability, and a selected asymmetric power sideslip maneuver showing rudder float characteristics with and without ice. It should be noted that on all stability and control flights lateral-directional data was acquired, however, these data were not analyzed for this report for the reasons previously mentioned. It is our hope at KSR that future contracts will allow us to analyze this additional data and verify it with simulation techniques.

THIS PAGE INTENTIONALLY LEFT BLANK

2.0 LIST OF SYMBOLS

SYMBOL	DEFINITION
A_X	longitudinal acceleration (body axis)
A_Y	lateral acceleration (body axis)
A_Z	vertical acceleration (body axis) positive downward
b	wingspan
b_a	aileron span
b_e	elevator span
b_r	rudder span
$\bar{c}$	wing mean aerodynamic chord (MAC)
c_a	average aileron chord
c_e	average elevator chord
c_r	average rudder chord
c.g.	center of gravity
C_D	drag coefficient, $D/\frac{1}{2}\rho V^2 S_W$
$C_{h_{\delta_r}}$	$\partial C_h/\partial\delta_r$
$C_{h_{r_\beta}}$	$\partial C_h/\partial r_\beta$
C_L	lift coefficient, $L/\frac{1}{2}\rho V^2 S_w$
$C_{L_{\delta_e}}$	$\partial C_L/\partial\delta_e$
$C_{L_{\dot\alpha}}$	$\partial C_L/\partial \left(\frac{\dot\alpha\bar{c}}{2V}\right)$
C_{L_q}	$\partial C_L/\partial \left(\frac{q\bar{c}}{2V}\right)$

SYMBOL	DEFINITION
C_m	pitching moment coefficient
C_{m_q}	$\partial C_m/\partial\ (\frac{q\bar{c}}{2V})$
$C_{m_{\dot{\alpha}}}$	$\partial C_m/\partial\ (\frac{\dot{\alpha}\bar{c}}{2V})$
$C_{m_{\delta_e}}$	$\partial C_m/\partial \delta_e$
C_P	$P/pn^3\ D_p{}^5$
C_T	$F/pn^2\ D_p{}^4$
D	drag
D_p	propeller diameter
DAS	data acquisition system
F	thrust
F_a	wheel force due to ailerons
F_e	wheel force due to elevators
F_g	gross thrust (engine axis)
F_n	net thrust (engine axis)
F_r	rudder pedal force or ram drag (stability axis)
F_y	aerodynamic force along the Y-axis
g	acceleration due to gravity
I_{XX}	moment of inertia about X axis
I_{YY}	moment of inertia about Y axis

LIST OF SYMBOLS (Cont'd)

SYMBOL	DEFINITION
I_{ZZ}	moment of inertia about Z axis
I_{XZ}	XZ product of inertia
ITT	turbine temperature
J	$V/n\ D_p$
L	lift or rolling moment
M	pitching moment or Mach number
MAC	mean aerodynamic chord
n	normal load factor, g's, $n = -A_Z$ or propeller speed
$n_{x_{wind}}$	wind axis load factor, x-direction
$n_{z_{wind}}$	wind axis load factor, z-direction
N	yawing moment or correction exponent for the thrust model
G	gas generator RPM
P	pressure
P	propeller
p	roll rate
P	power
q	dynamic pressure or pitch rate
r	yaw rate
S_W	wing area
T	temperature
V_c	calibrated airspeed

LIST OF SYMBOLS (Cont'd)

SYMBOLS	DEFINITION
V_g	ground speed
V_t, V	true airspeed
W	weight
W_a	air flow rate
W_f	fuel flow rate
x, y, z	aircraft coordinate axes - defined in Section 6
α	angle of attack of longitudinal body
α_η	angle of attack of horizontal stabilizer
β	sideslip angle
δ	control or trim surface deflection
δ	normalized ambient pressure ratio
Δ	differential element (generic)
ε	downwash angle at horizontal stabilizer
λ	inclination angle
ε_o	downwash angle at horizontal stabilizer for $\alpha = 0$
ρ	air density
Θ	pitch angle
Φ	roll (bank) angle
φ	yaw angle
δ_{t_2}	normalized total pressure ratio at the compressor face
θ_{t_2}	normalized total temperature ratio at the compressor face
γ	flight path angle

LIST OF SYMBOLS (Cont'd)

SUBSCRIPT	DEFINITION
a	aileron
A	aerodynamic
A/C	aircraft
C	control column
e	elevator
f	flap
L	left
r	rudder
R	right
t	test
t	trim
T	total
w	control wheel

THIS PAGE INTENTIONALLY LEFT BLANK

3. AIRPLANE

3.1. General Airplane Desciption

The De Havilland Twin Otter is a 13 to 20 passenger, one or two crew, turboprop airplane used primarily for commuter transportation. Maximum range is 700 n.m (at 10,000 ft.) with a 45 minute reserve. Maximum cruise speed at 10,000 feet is 165 KTAS. The airplane operating envelope is shown in Figure 3.1.1, and the geometry and operating weights are shown in Figure 3.1.2.

The airplane is powered by two Pratt and Whitney (UACL) PT6A-20 engines, each flat rated at 550 shaft horsepower and driving a Hartzell three bladed, constant speed, reversible, metal propeller, model H3-B3TN-3, blade T10173+1.

The primary flight control system is fully reversible. A gear tab is fitted to the rudder to lighten control forces and a tab fitted to the starboard elevator is linked to the flaps to control longitudinal trim during flap retraction and extension. The horizontal tail has fixed incidence. Geared trim tabs are located on both ailerons. The flaps are hydraulically actuated and incorporate a hand pump in the crew compartment to provide emergency pressure. No speed brakes or spoilers are installed. Figure 3.1.2 shows the location of the flight control system layout. Stall warning is visual and aural. No stick shaker is installed.

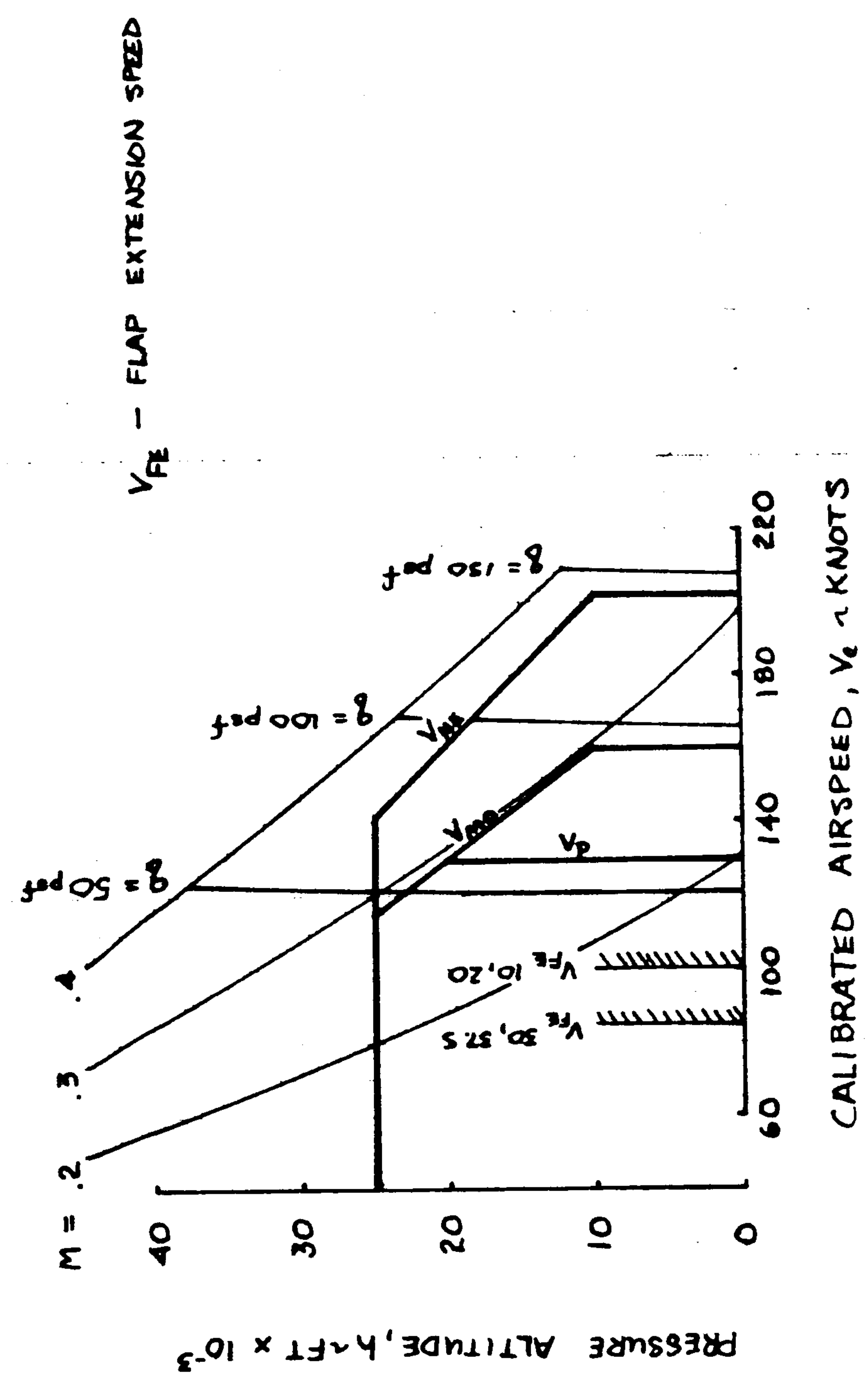

			REVISED	DATE		
CALC	J.K.J.	3/6/86			AIRPLANE OPERATING ENVELOPE	Fig. 3.1.1
CHECK						DHC-6-004
APPD						
APPD					KOHLMAN SYSTEMS RESEARCH - LAWRENCE KANSAS	3.1.2
DRAWN	J.K.J.	3/6/86				

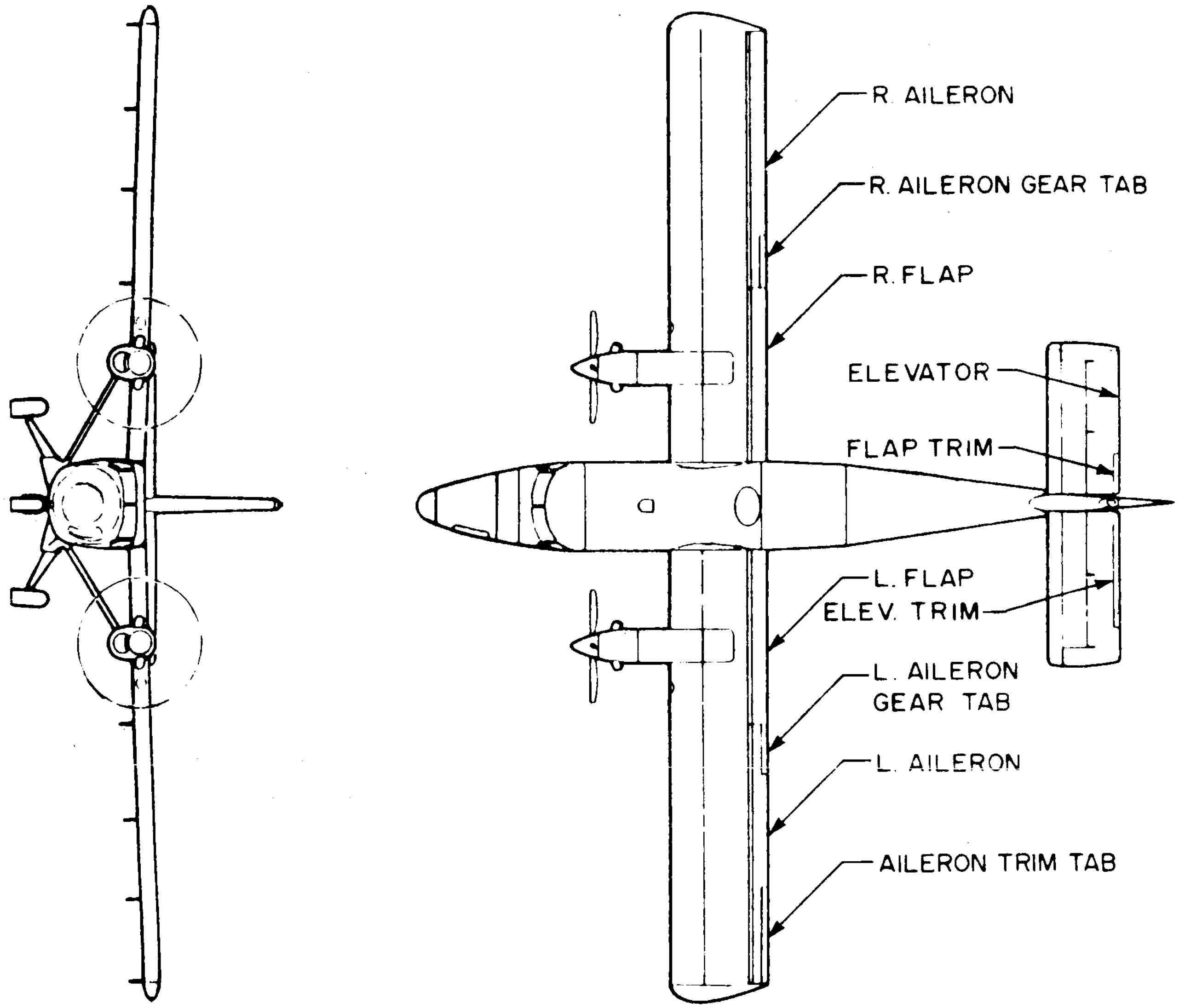

MAX. T/O WT. 11,579 LB

MAX. LANDING WT 11,400 LB.

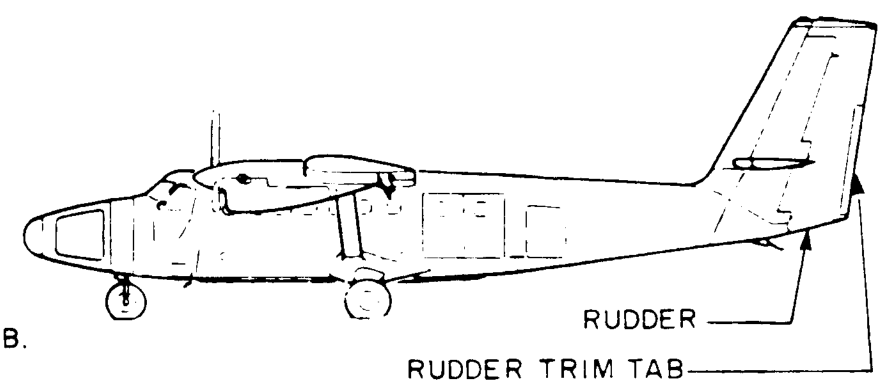

NOTE: DRAWING NOT TO SCALE.

			REVISED	DATE		
CALC					AIRPLANE GEOMETRY	Fig.3.1.2
CHECK	JYJ	3/14/86				DHC-6-001
APPD						
APPD					KOHLMAN SYSTEMS RESEARCH. LAWRENCE KANSAS	3.1.3
DRAWN						

THIS PAGE INTENTIONALLY LEFT BLANK

3.2. Test Airplane

The test airplane (N607, SN 04) instrumentation included control surface positions, pilot forces, engine data, air data, and inertial data. The KSR Data Acquisition System (DAS) was mounted inside the cabin near the aircraft, c.g. A Rosemount differential pressure angle of attack and sideslip sensor was mounted on a nose boom. This sensor is detailed in Section 5.2, 'Special Sensors'.

Several geometric constants were used to process the flight test data. These are listed in Table 3.2.1. The wing area, span, and mean aerodynamic chord (MAC) were used to non-dimensionalize the aerodynamic coefficients. The standard c.g. location is the point where all aerodynamic forces are assumed to act. A standard moment transformation is then used to transfer the moments to the actual c.g. The propeller and nozzle locations are where the propeller and jet forces act.

TABLE 3.2.1

DE HAVILLAND TWIN OTTER BASIC CONSTANTS LIST

	PARAMETER	UNITS	VALUE
1	WING AREA	SQ. FEET	420.03
2	WING SPAN	INCHES	780.000
3	ASPECT RATIO		10.00
4	M.A.C.	INCHES	78.000
5	LEADING EDGE STATION	INCHES	188.240
6	F.S. OF ALPHA/BETA SENSORS	INCHES	-123.5
7	AILERON AREA (EACH)	SQ. FEET	14.68
8	ELEVATOR AREA (EACH SIDE)	SQ. FEET	21.61
9	RUDDER AREA	SQ. FEET	33.55
10	AVERAGE AILERON CHORD	INCHES	10.500
11	AVERAGE ELEVATOR CHORD	INCHES	26.600
12	AVERAGE RUDDER CHORD	INCHES	29.000
13	STANDARD LONGITUDINAL C.G.	INCHES	223.058
14	STANDARD VERTICAL C.G.	INCHES	12.84
15	F.S. INLET	INCHES	131.44
16	WL. INLET	INCHES	29.6800
17	B.L. INLET	INCHES	110.000
18	FS. NOZZLE	INCHES	141.8
19	WL. NOZZLE	INCHES	43.43
20	B.L. NOZZLE	INCHES	110.000
21	FS. PROPELLER	INCHES	124.49
22	WL. PROPELLER	INCHES	43.43
23	B.L. PROPELLER	INCHES	110.000
24	ENGINE TOE-OUT ANGLE	DEG	0.0
25	ENGINE INCIDENCE ANGLE	DEG	0.0
26	100% NG	RPM	37468.
27	RAM RECOVERY FACTOR		1.00
28	NUMBER OF ENGINES		2.0
29	X LOCATION H-TAIL (25% MAC)	INCHES	511.93
30	Z LOCATION H-TAIL (25% MAC)	INCHES	54.00
31	X LOCATION V-TAIL (25% MAC)	INCHES	519.500
32	V LOCATION V-TAIL (25% MAC)	INCHES	81.000
33	STANDARD FLAP SETTING 1	DEG	10.0
34	STANDARD FLAP SETTING 2	DEG	20.0
35	STANDARD FLAP SETTING 3	DEG	37.5
36	FORCE WHEEL RADIUS	INCHES	5.25
37	GROUND DECK ANGLE	DEG	-1.5
38	D.A.S. SAMPLE RATE	SPS	8.567
39	PROP. DIAMETER	INCHES	102.0

3.3. Weights, Center of Gravity, and Inertias

The weight, center of gravity (c.g.) and inertias for the aircraft were determined from a combination of manufacturer's data and from experimental tests, measurements, and computations by KSR. The weight of the aircraft was measured in flight by subtracting the measured value of fuel used from the initial weight of the aircraft with full fuel, crew and flight test equipment. The zero fuel weight was determined by weighing the aircraft. The fuel used measurement was confirmed by weighing the aircraft before and after a number of the early flights. The fuel used measurement was found to be accurate to within 50 pounds. Between NASA flights 11 and 12, (KSR flights 6 and 7), additional equipment was installed in the aircraft. Therefore, two sets of plots for aircraft weight, c.g., and inertias are used. One set is valid for flights 6 through 11 and a second for flights 12 and on.

Since weight is the primary variable for determining the center of gravity and inertias during any given flight, changes in their values have been expressed in terms of fuel used. The same fuel burning sequence was used for all test flights. The initial weight, c.g. and inertias of the aircraft for each flight were adjusted for the addition of observers and test equipment.

The center of gravity position in flight was determined as a function of the fuel used. The longitudinal position of the center of gravity was established based on information contained in the Pilot's Operating Handbook (P.O.H.) and data from the zero fuel weighing. The vertical center of gravity was determined from specially provided manufacturer's data. No corrections were made for fuel slosh with change in attitude of the aircraft.

The coordinates used to measure the X and Z c.g. location are shown in Figure 3.3.1. The origin is located 21 inches aft of the nose, in the forward baggage compartment. Waterline and fuselage station are measured positive upward and aft from this point. Because this sign convention is contrary to the conventional aerodynamic body axis coordinates (positive X forward and Z downward), the signs have been changed in the KSR flight test data and are expressed in feet for consistency of that data set. Thus, the leading edge of the MAC would be listed as -15.69 feet in the KSR data base. The lateral (Y-axis) location of the c.g. is assumed to be zero (i.e., lies in the X-Z plane).

Moments of inertia (Ixx, Iyy, Izz, Ixz) were calculated based on manufacturer's data for the aircraft with empty tanks and with eight fuel loadings. The aircraft c.g. and inertia data for flights 6 through 11 are presented in Figures 3.3.2a thru 3.3.2g. For Flight 12 and on, this data is presented in Figures 3.3.3a thru 3.3.3g. The effects of crew and test equipment were accounted for, however, the dynamic effects of fuel slosh were not. This could cause variations of damping and momentary aircraft response to control inputs during more violent maneuvers.

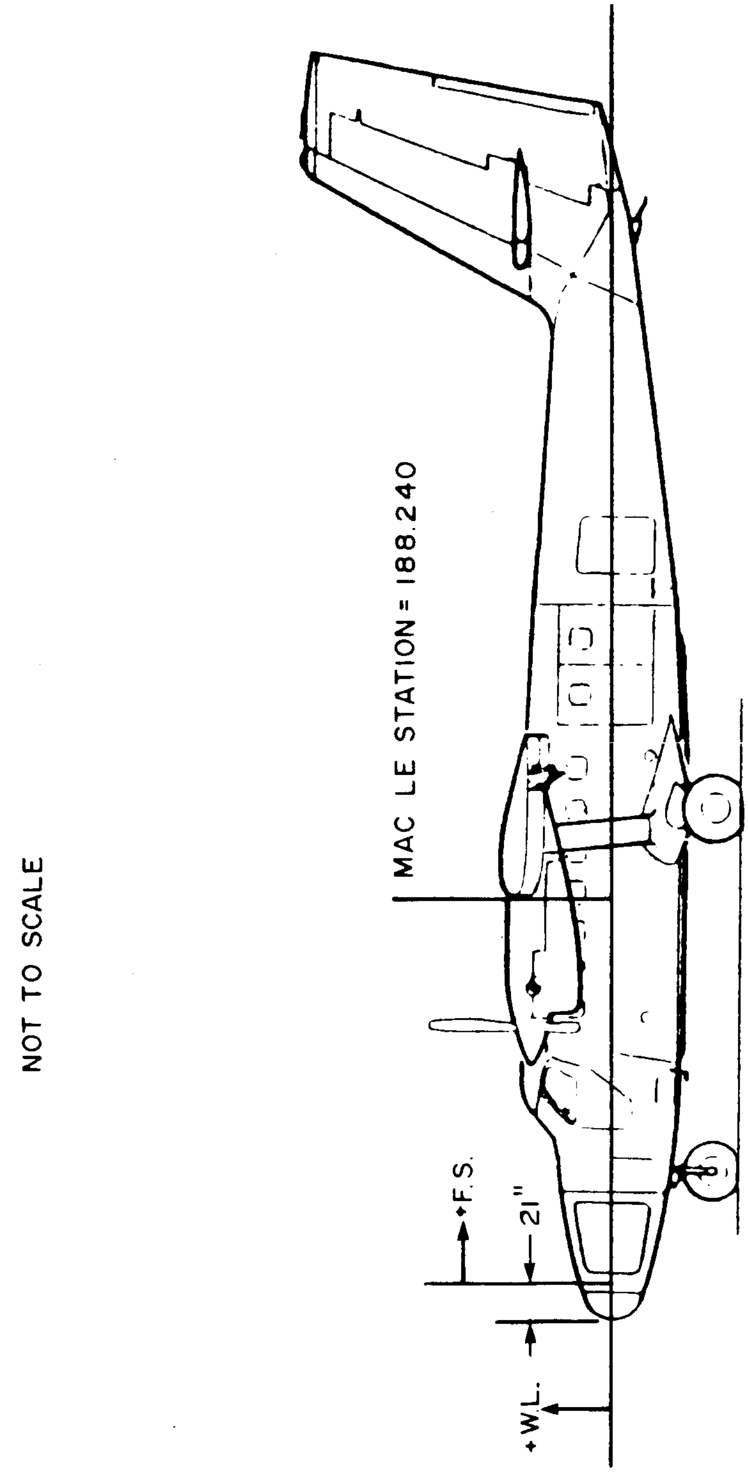

CALC			REVISED	DATE	FUSELAGE STATION AND WATERLINE REFERENCES	Fig. 3.3.3
CHECK	J.J.	3/14/86				DHC-6-004
APPD						
APPD					KOHLMAN SYSTEMS RESEARCH - LAWRENCE KANSAS	3.3.3
DRAWN						

Aircraft Weight	X C.G. Position (ft.)
9053.500	-17.39500
9428.500	-17.37266
9828.500	-17.35071
10228.50	-17.33048
10628.50	-17.31177
10828.50	-17.30293
11028.50	-17.29441
11228.50	-17.28620
11428.50	-17.27828

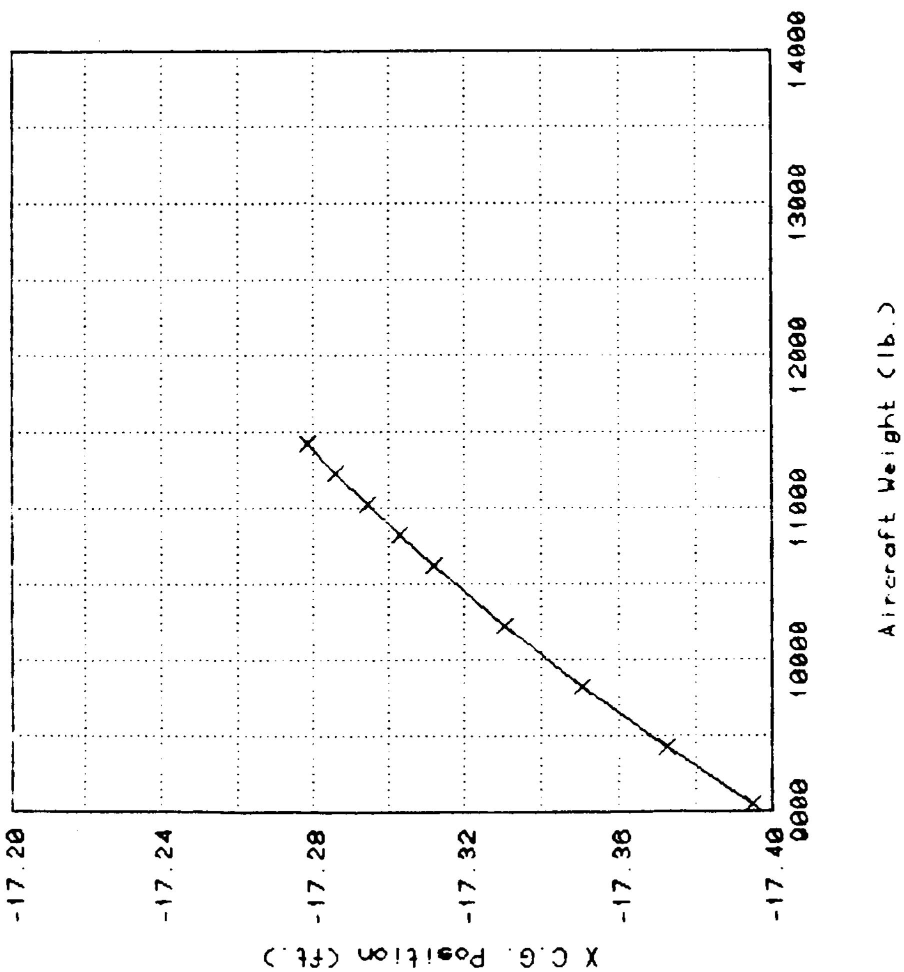

CALC		02/21/86	REVISED	DATE	FOR NASA FLIGHTS 6-11
CHECK	J.J.J.	3/14/86			Mass Model - X C.G.
APPD					Fig. 3.3.2a
APPD					DHC-6-004
TIME	16:25:40				KOHLMAN SYSTEMS RESEARCH
					3.3.4

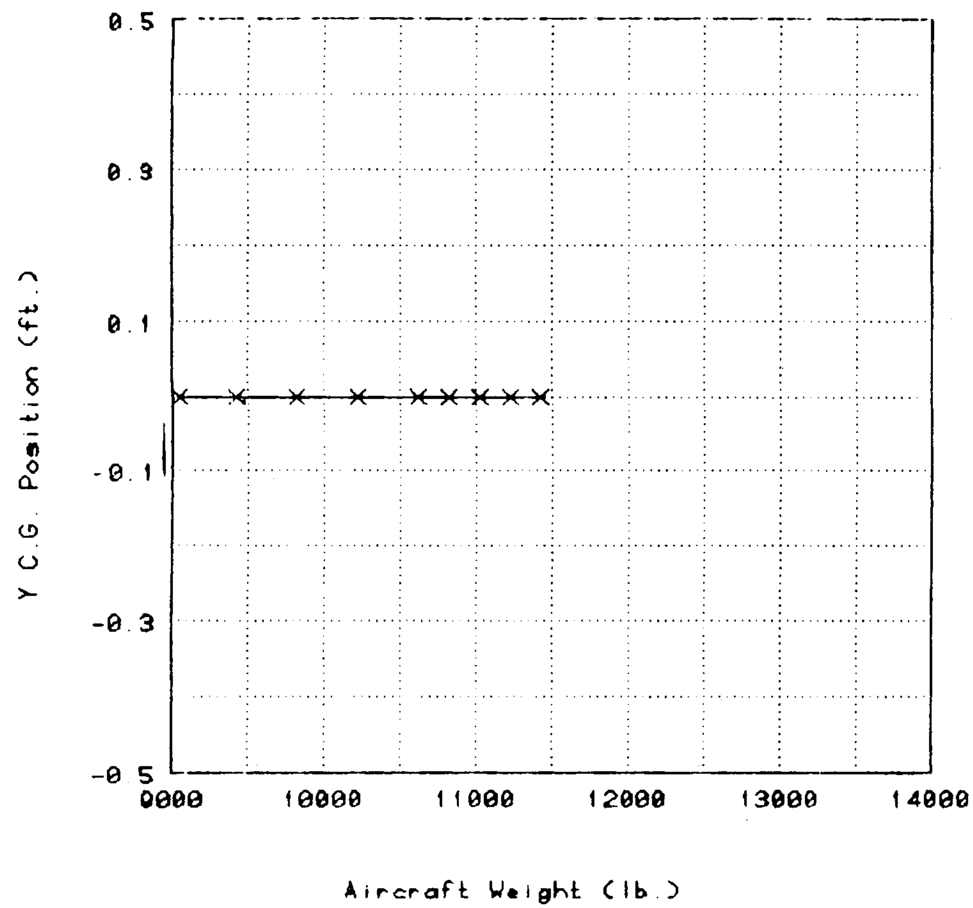

Aircraft Weight	Y C.G. Position (ft.)
9053.500	.0000000e+00
9428.500	.0000000e+00
9828.500	.0000000e+00
10228.50	.0000000e+00
10628.50	.0000000e+00
10828.50	.0000000e+00
11028.50	.0000000e+00
11228.50	.0000000e+00
11428.50	.0000000e+00

LC		02/21/86	REVISED	DATE
CHECK	J.Z.J.	3/14/86		
APPD				
APPD				
TIME	16:27:21			

FOR NASA FLIGHTS 6-11
Mass Model - Y C.G.

Fig. 3.3.2b

DHC-6-004

KOHLMAN SYSTEMS RESEARCH

3.3.5

Aircraft Weight	Z C.G. Position (ft.)
9053.500	-1.664167
9428.500	-1.502357
9828.500	-1.353554
10228.50	-1.223621
10628.50	-1.110073
10828.50	-1.058758
11028.50	-1.010067
11228.50	-.9657042
11428.50	-.9234838

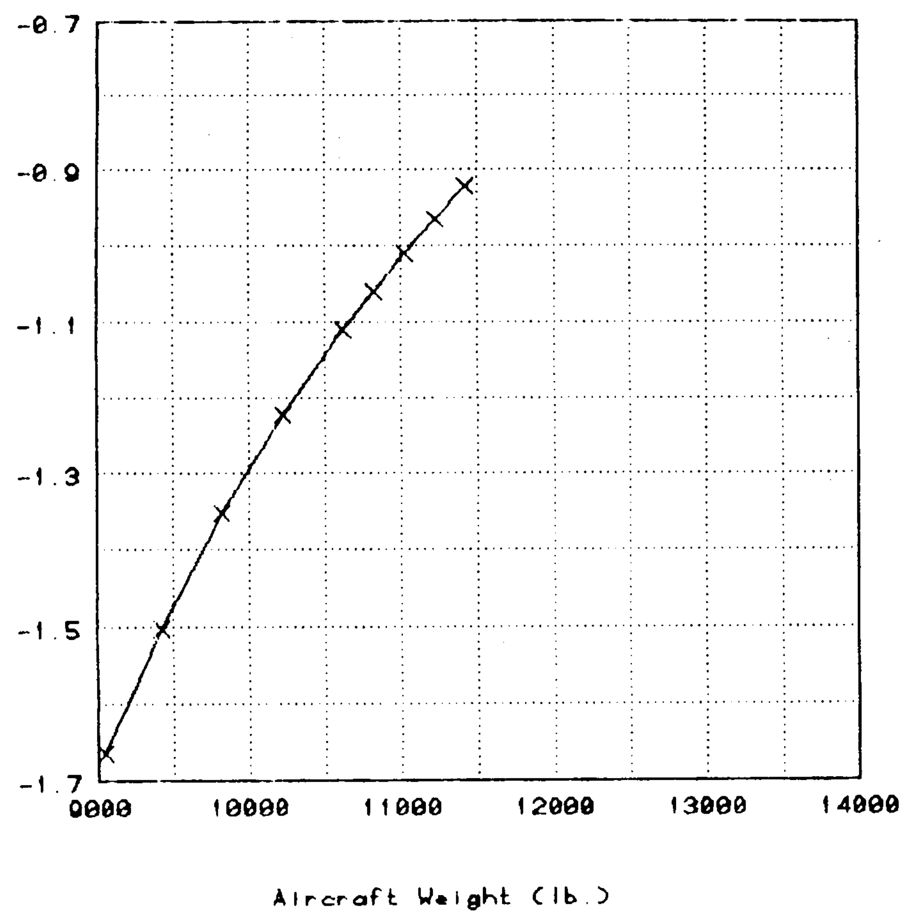

CALC		02/21/86	REVISED	DATE	FOR NASA FLIGHTS 6-11 Mass Model - Z C.G.
CHECK	J.Z.J	3/14/86			
APPD					
APPD					
TIME	16:29:00				KOHLMAN SYSTEMS RESEARCH

Fig. 3.3.2c

DHC-6-004

Aircraft Weight	IXX (slug-ft**2)
9053.500	15645.00
9428.500	15828.37
9828.500	15977.65
10228.50	16006.50
10628.50	16192.61
10828.50	16234.55
11028.50	16267.87
11228.50	16299.92
11428.50	16327.98

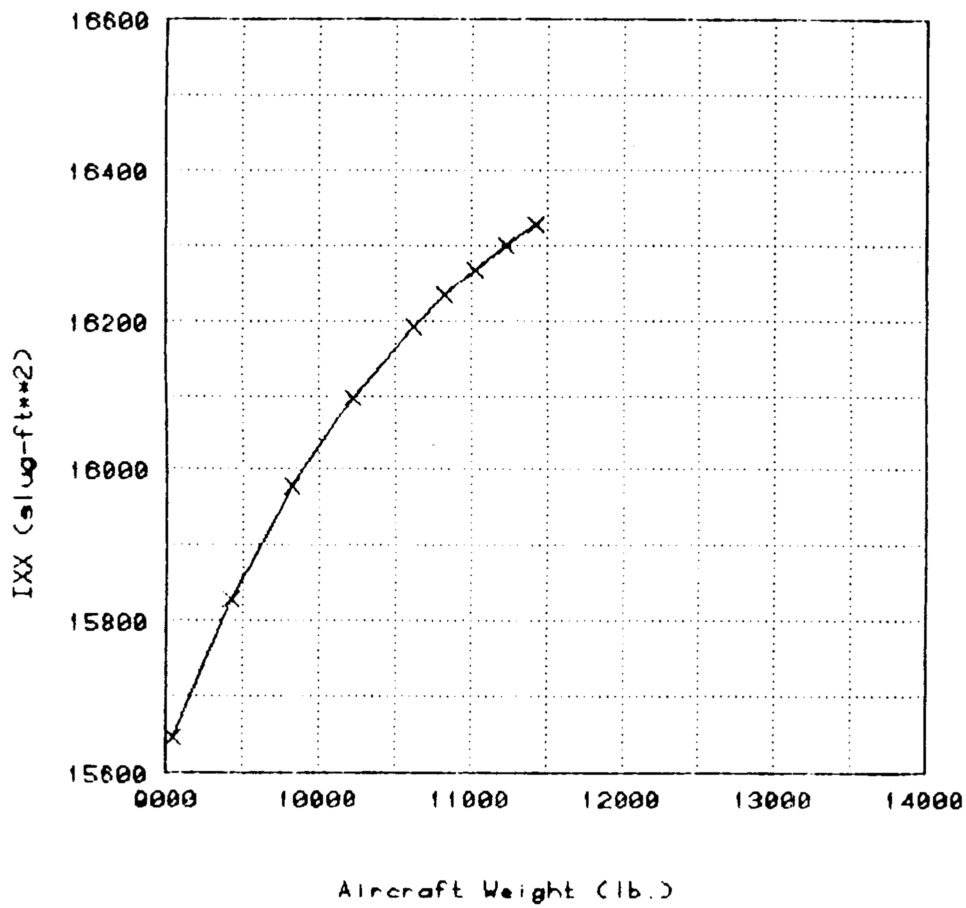

ALC		02/21/86	REVISED	DATE
CHECK	J.L.J.	3/14/86		
APPD				
APPD				
TIME	16:30:41			

FOR NASA FLIGHTS 6-11

Mass Model - IXX

KOHLMAN SYSTEMS RESEARCH

Fig. 3.3.2d

DHC-6-004

3.3.7

Aircraft Weight	IYY (slug-ft**2)
9053.500	22039.00
9428.500	22365.28
9828.500	22677.60
10228.50	22958.82
10628.50	23206.81
10828.50	23322.21
11028.50	23432.42
11228.50	23544.28
11428.50	23642.00

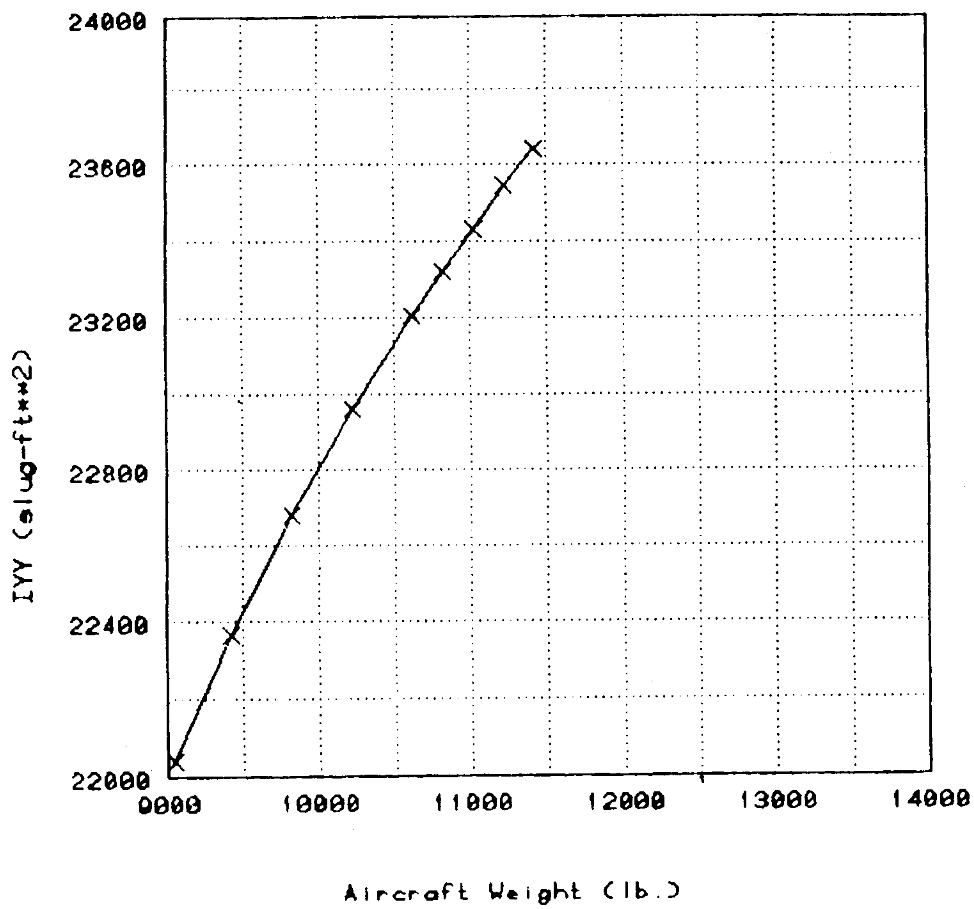

CALC		02/21/86	REVISED	DATE
CHECK	J.J.J.	3/14/86		
APPD				
APPD				
TIME	16:32:21			

FOR NASA FLIGHTS 6-11

Mass Model - IYY

Fig. 3.3.2e

DHC-6-004

KOHLMAN SYSTEMS RESEARCH

3.3.8

Aircraft Weight	IZZ (slug-ft**2)
9053.500	35304.00
9428.500	35547.30
9828.500	35730.45
10228.50	35918.02
10628.50	36110.20
10828.50	36206.16
11028.50	36302.05
11228.50	36397.88
11428.50	36493.61

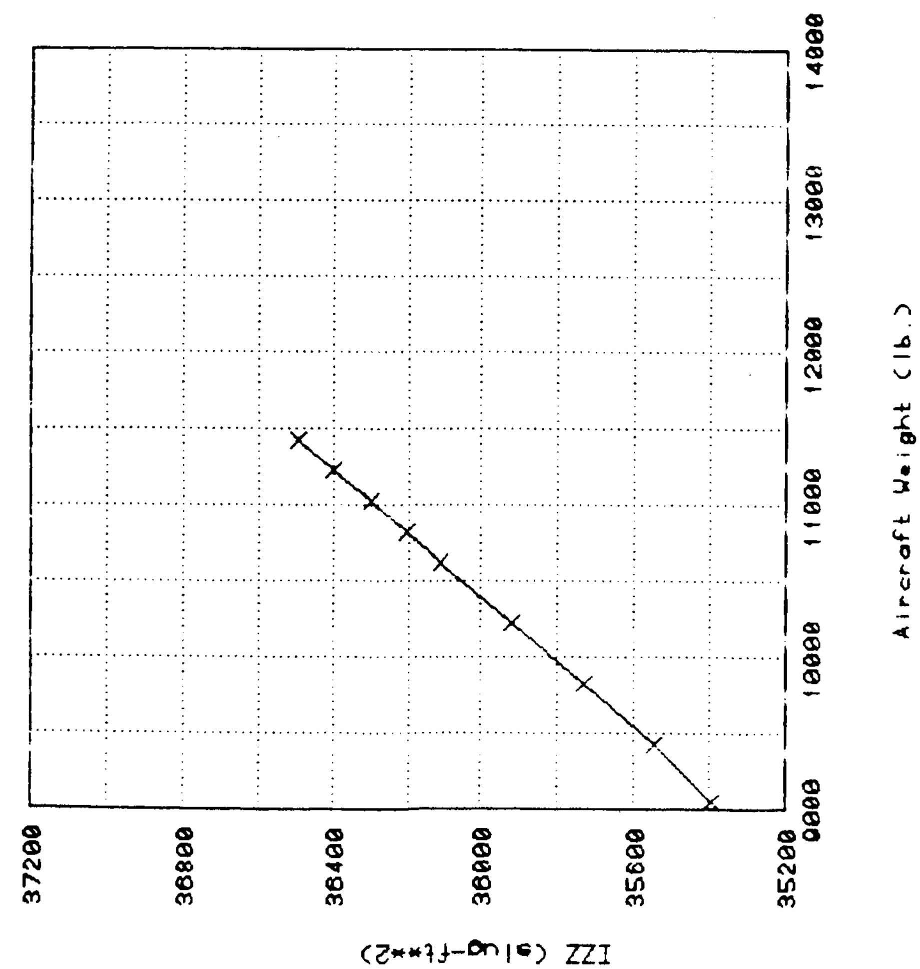

CALC		02/21/86	REVISED	DATE	FOR NASA FLIGHTS 6-11 Mass Model - IZZ	Fig. 3.3.2f
CHECK	JJJ	3/14/86				DHC-6-004
APPD						
APPD						
TIME	16:34:02				KOHLMAN SYSTEMS RESEARCH	3.3.9

Aircraft Weight	IXZ (slug-ft**2)
9053.500	1048.000
9428.500	1072.557
9828.500	1093.221
10228.50	1100.820
10628.50	1122.598
10828.50	1127.000
11028.50	1132.740
11228.50	1137.007
11428.50	1140.736

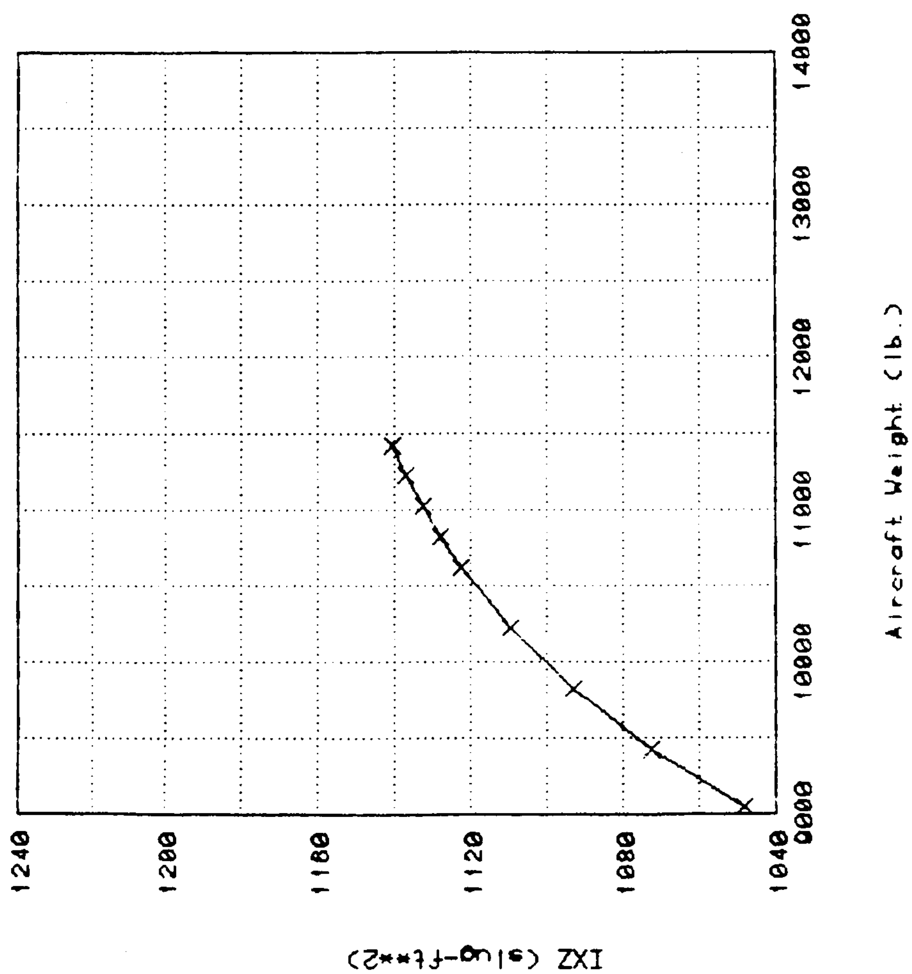

CALC		02/21/86	REVISED	DATE
CHECK	J.Y.J.	3/14/86		
APPD				
APPD				
TIME	16:35:42			

FOR NASA FLIGHTS 6-11

Mass Model - IXZ

KOHLMAN SYSTEMS RESEARCH

Fig. 3.3.2g

DHC-6-004

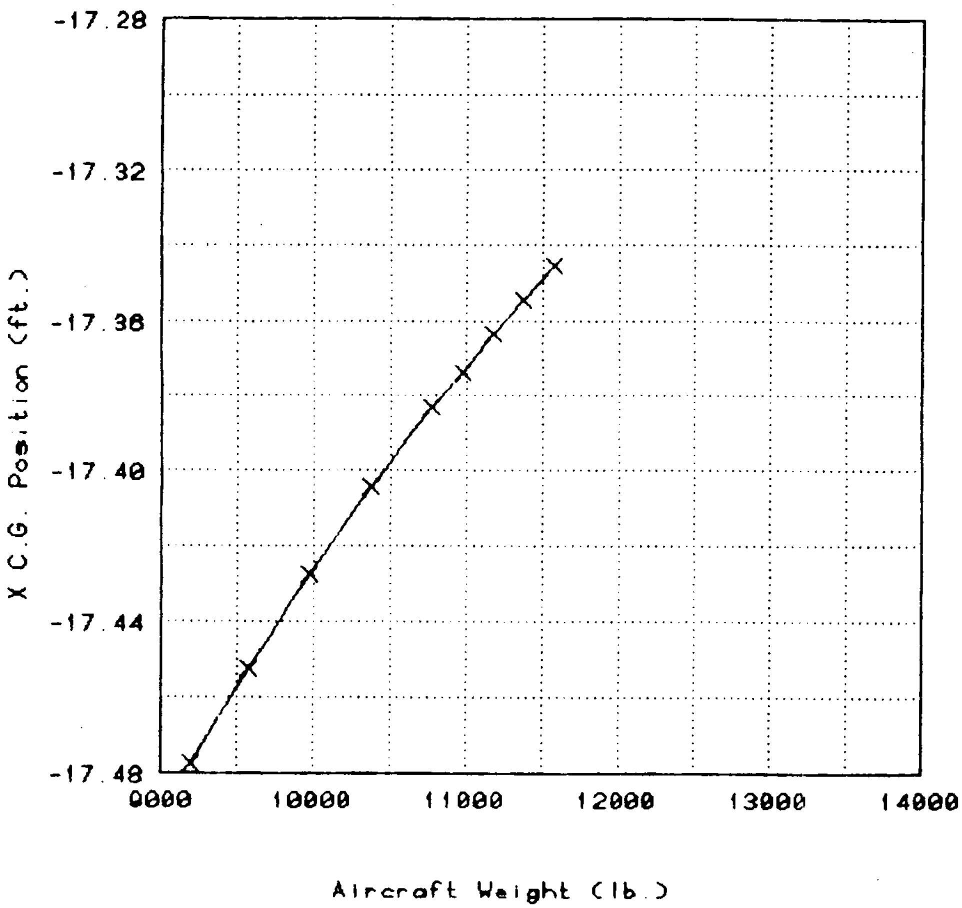

Aircraft Weight	X C.G. Position (ft.)
9205.500	-17.47750
9580.500	-17.45228
9980.500	-17.42748
10380.50	-17.40458
10780.50	-17.38930
10980.50	-17.37337
11180.50	-17.36371
11380.50	-17.35430
11580.50	-17.34530

CALC		02/21/86	REVISED	DATE
CHECK	J.Y.J.	3/14/86		
APPD				
APPD				
TIME	16:07:18			

FOR NASA FLIGHTS 12-25

Mass Model - X C.G

KOHLMAN SYSTEMS RESEARCH

Fig.3.3.3a

DHC-6-004

3.3.11

Aircraft Weight	Y C.G. Position (ft.)
9205.500	.0000000e+00
9580.500	.0000000e+00
9980.500	.0000000e+00
10380.50	.0000000e+00
10780.50	.0000000e+00
10980.50	.0000000e+00
11180.50	.0000000e+00
11380 50	.0000000e+00
11580.50	.0000000e+00

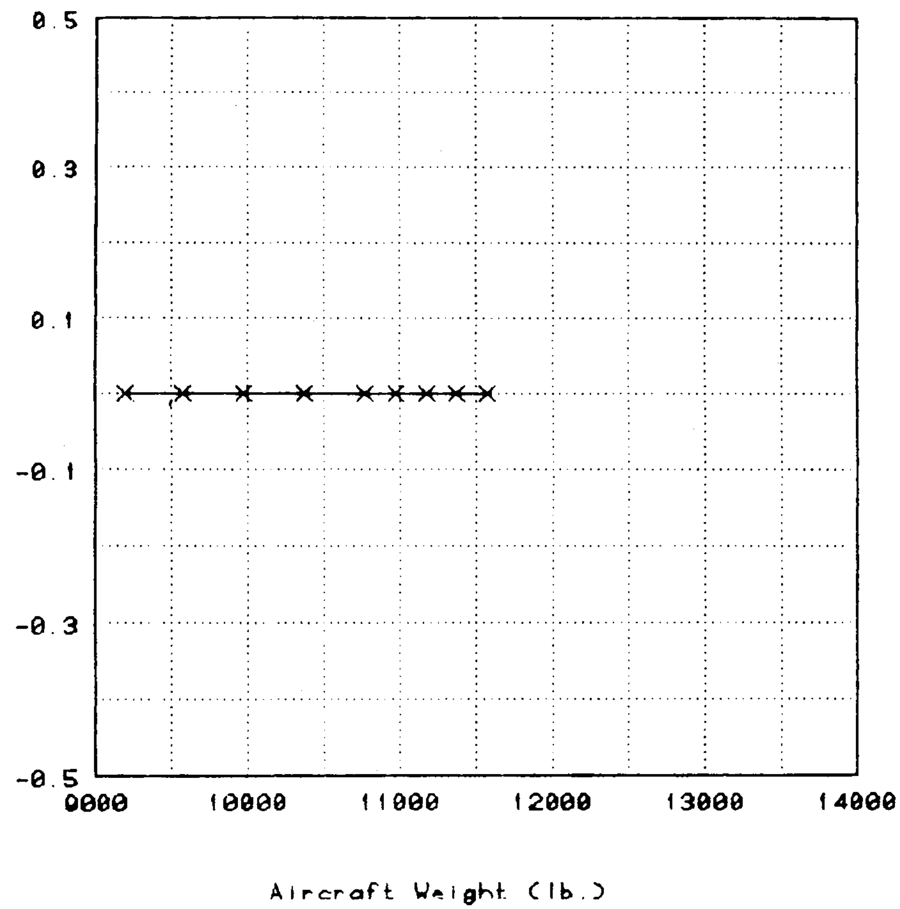

CALC		02/21/86	REVISED	DATE
CHECK	J.G.J.	3/14/86		
APPD				
APPD				
TIME	16:08:58			

FOR NASA FLIGHTS 12-25

Mass Model - Y C.G.

KOHLMAN SYSTEMS RESEARCH

Fig.3.3.3b

DHC-6-004

3.3.12

Aircraft Weight	Z C.G. Position (ft.)
9205.500	-1.664167
9580.500	-1.504024
9980.500	-1.357061
10380.50	-1.230072
10780.50	-1.117885
10980.50	-1.067130
11180.50	-1.019847
11380.50	-.9750330
11580.50	-.9332057

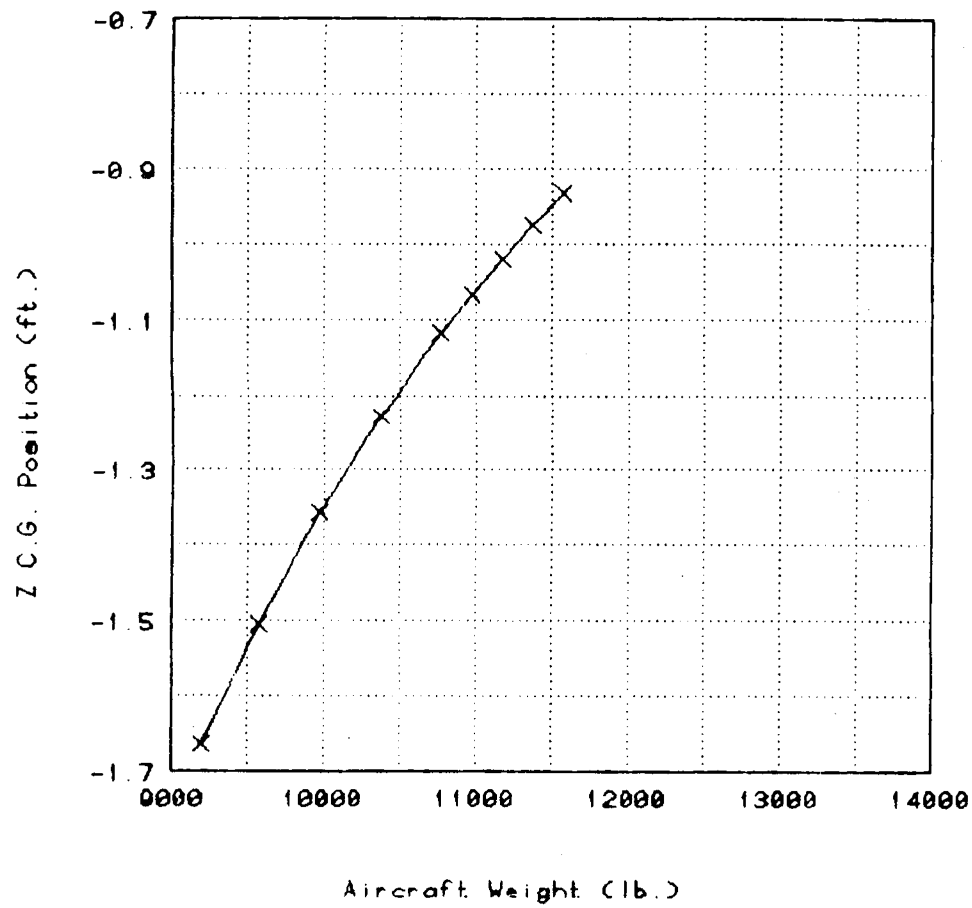

LC		02/21/86	REVISED	DATE	FOR NASA FLIGHTS 12-25
CHECK	JLJ	3/4/86			Mass Model - Z C.G.
APPD					
APPD					
TIME	16:10:30				KOHLMAN SYSTEMS RESEARCH

Fig. 3.3.3c

DHC-6-004

3.3.13

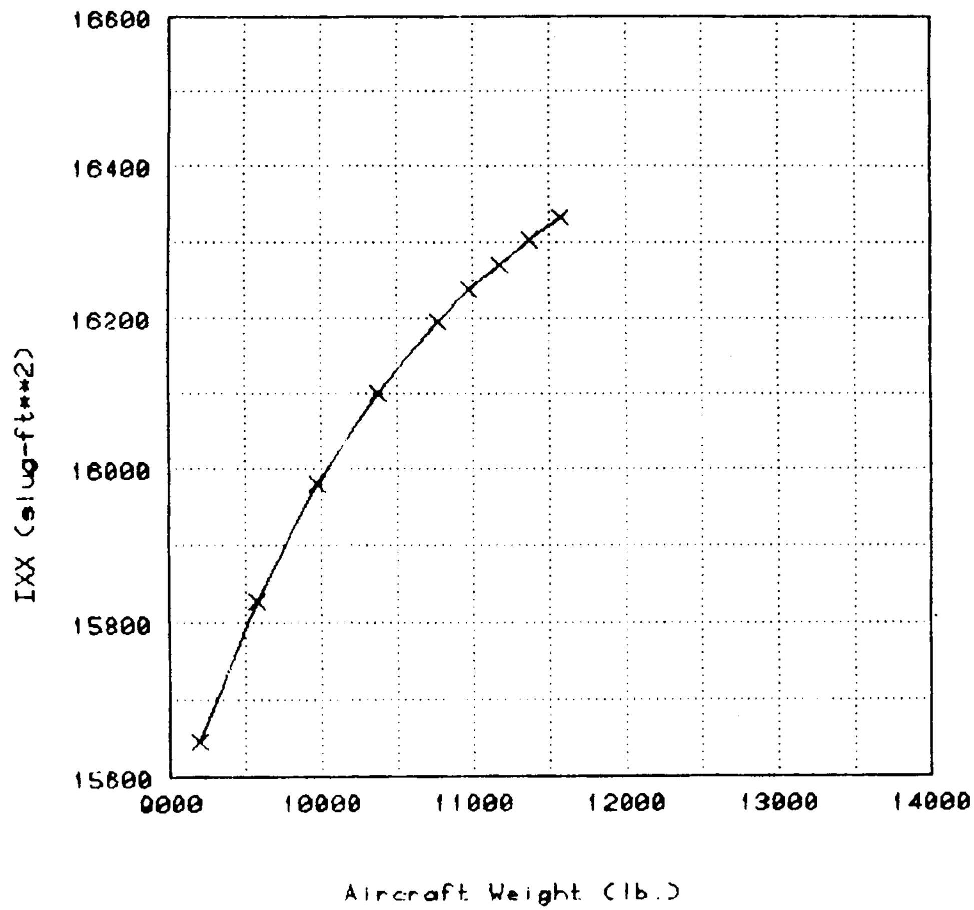

Aircraft Weight	IXX (slug-ft**2)
9205.500	15645.00
9580.500	15828.81
9080.500	15979.65
10380.50	16008.90
10780.50	16108.05
10980.50	16237.41
11180.50	16271.14
11380.50	16303.40
11580.50	16332.04

CALC		02/21/86	REVISED	DATE
CHECK	J.Y.J.	3/14/86		
APPD				
APPD				
TIME	16:12:10			

FOR NASA FLIGHTS 12-25

Mass Model - IXX

KOHLMAN SYSTEMS RESEARCH

Fig. 3.3.3d

DHC-6-004

3.3.14

Aircraft Weight	IYY (slug-ft**2)
9205.500	22132.00
9580.500	22459.57
9080.500	22774.15
10380.50	23053.31
10780.50	23305.88
10980.50	23422.00
11180.50	23532.90
11380.50	23640.45
11580.50	23748.80

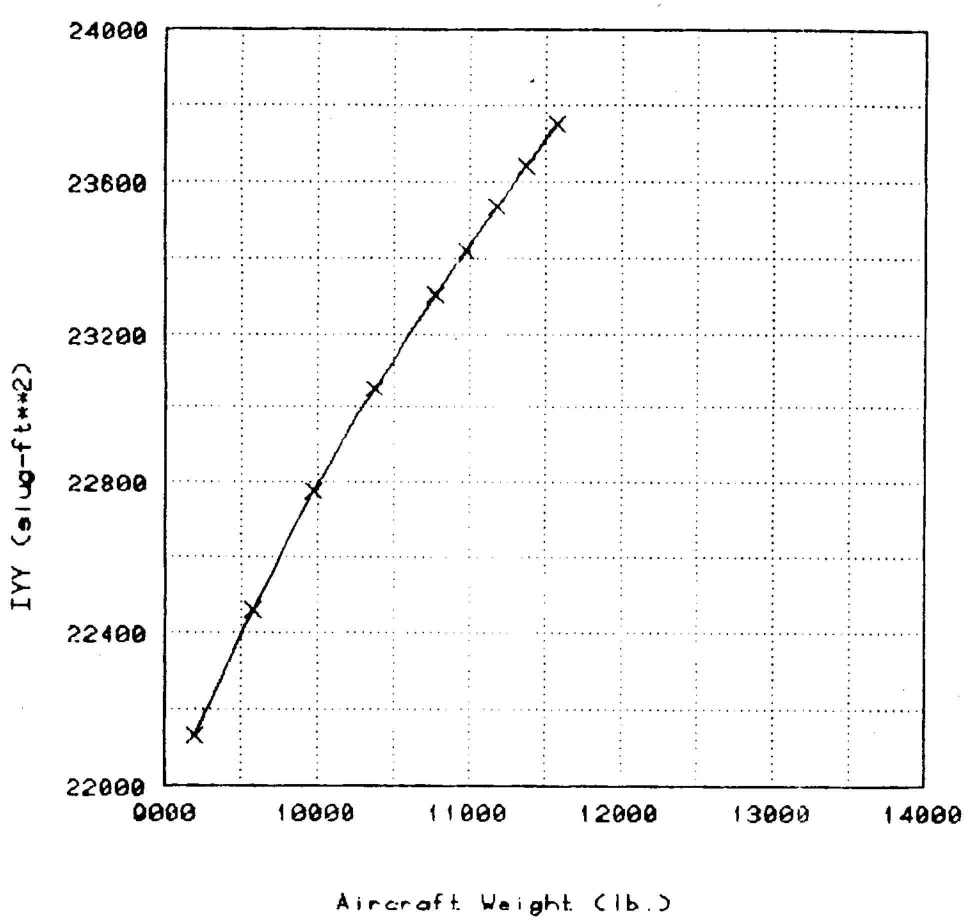

CALC		02/21/86	REVISED	DATE
CHECK	[signature]	3/14/86		
APPD				
APPD				
TIME	16:14:00			

FOR NASA FLIGHTS 12-25

Mass Model - IYY

KOHLMAN SYSTEMS RESEARCH

Fig. 3.3.3e

DHC-6-004

3.3.15

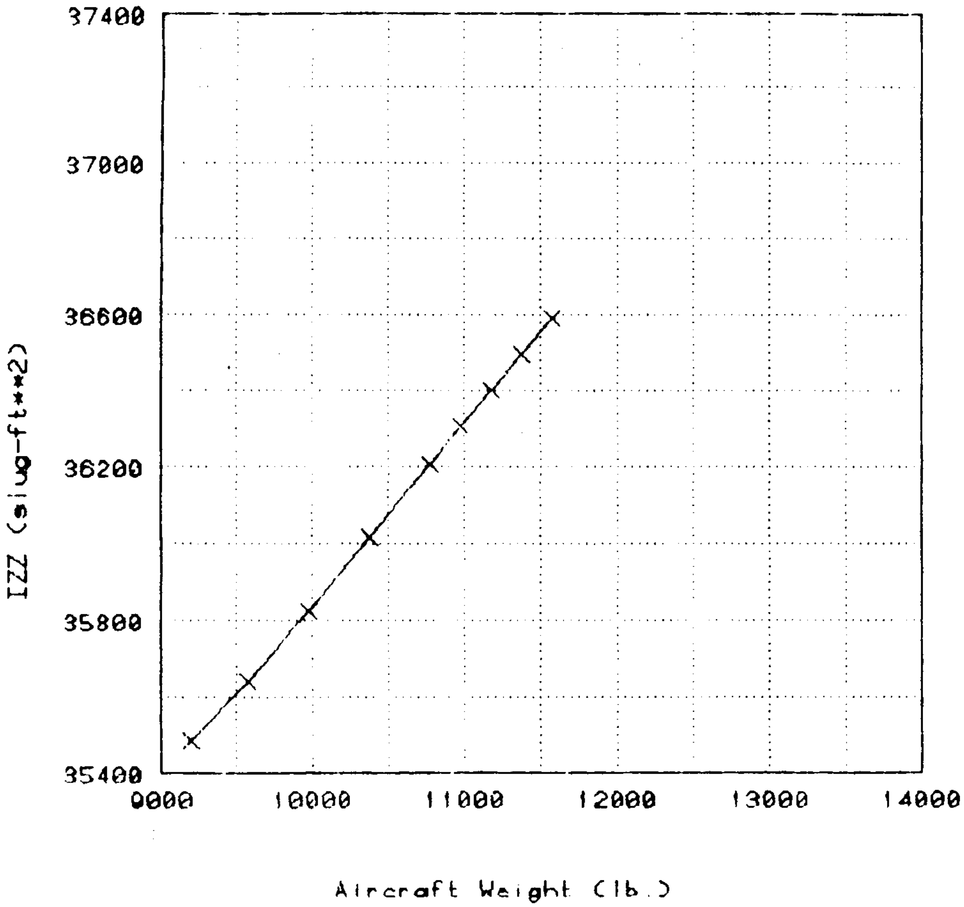

Aircraft Weight	IZZ (slug-ft**2)
9205.500	35487.00
9580.500	35641.46
9980.500	35825.50
10380.50	36015.91
10780.50	36208.81
10980.50	36303.00
11180.50	36309.27
11380.50	36405.35
11580.50	36501.35

CALC		02/21/86	REVISED	DATE
CHECK	J.G.J.	3/14/86		
APPD				
APPD				
TIME	16:15:45			

FOR NASA FLIGHTS 12-25

Mass Model - IZZ

KOHLMAN SYSTEMS RESEARCH

Fig. 3.3.3f

DHC-6-004

3.3.16

Aircraft Weight	IXZ (slug-ft**2)
9205.500	1048.000
9580.500	1076.201
9080.500	1100.053
10380.50	1118.950
10780.50	1133.974
10980.50	1140.240
11180.50	1145.775
11380.50	1150.737
11580.50	1155.091

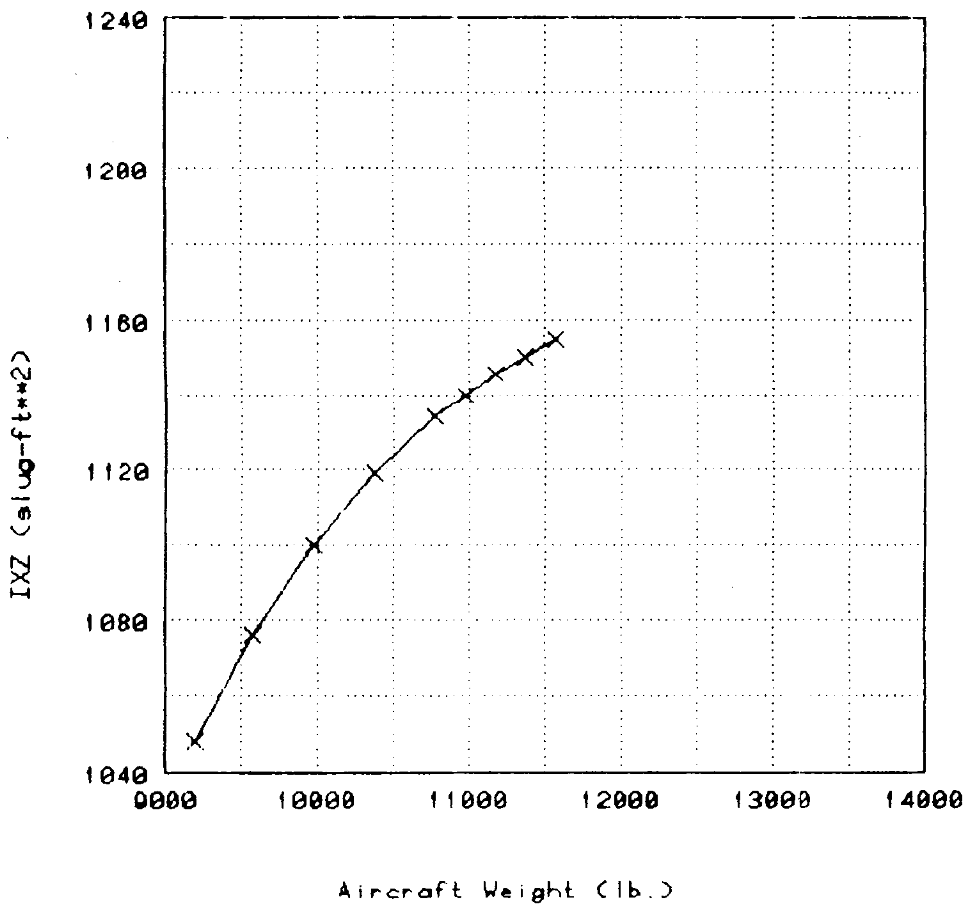

CALC		02/21/86	REVISED	DATE	FOR NASA FLIGHTS 12-25 Mass Model - IXZ	Fig. 3.3.33
CHECK	J.G.J.	3/14/86				DHC-6-004
APPD						
APPD						
TIME	16 16 24				KOHLMAN SYSTEMS RESEARCH	3.3.17

THIS PAGE INTENTIONALLY LEFT BLANK

4. FLIGHT TEST OPERATION

Data for this report were gathered in 18 data flights totaling 38.9 hours. The test airplane was the NASA Lewis Research Center modified De Havilland Twin Otter which has been equipped for icing research.

A summary of the total flight test program is given in Table 4.1. Aircraft instrumentation started in September 1985 and data system installation and calibration were completed by the end of the month.

A typical flight began with a ground transducer check. Every parameter was checked for operation and its counts value hand recorded. The flight test engineer briefed the pilots on the maneuvers to be flown. Before takeoff, three preflight runs were recorded on the DAS. A "zero" run data record was taken with the airplane static, engines at idle, and the controls at a pre-determined position. Then a data record of a control sweep in each axis was taken. An engine run-up was used to check engine parameters. At this time, the cockpit engine indications were hand recorded. After the flight, these steps were repeated. The values from the "zero" runs were used to correct bias errors in some parameters, such as angular rates, air data, and forces.

TABLE 4.1

TWIN OTTER FLIGHT PROGRAM SUMMARY

DATE (1985)	FLT. NO.*	FLIGHT TIME TOTAL	PERF. (DRY AIR)	S & C (DRY AIR)	PERF. (ICE)	S & C (ICE)	MISC.	REMARKS
27 Sep	1 (6)	1.4					1.4	System Check Out
30 Sep	2 (7)	2.4					2.4	Airspeed Cal.
1 Oct	3 (8)	2.0		1.0			1.0	Finished Airspeed Cal.
3 Oct	4 (9)	2.9		2.9				
4 Oct	5 (10)	2.1		2.1				
23 Oct	6 (11)	1.9	1.9					
19 Nov	7 (12)	1.1					1.1	System Check Out
21 Nov	8 (13)	2.6			2.6			Airspeed Failure
4 Dec	10 (15)	2.8				2.8		
4 Dec	11 (16)	2.2				2.2		
5 Dec	12 (17)	1.9				1.9		
12 Dec	19 (19)	1.8			1.8			
12 Dec	20 (20)	1.9			1.4	.5		
13 Dec	21 (21)	2.2			2.2			
14 Dec	22 (22)	3.0			1.0	2.0		
16 Dec	23 (23)	2.5				2.5		
18 Dec	24 (24)	1.8	1.8					
19 Dec	25 (25)	2.4		2.4				
Total Hours		38.9	3.7	8.4	9.0	11.9	5.9	

PERF. - Performance
S & C - Stability and Control
MISC. - Miscellaneous

DRY AIR - Baseline Flights
ICE - Icing Data Flights

* Numbers in parenthesis represent the NASA flight test numbering system.

5. DATA ACQUISITION AND ANALYSIS

5.1. Data Acquisition

The data for this report were recorded on the KSR DAS. The DAS records data with 12 bits of resolution at approximately 8.6 samples per second. All channels are sampled within a one-millisecond time interval and then recorded on tape. This effectively eliminates time skews due to sequential sampling. The parameters recorded by this system are listed in Table 5.1.1.

Figure 5.1.1 shows the DAS which includes the computer, computer controls and display, tape recorder, and signal conditioning. The KSR inertial transducer package which contains three linear accelerometers, three rate gyros, and an attitude gyro was mounted near the longitudinal and vertical c.g. but to the left of the lateral c.g.

TABLE 5.1.1

RECORDED DATA

NASA TWIN OTTER DHC-6-004

VARIABLE #	VARIABLE	VARIABLE NAME	UNITS
1	FILCNT	FILE COUNTER	--------
2	BLKCNT	BLOCK COUNTER	--------
3	ESB	ENGINEER'S STATUS BYTE	--------
4	ASB	AIRCRAFT STATUS BYTE	
		PAUSE EVENT	
		ROSEMOUNT HEAT	
		GEAR POSITION	
		GYRO ERECTION MARKER	
		PILOT EVENT	
5	TIME	TIME	(SEC)
6	AX	LONGITUDINAL ACCELERATION	(G)
7	AY	LATERAL ACCELERATION	(G)
8	AZ	Z-DIRECTION ACCELERATION	(G)
9	PITCH_RATE	PITCH RATE	(DEG/SEC)
10	ROLL_RATE	ROLL RATE	(DEG/SEC)
11	YAW_RATE	YAW RATE	(DEG/SEC)
12	PITCH_ATT	PITCH ATTITUDE	(DEG)
13	ROLL_ATT	ROLL ATTITUDE	(DEG)
14	DELP_ALPHA	PRESSURE ALPHA	(PSF)
15	DELP_BETA	PRESSURE BETA	(PSF)
16	DELP_REF	PRESSURE REFERENCE	(PSF)
17	DELTA_A_L	AILERON DEFLECTION	(DEG)
18	---------	------------------	EMPTY

19	DELTA_E	ELEVATOR DEFLECTION	(DEG)
20	DELTA_R	RUDDER DEFLECTION	(DEG)
21	FLAP	FLAP POSITION	(DEG)
22	-------	-------------------	EMPTY
23	-------	-------------------	EMPTY
24	-------	-------------------	EMPTY
25	-------	-------------------	EMPTY
26	-------	-------------------	EMPTY
27	-------	-------------------	EMPTY
28	-------	-------------------	EMPTY
29	-------	-------------------	EMPTY
30	-------	-------------------	EMPTY
31	-------	-------------------	EMPTY
32	DIFF_PRESS	DIFFERENTIAL PRESSURE	(PSF)
33	AIR_TEMP	INDICATED TOTAL TEMPERATURE	(DEG_K)
34	INERT_VREF	VERTICAL GYRO REFERENCE VOLTAGE	(VOLT)
35	STAT_PRESS	STATIC PRESSURE	(PSF)
36	CPT_VREF	REFERENCE VOLTAGE	(VOLT)
37	BATTERY_A	REFERENCE BATTERY BOARD 1	(VOLT)
38	-------	-------------------	EMPTY
39	FUEL_USED	FUEL USED	(LB)
40	PAF	PILOT AILERON FORCE	(LB)
41	PEF	PILOT ELEVATOR FORCE	(LB)
42	PRF_L	PILOT RUDDER FORCE LEFT	(LB)
43	PRF_R	PILOT RUDDER FORCE RIGHT	(LB)
44	-------	-------------------	EMPTY
45	-------	-------------------	EMPTY

46	-------	-------------------	EMPTY
47	-------	-------------------	EMPTY
48	-------	-------------------	EMPTY
49	N1_L	GAS GENERATOR RPM-N1 LEFT	(%)
50	N1_R	GAS GENERATOR RPM-N1 RIGHT	(%)
51	PROP_RPM_L	PROPELLER RPM LEFT	(%)
52	PROP_RPM_R	PROPELLER RPM RIGHT	(%)
53	TORQUE_L	ENGINE TORQUE PRESSURE LEFT	(PSI)
54	TORQUE_R	ENGINE TORQUE PRESSURE RIGHT	(PSI)
55	FUEL-FLO_L	INDICATED FUEL FLOW LEFT ENGINE	(LB/HR)
56	FUEL_FLO_R	INDICATED FUEL FLOW RIGHT ENGINE	(LB/HR)
57	FUELTEMP_L	FUEL TEMPERATURE LEFT ENGINE	(DEG_K)
58	FUELTEMP_R	FUEL TEMPERATURE RIGHT ENGINE	(DEG_K)
59	-------	-------------------	EMPTY
60	-------	-------------------	EMPTY
61	-------	-------------------	EMPTY
62	-------	-------------------	EMPTY
63	-------	-------------------	EMPTY
64	JOHNS_WILL	LIQUID WATER CONTENT INDICATOR	(VOLT)
65	LEIGH	ICE DETECTOR UNIT	(VOLT)
66	ROSEMOUNT	ICE DETECTOR UNIT	(VOLT)
67	GEN_EAST	DEW POINT HYGROMETER	(VOLT)
68	-------	-------------------	EMPTY
69	-------	-------------------	EMPTY
70	-------	-------------------	EMPTY
71	BATTERY_B	REFERENCE BATTERY BOARD 2	(VOLT)

ORIGINAL PAGE IS
OF POOR QUALITY

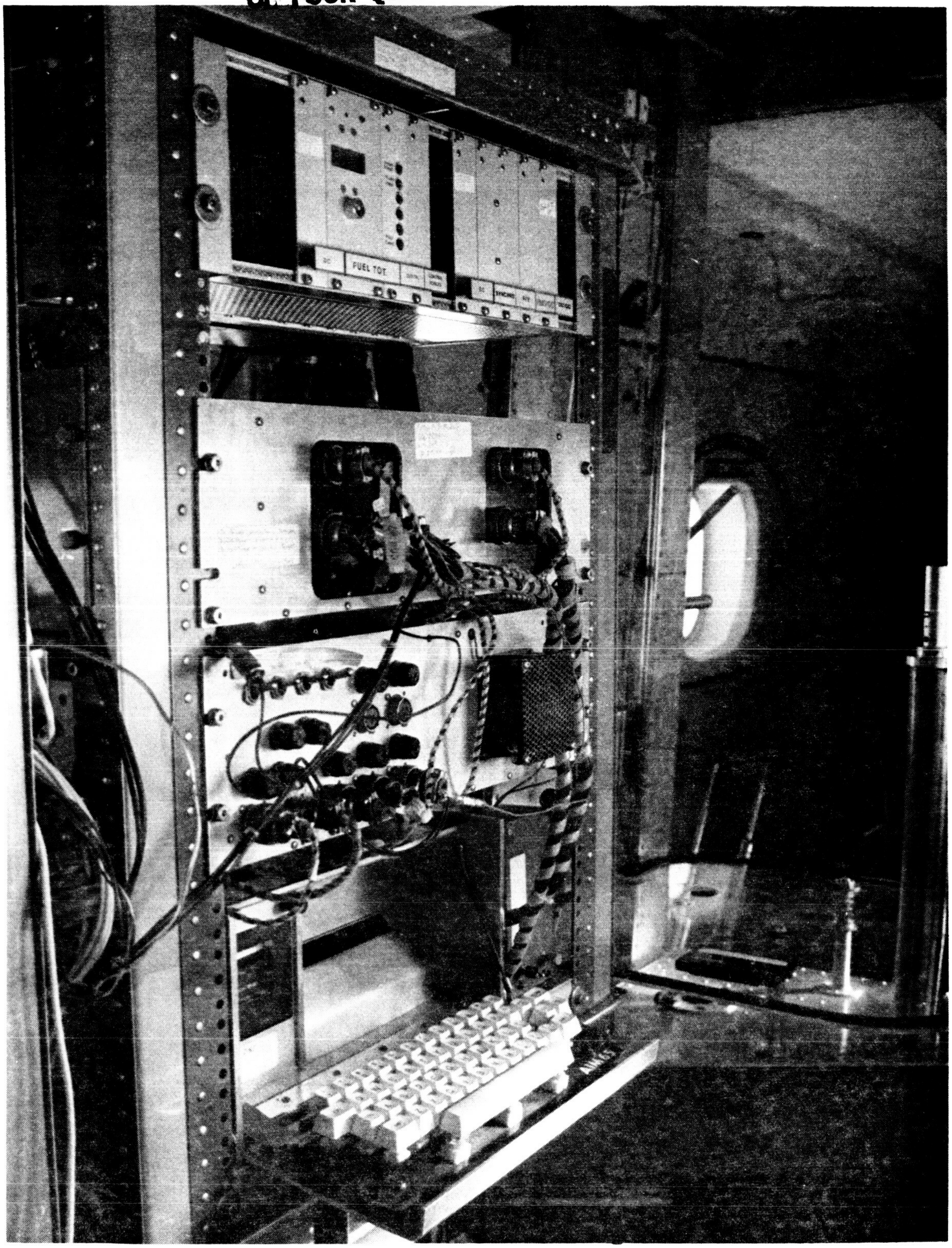

CALC		REVISED	DATE	KSR DATA ACQUISITION SYSTEM	Fig. 5.1.1
CHECK	J.L.J. 3/14/86				
APPD					PMC-6-004
APPD					
DRAWN				KOHLMAN SYSTEMS RESEARCH LAWRENCE KANSAS	5.1.5

THIS PAGE INTENTIONALLY LEFT BLANK

5.2. Special Sensors

Special sensors were installed on the test airplane as described in the following paragraphs.

5.2.1. Trailing Cone

To calibrate the airplane's airspeed system, a trailing cone was used to measure atmospheric pressure. The cone was trailed approximately 100 feet behind the airplane on a flexible tube which entered the aircraft through a metal tube connected to the aircraft at an opening created by removing the tail skid. A previous inflight inspection confirmed that the cone trailed well in all configurations. Static ports were located approximately 5 cone diameters forward of the cone where the pressure is uninfluenced by either the cone or the airplane. Cone static pressure was sensed by an independent pressure transducer. Calibration methods are described in Section 7.3.

5.2.2. Primary Control Force Measurement

KSR has developed a system to measure column, wheel, pedal, and toe brake forces. Elevator and aileron control forces are measured with the force wheel shown in Figure 5.2.1. Rudder and toe brake forces are measured with the pedal system shown in Figure 5.2.2.

ORIGINAL PAGE IS
OF POOR QUALITY

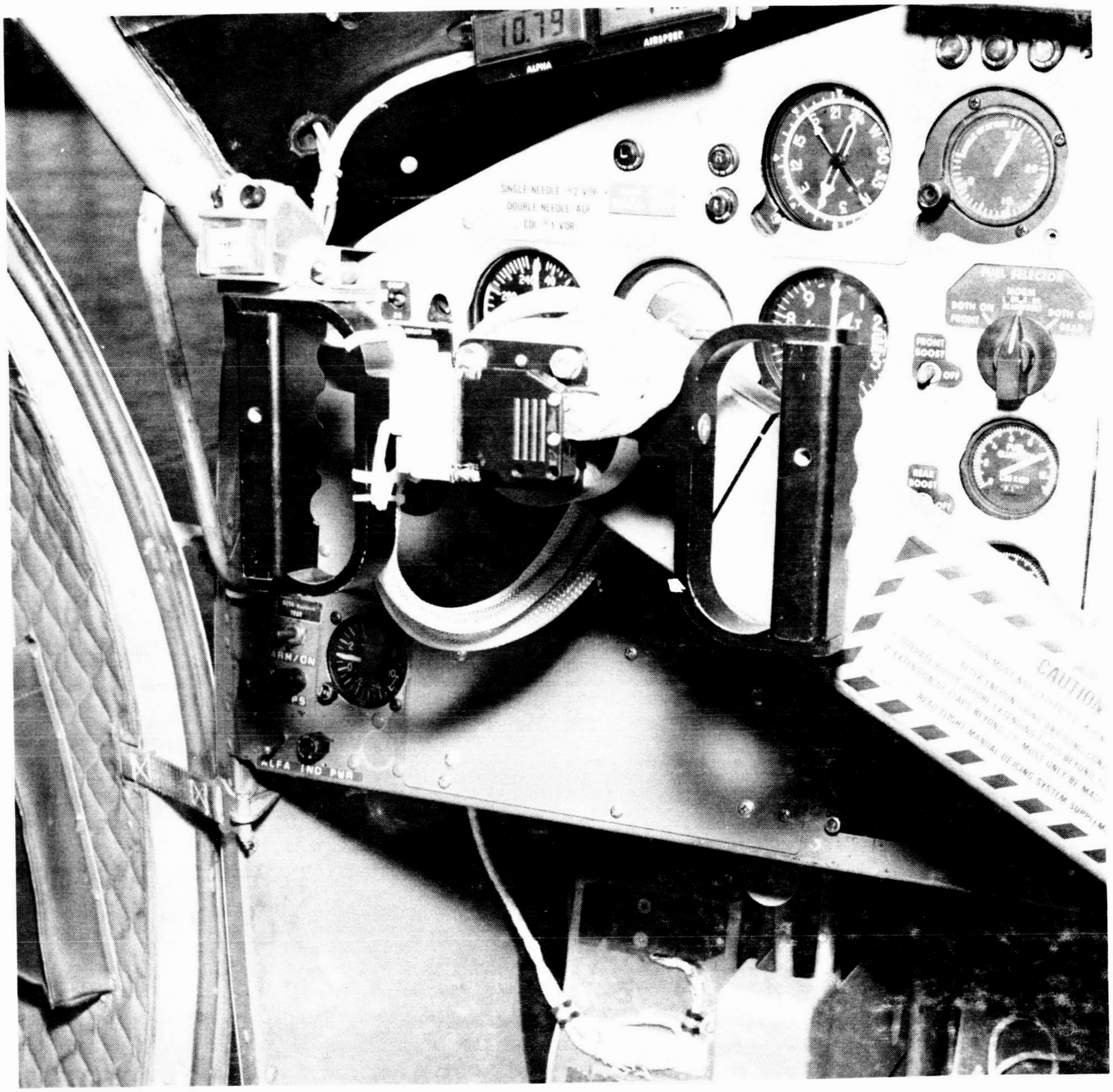

			REVISED	DATE
CALC				
CHECK	[signature]	3/14/86		
APPD				
APPD				
DRAWN				

KSP FORCE [illegible]

Fig. 5.2.1

[illegible]-6-004

KOHLMAN SYSTEMS RESEARCH
LAWRENCE KANSAS

5.2.2

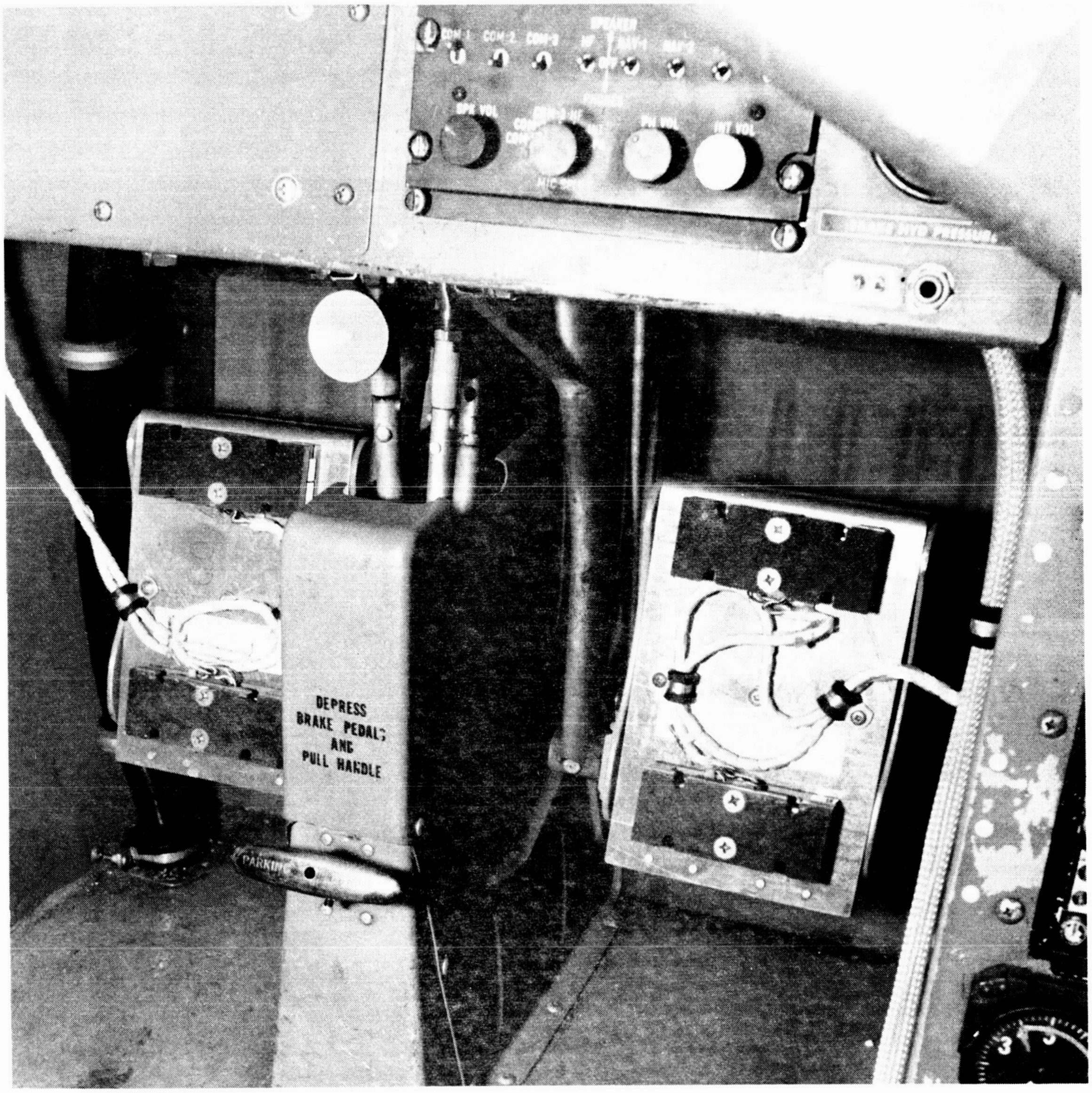

CALC		REVISED	DATE
CHECK	J.J. 3/14/86		
APPD			
APPD			
DRAWN			

KSR FORCE PEDALS

Fig.5.2.2

DHC-6-00?

KOHLMAN SYSTEMS RESEARCH
LAWRENCE KANSAS

5.2.3

5.2.3. Angle of Attack and Sideslip Sensors

A Rosemount Model 858AJ Type Flow Angle Sensor to measure angle of attack and sideslip was installed on the aircraft noseboom. The system consisted of five pressure ports; one located at most forward point and four others located to the left, right, above and below the forward port. The geometric layout of the system is illustrated in Figure 5.2.3. A change in angle of attack (alpha) or sideslip (beta) resulted in a change in differential pressure between the respective pressure ports. Calibration methods are described in Section 7.3.

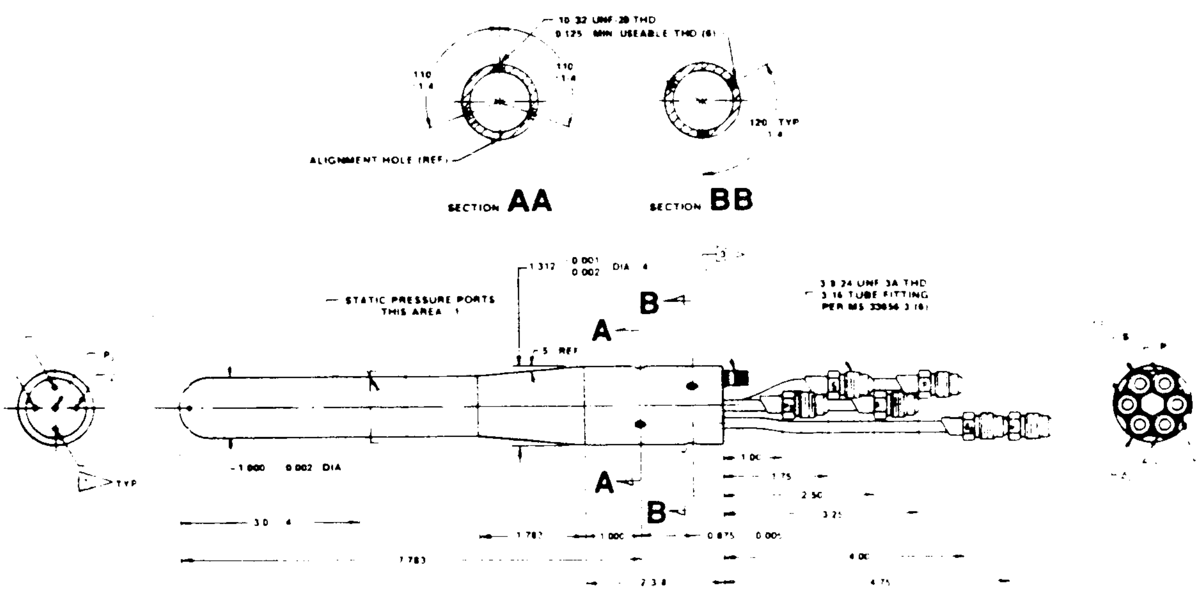

CALC			REVISED	DATE	ROSEMOUNT MODEL 858AJ TYPE FLOW ANGLE SENSOR	Fig.5.2.3
CHECK	[signature]	3/14/86				DHC-6-004
APPD						
APPD					KOHLMAN SYSTEMS RESEARCH. LAWRENCE KANSAS	5.2.5
DRAWN						

THIS PAGE INTENTIONALLY LEFT BLANK

5.3. Data Analysis

The data were processed on a Cadmus 9000 microcomputer and a Gould SEL 32/77 minicomputer both located at KSR in Lawrence, Kansas. A block diagram of the data management system is shown in Figures 5.3.1a and 5.1.3b. This data management system was designed to function with the KSR DAS.

The initial phase of the processing involved transferring the flight tapes to the Cadmus in a raw data format. The data are then converted to engineering units, and the air data are corrected for position error. Also computed are the weight and balance, inertias, linear accelerations at the center of gravity, corrections to alpha and beta due to angular rates and boom bending, thrust, and other parameters required for subsequent analysis programs.

The flight test data base was then transferred to the SEL where it is saved on magnetic tape for subsequent data analysis. The data analysis techniques are discussed in Section 7. The flight test data base was stored in unformatted, 200-word blocks (each word is 32 bits). Each block represents one time-slice of flight test data, and every measured or derived parameter occupies a specific word as listed in Table A.1 in Appendix A.

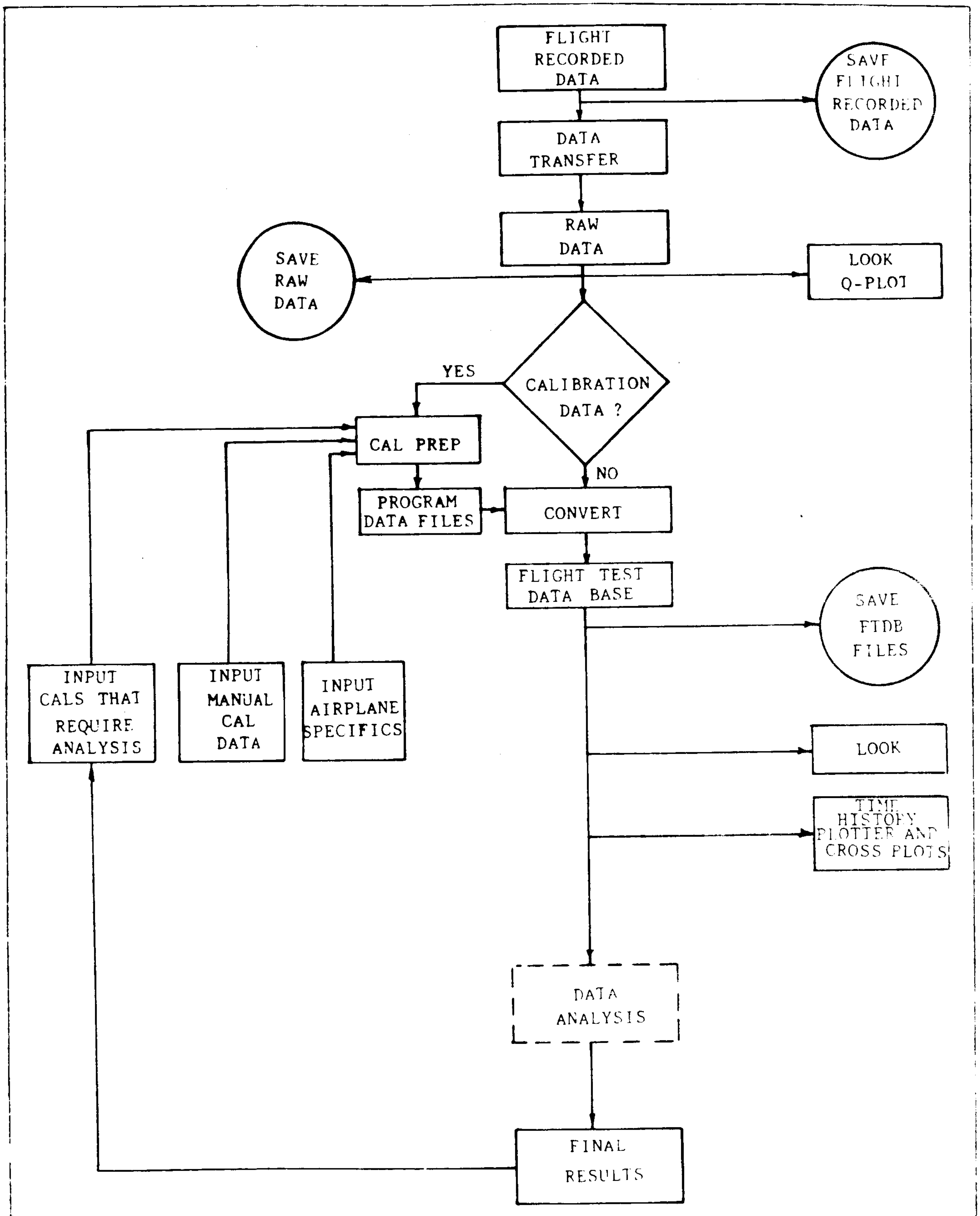

CALC	REVISED	DATE	KSR DATA MANAGEMENT SYSTEM - TRANSFER AND CALIBRATION	FIG. 5.3.1a
CHECK 3/11/86				DHC-6-004
APPD				
APPD			KOHLMAN SYSTEMS RESEARCH	5.3.2
DRAWN			LAWRENCE KANSAS	

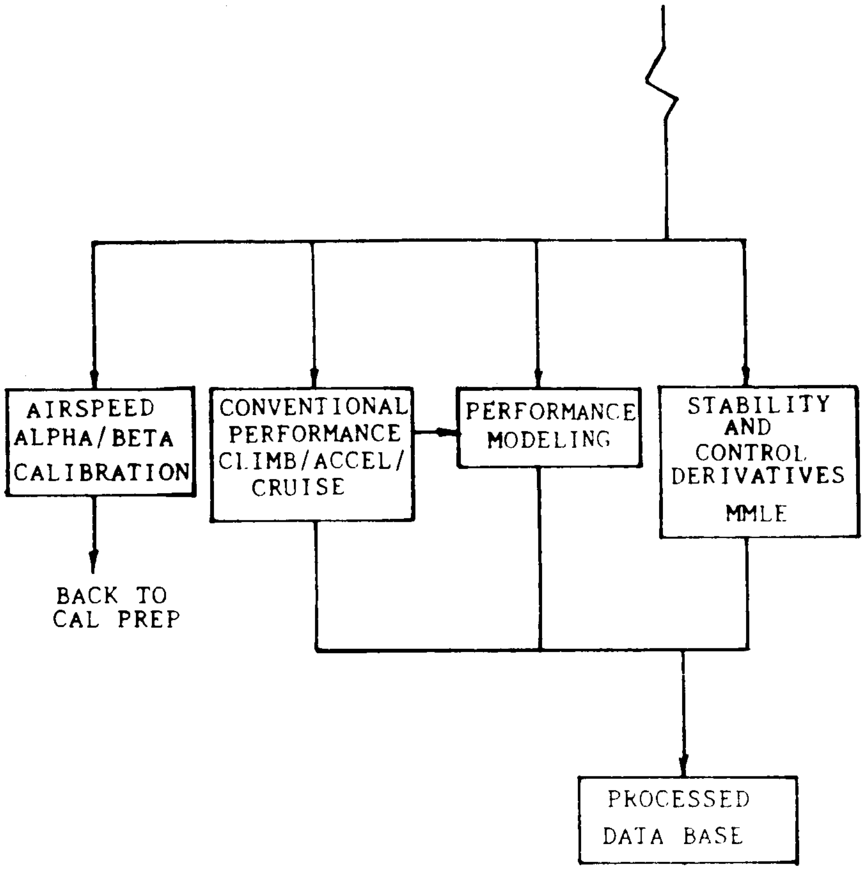

CHK: 3/14/86	REVISED / DATE	KSR DATA MANAGEMENT SYSTEM - DATA ANALYSIS	FIG. 5.3.1b
			DHC-6-004
		KOHLMAN SYSTEMS RESEARCH	5.3.3

THIS PAGE INTENTIONALLY LEFT BLANK

6. AXIS SYSTEM AND SIGN CONVENTIONS

The axis system and sign conventions used in this report are defined in Figures 6.1 and 6.2. Figure 6.1 shows the sign conventions used for body motion and Figure 6.2 shows the sign conventions for the control surface deflections. Rudder and aileron trim have the same conventions as rudder and aileron deflection. Positive control forces move pilot control positions in a positive direction.

PRECEDING PAGE BLANK NOT FILMED

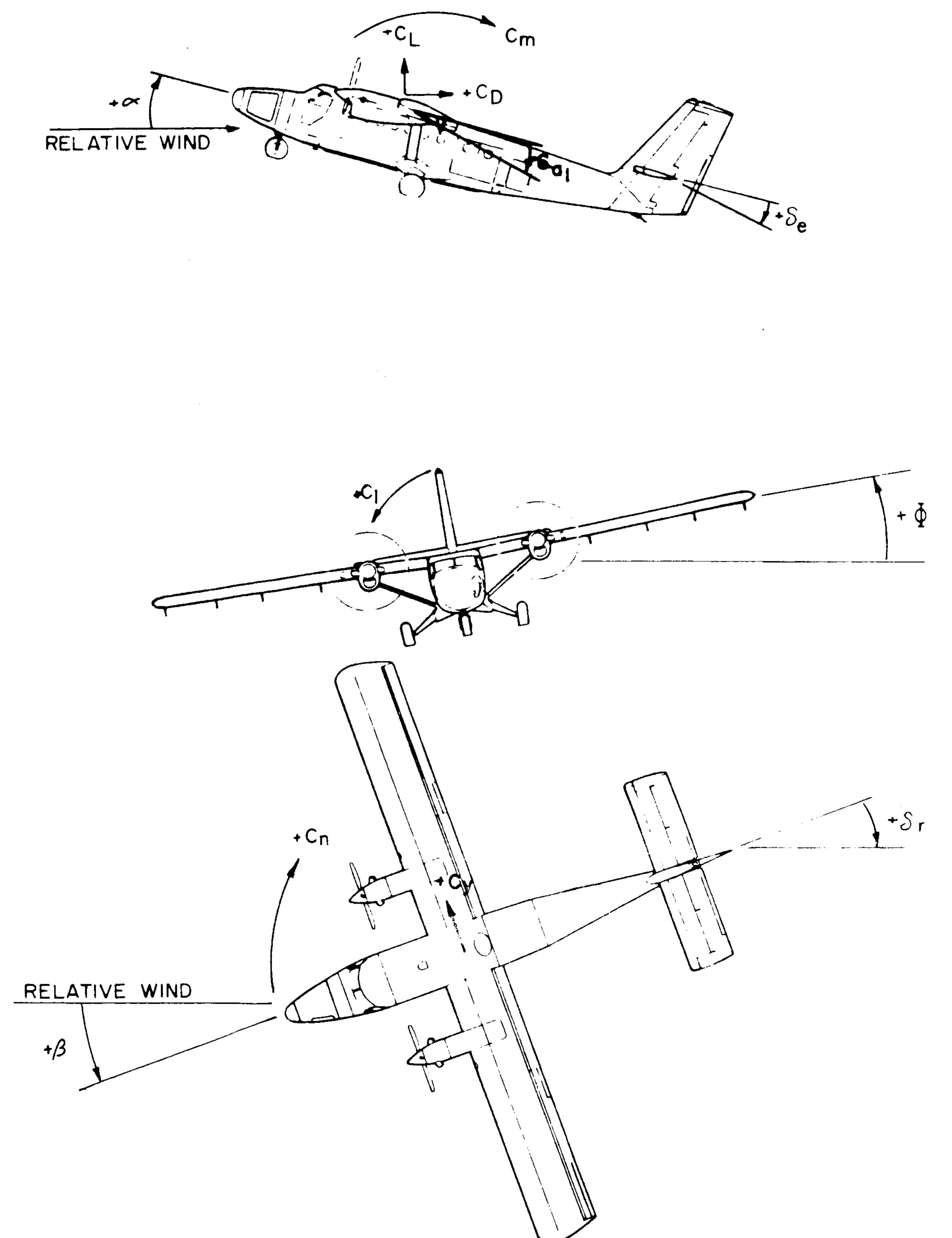

			REVISED	DATE		
CALC					AIRPLANE AXIS SYSTEM	Fig. 6.?
CHECK	J.J.G.	3/14/86				DHC-6-004
APPD						
APPD						
DRAWN					KOHLMAN SYSTEMS RESEARCH LAWRENCE KANSAS	6.2

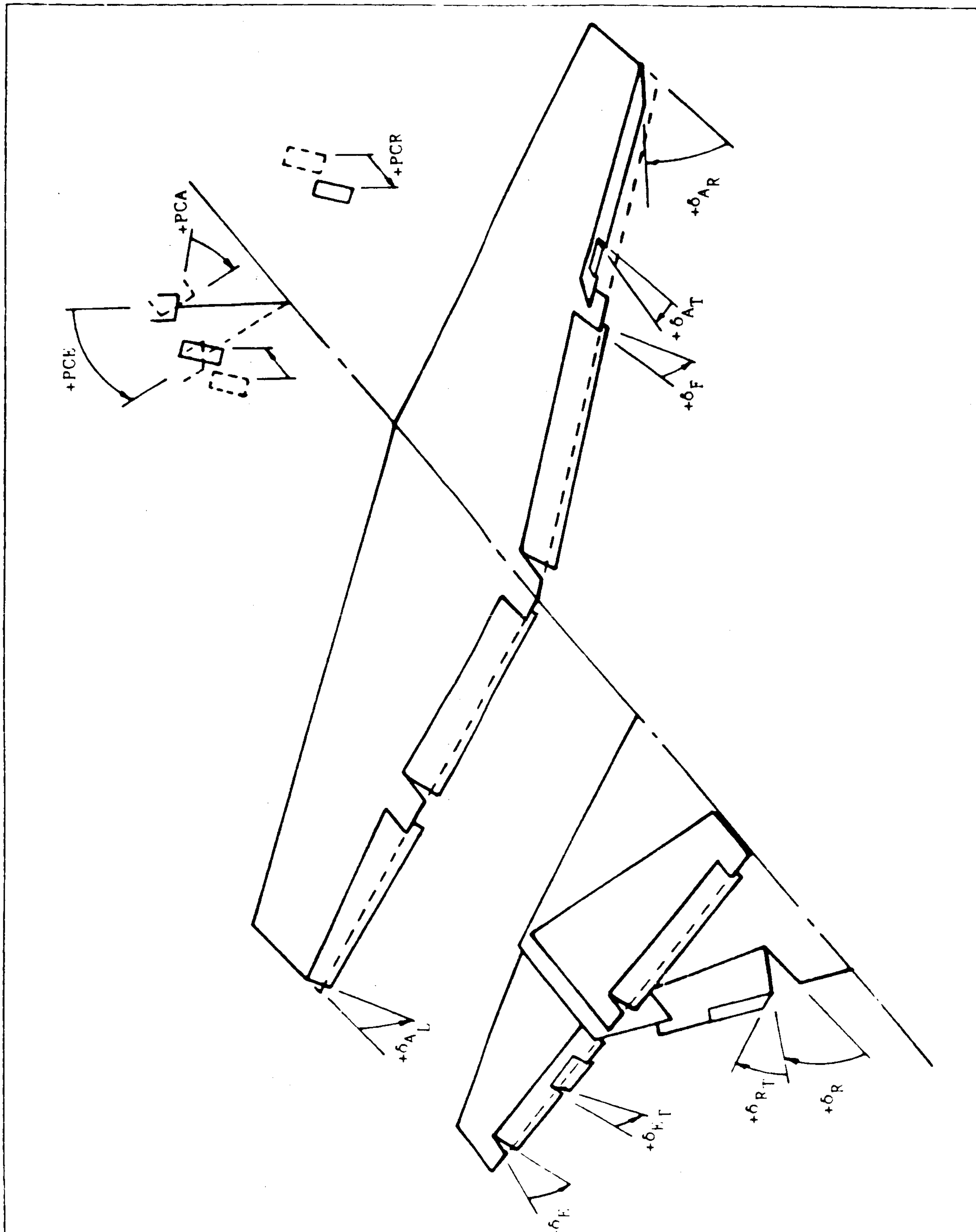

CALC		REVISED	DATE	CONTROL DEFLECTION SIGN CONVENTIONS
CHECK	CJJ 3/14/86			
APPD				
APPD				
DRAWN	2/14/85			KOHLMAN SYSTEMS RESEARCH LAWRENCE KANSAS

FIG. 6.2

DHC-6-004

THIS PAGE INTENTIONALLY LEFT BLANK

7. FLIGHT TEST ANALYSIS TECHNIQUES

This section gives a general outline of the various techniques used by Kohlman Systems Research to obtain the results presented in Section 8.

7.1. Stability and Control Derivative Methods

The primary method used to determine stability derivatives is the Modified Maximum Likelihood Estimation technique (MMLE).

The MMLE method is based on an assumed mathematical model of the airplane's aerodynamic and inertial characteristics. Initial conditions and dynamic control inputs measured in flight are applied to the model and the response of the model is compared to that of the airplane. The difference is a response error. The MMLE program then changes the aerodynamic derivatives by a computational algorithm to reduce the response error. The new derivatives are used in the math model to compute a new response error. This iteration procedure continues until a specified convergence criterion is met. The final derivatives represent airplane aerodynamic characteristics that maximize the likelihood that the error between airplane and mathematical model responses will be minimized.

ORIGINAL PAGE IS
OF POOR QUALITY

The accuracy and consistency of results obtained by MMLE methods are dependent on many different factors. First, the model must reasonably represent the airplane. Since the model is linear, any nonlinearities during a maneuver will affect the results. Good results achieved during relatively linear, small perturbation maneuvers will represent only local slopes.

It was found on the lowest speed flight test runs, buffet due to ice accretion caused the MMLE analysis to converge poorly or not at all. Therefore, in general, the lowest speed data points for all configurations were not included in the analysis.

Since the MMLE program will attempt to match whatever actual response is presented to it, it is important to minimize the sources of error in the recorded data. Air turbulence can be minimized by doing tests only when the air is smooth. Data system noise minimization requires a data system having a very high signal to noise ratio. Bias errors in calibration curves used to produce the data do not affect the analysis. However changes in sensitivity or slope of the calibration curves do. Time skews, caused by sampling between channels at too slow a rate, produce subtle errors that can go undetected. Great care has been taken to eliminate these problems.

The final non-dimensional derivatives obtained from MMLE are dependent on the initial conditions of the maneuver (airspeed and altitude) and the airplane weight and moments of inertia. The MMLE program will attempt to correct any errors in these parameters by adjusting the derivatives. For example, if the roll inertia is calculated to be higher than it actually is, the MMLE derived roll power $C_{\ell_{\delta_a}}$ will be higher than it actually is. This illustrates the importance of obtaining accurate airspeed calibrations, weight and inertia data, and accurate calibration of the data acquisition system.

An illustration of the ability of the MMLE program to match the model response to the airplane response is provided in Figure 7.1.1 which presents time histories for an elevator doublet. The quality of these matches provide confidence in the accuracy of the derived stability derivatives. However, these results are collected for many runs over a wide range of flight conditions, thus some judgement is involved in arriving at the stability derivative curves.

Careful interpretation was required for each data point produced by MMLE. Important characteristics included the level of excitation of particular parameters, the quality of the time history match provided by the MMLE program, and the nature of the dynamic maneuver. Full documentation of each individual MMLE data point is available for inspection and further interpretation as required.

The MMLE results, combined with theoretical aerodynamics and judgements on the quality of individual maneuvers, were used to form derivative curves that are believed to represent the airplane as accurately as possible.

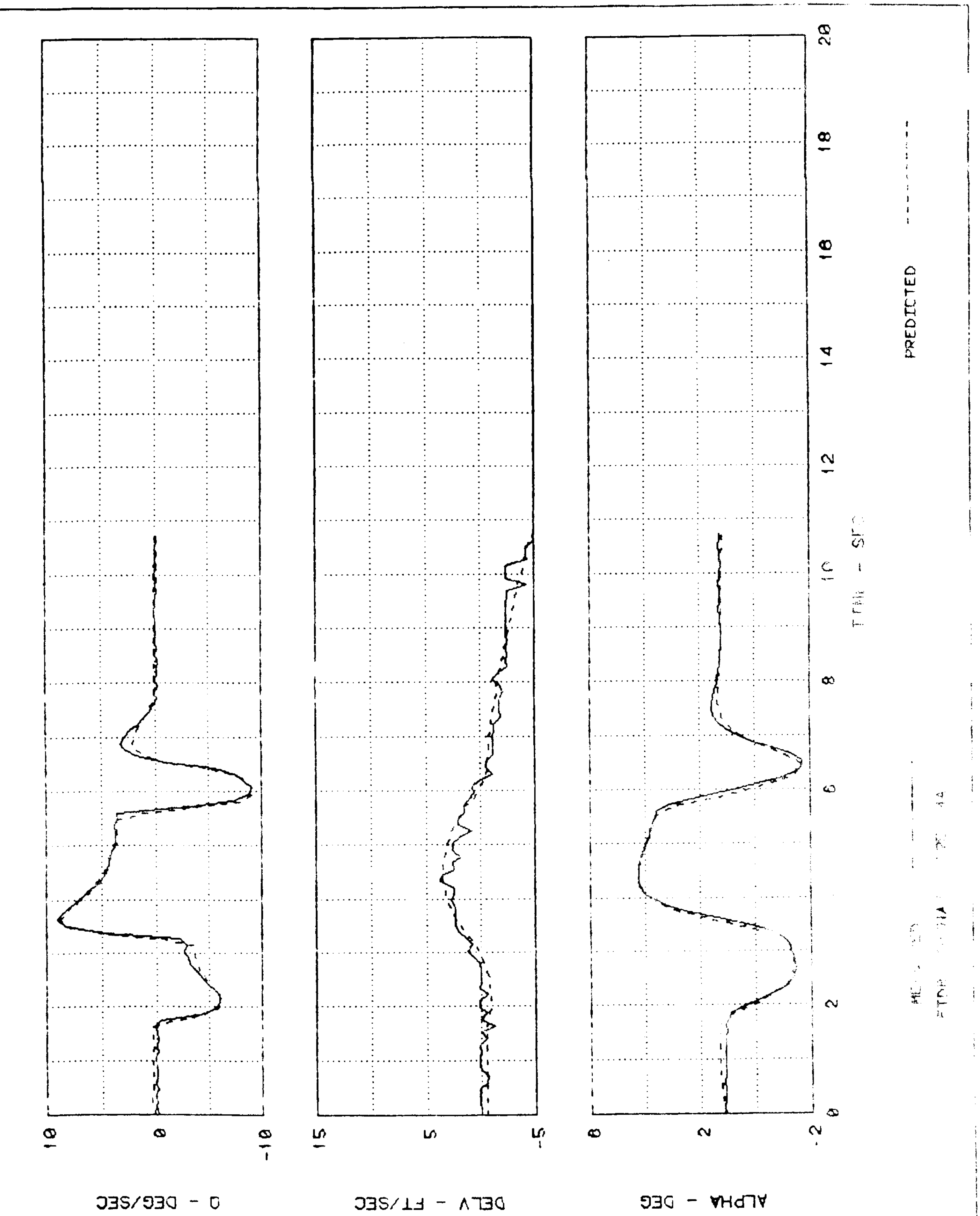

CALC		03/04/86	REVISED	DATE	TEST DATA AND MMLE MATCH FOR LONGITUDINAL DOUBLET (FLAPS 0)	Fig. 7.1.1a
CHECK	J.G.J.	3/14/86				DHC-6-004
APPD						
APPD					KOHLMAN SYSTEMS RESEARCH	7.1.4
TIME	14:56:24					

7.2. Performance Modeling Methods

Performance modeling is a technique developed by KSR through which a complete model of the propulsion system and the static longitudinal aerodynamic coefficients of the airplane are defined. This is done by performing a series of level flight full and partial power accelerations over the flight envelope.

The first step in performance modeling is to define a propulsion system model from the engine deck provided by the engine manufacturer and the propeller characteristics from the propeller manufacturer. The net jet thrust calculated from the deck is used directly, while inflight measured torque and propeller rpm are used to calculate shaft horsepower.

Once the propulsion model is defined, the aerodynamic lift and drag models are determined in terms of:

a) $C_{L_{A/C}}$ vs. α

b) C_D vs. $C_{L_{A/C}}^2$

c) $C_{m_{untrimmed}}$ vs. α

The forces and moments pertinent to the steady state analysis are shown in Figure 7.2.1. The airplane lift coefficient is generated with the following equations.

$$C_{L_{A/C}} = [\, W \cdot n_{z_{wind}} - F_P \sin(\alpha + \lambda_P) - F_J \sin(\alpha + \lambda_J) \,]/\bar{q}S$$

where: $C_{L_{untrimmed}} = C_{L_{A/C}} - C_{L_{\delta_e}} \delta_e$

$C_{L_{\delta_e}}$ from MMLE data reduction

λ_P propeller inclination angle

λ_J jet exhaust inclination angle

F_J net jet thrust

The airplane trim drag $C_{D_{\delta_e}}$ cannot be determined from the maneuvers performed. Therefore a trimmed drag coefficient is generated from:

$$C_D = [F_P \cos(\alpha + \lambda_P) + F_J \cos(\alpha + \lambda_J) - W \cdot n_{x_{wind}} \,]/\bar{q}S$$

Untrimmed (δ_e = 0) pitching moment coefficient data were also derived from the performance maneuvers. The governing equations are:

$$C_{m_{untrimmed}} = C_{L_{unt}} \Delta\bar{X} - C_{m_{\delta_e}} \delta_e - C_{m_T} - C_D \Delta\bar{Z}$$

where: $\Delta\bar{X} = (X_{cg_{std}} - X_{cg_{tst}})$

$$\Delta\bar{Z} = (Z_{cg_{std}} - Z_{cg_{tst}})$$

$$C_{m_T} = \frac{-(F_J Z_{T_J} + F_P Z_{T_P})}{\bar{q} S \bar{c}}$$

$C_{m_{\delta_e}}$ and $C_{L_{\delta_e}}$, are predicted from MMLE. Z_{T_P} and Z_{T_J} are a function of airplane geometry and c.g. position.

A summary of the performance flight tests is presented in Table 7.2.1. These tests consist of a series of accelerations and decelerations at selected torque settings and weight-pressure ratios (W/δ).

The various airplane configurations evaluated during these maneuvers are listed below:

CONFIGURATION	FLAPS	GEAR
Cruise	0	Down
Approach	10	Down
Approach	20	Down
Takeoff	0	Down
Takeoff	10	Down
Landing	37.5	Down

At the time the data was being analyzed, it was felt that the KSR torque readings were in error when compared to values recorded in previous flight test by NASA. The evidence of this effect was most noticeable in the drag polar. After much discussion it was decided to adjust the torque readings so that the KSR drag polar matched the NASA drag polar shown in the NASA report given at the AIAA 23rd Aerospace Sciences Meeting (paper number AIAA-85-0468). To match this drag polar 45 foot-pounds of torque was subtracted from the recorded torque value of each engine. The flight test data base mag tapes that were made for NASA do not have this adjustment made for the engine torque so that the user could make any changes as deemed necessary.

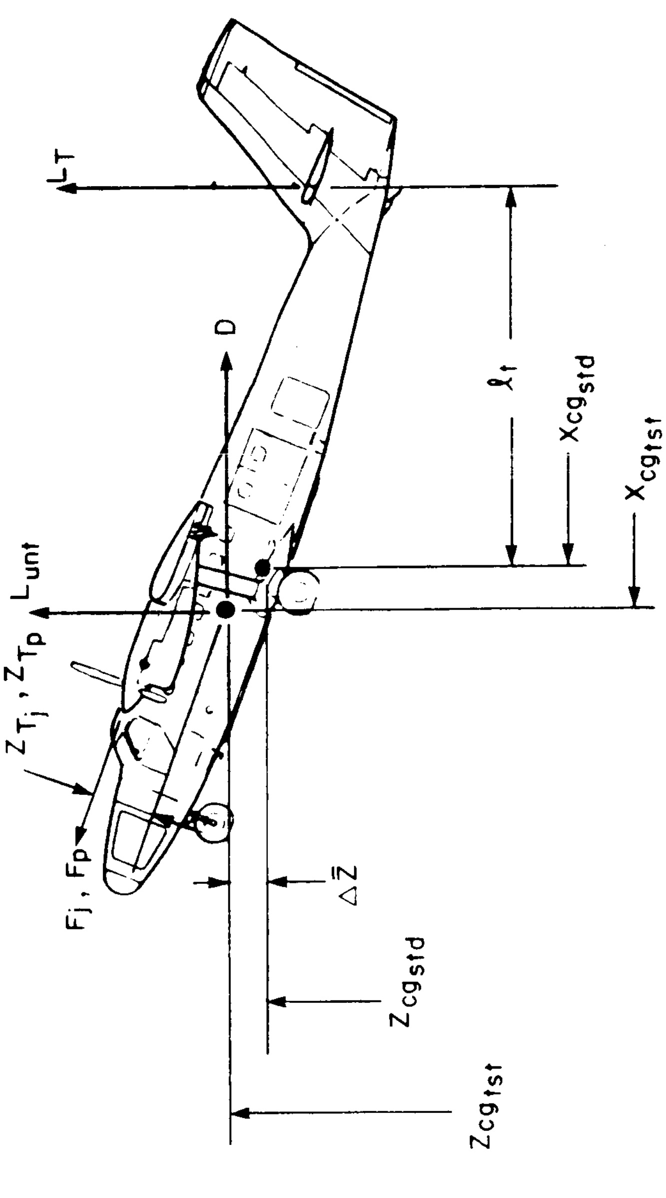

			REVISED	DATE		
CALC					FORCES AND MOMENTS USED FOR PERFORMANCE ANALYSIS	Fig. 7.2.?
CHECK	C.Y.J.	3/14/86				DHC-6-004
APPD						
APPD						
DRAWN					KOHLMAN SYSTEMS RESEARCH - LAWRENCE KANSAS	7.2.5

TABLE 7.2.1

PERFORMANCE FLIGHT TEST SUMMARY

FLIGHT	CONFIGURATION	TESTS
6	Cruise, δ_F = 10, 20, 37.5 (DRY AIR)	13K W/δ
8	Cruise (ICE)	13K W/δ
19	Cruise (ICE)	13K W/δ
21	Cruise (ICE)	13K W/δ
22	Cruise (ICE)	13K W/δ
24	Cruise, δ_F = 10, 20, 37.5 (DRY AIR)	13K W/δ

7.3. Air Data Calibration Techniques

This section presents the techniques used to calibrate the air data measurement system. The static pressure system is corrected for static port position error. The delta-p alpha and beta systems are calibrated directly to degrees, which includes correction for upwash and sidewash.

Angle of attack and sideslip data were measured using a differential pressure system mounted on the nose boom of the airplane. The sensors used are detailed in Section 5.2, 'Special Sensors'.

7.3.1. Airspeed Calibration

The boom mounted forward of the nose of the aircraft contained static pressure ports located several diameters aft on the cylindrical shaft of the Rosemount Flow Angle Sensor. The ship's standard system (co-pilot's) pitot probe located on the right side of the aircraft nose was also utilized.

The airspeed calibration used a trailing cone extending more than one fuselage length behind the airplane in undisturbed air. A static pressure port located on the tube leading to the cone, well forward (at least 5 cone diameters) of the cone, was used to determine the true ambient pressure. The ambient pressure was compared to the indicated static pressure measured on the boom to determine the position error.

The airplane was stabilized at selected speeds and altitudes. Data were taken under stabilized conditions to prevent pneumatic lag from influencing the measurements. These data were analyzed using standard methods contained in Reference 4 and are presented in Figure 7.3.1.

ORIGI... OF POOR QUALITY

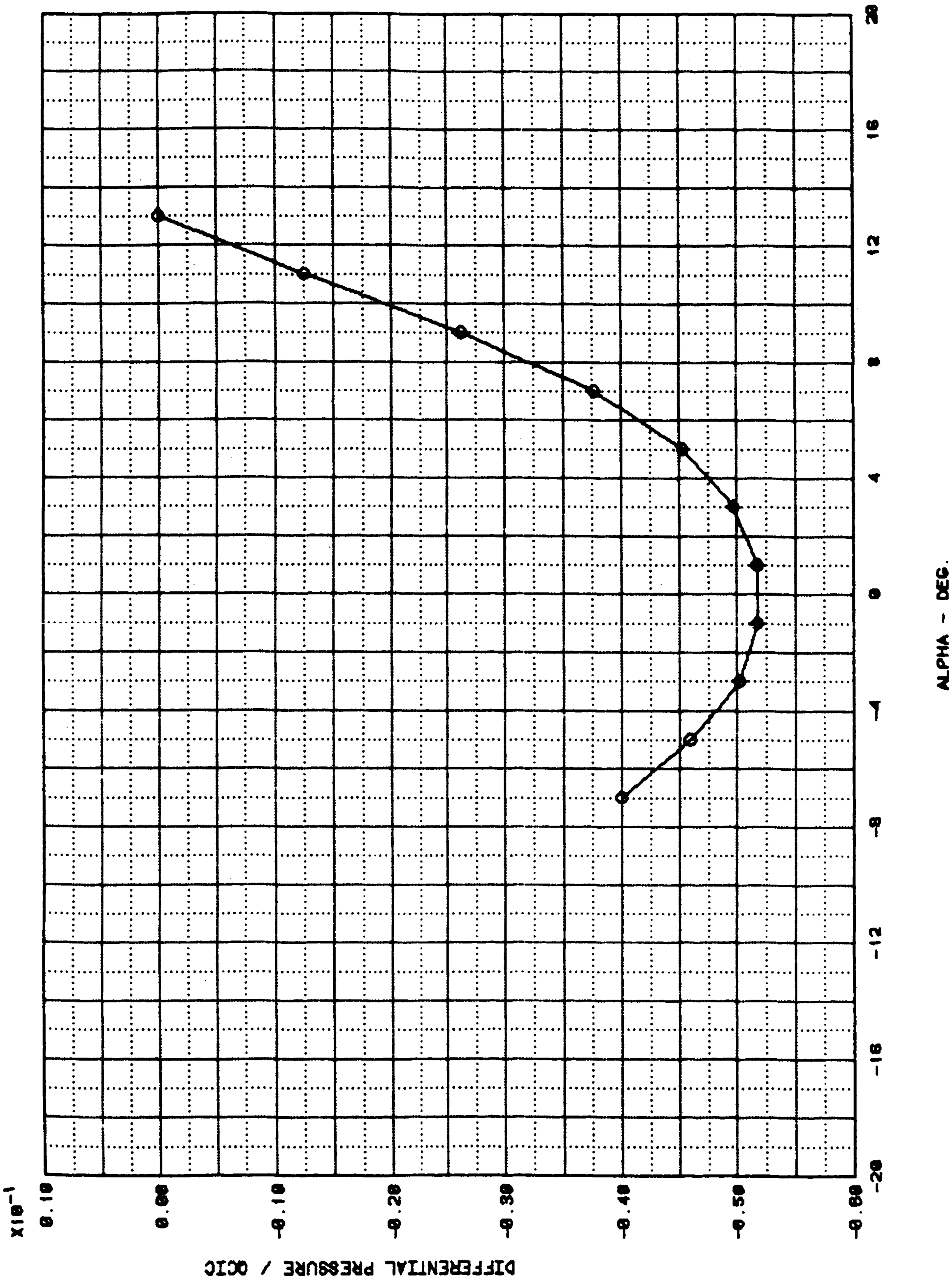

CALC		03/08/86	REVISED	DATE	POSITION CORRECTION	Fig. 7.3.1
CHECK	J.G.J.	3/14/86				
APPD					DE HAVILLAND TWIN OTTER	DHC-6-004
APPD	JLJ					
TIME	15:30:47				KOHLMAN SYSTEMS RESEARCH	7.3.3

7.3.2. Angle of Attack and Sideslip Calibration

The angle of attack and sideslip were measured using a Rosemount 858AJ probe (see Section 5.2). The 858AJ is supplied with a manufacturer calibration. These calibrations were used following a process of validation using actual flight test data.

The angle of attack calibration was verified by the analysis of stable points. With the aircraft stabilized at a constant altitude and airspeed the angle of attack is equal to the inverse tangent of the ratio of the longitudinal and normal body axis accelerations. The Rosemount calibration was verified using this method to validate its use during this flight test program.

The validation process was repeated on the angle of side-slip calibration using the dynamic calibration techniques described in Reference 6. This method involves the analysis of rudder doublets and compares the measured sideslip angle to a sideslip angle calculated from the inertial data. In addition to the validation of the Rosemount calibration this analysis procedure also facilitated the investigation of dynamic lag in sideslip measuring system. This lag was found to be insignificant for the flight conditions experienced in this flight program. The calibrations for angle of attack and sideslip are shown in Figures 7.3.2 and 7.3.3.

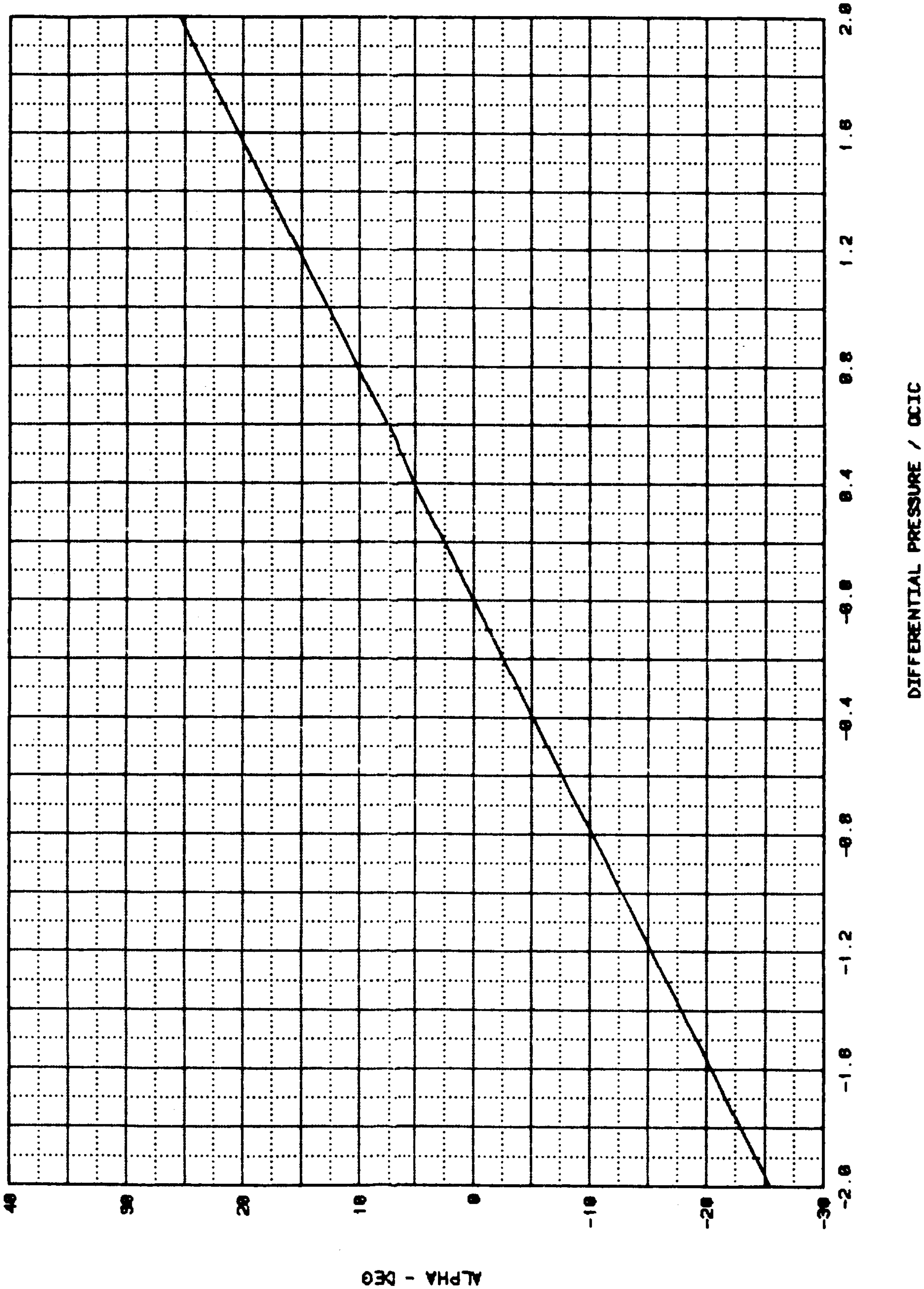

CALC		03/04/86	REVISED	DATE	ROSEMOUNT PROBE ALPHA CAL	Fig. 7.3.2
CHECK	J.L.J.	3/14/86				
APPD					DE HAVILLAND TWIN OTTER	DHC-6-004
APPD	JLJ					
TIME	10:30:48				KOHLMAN SYSTEMS RESEARCH	7.3.5

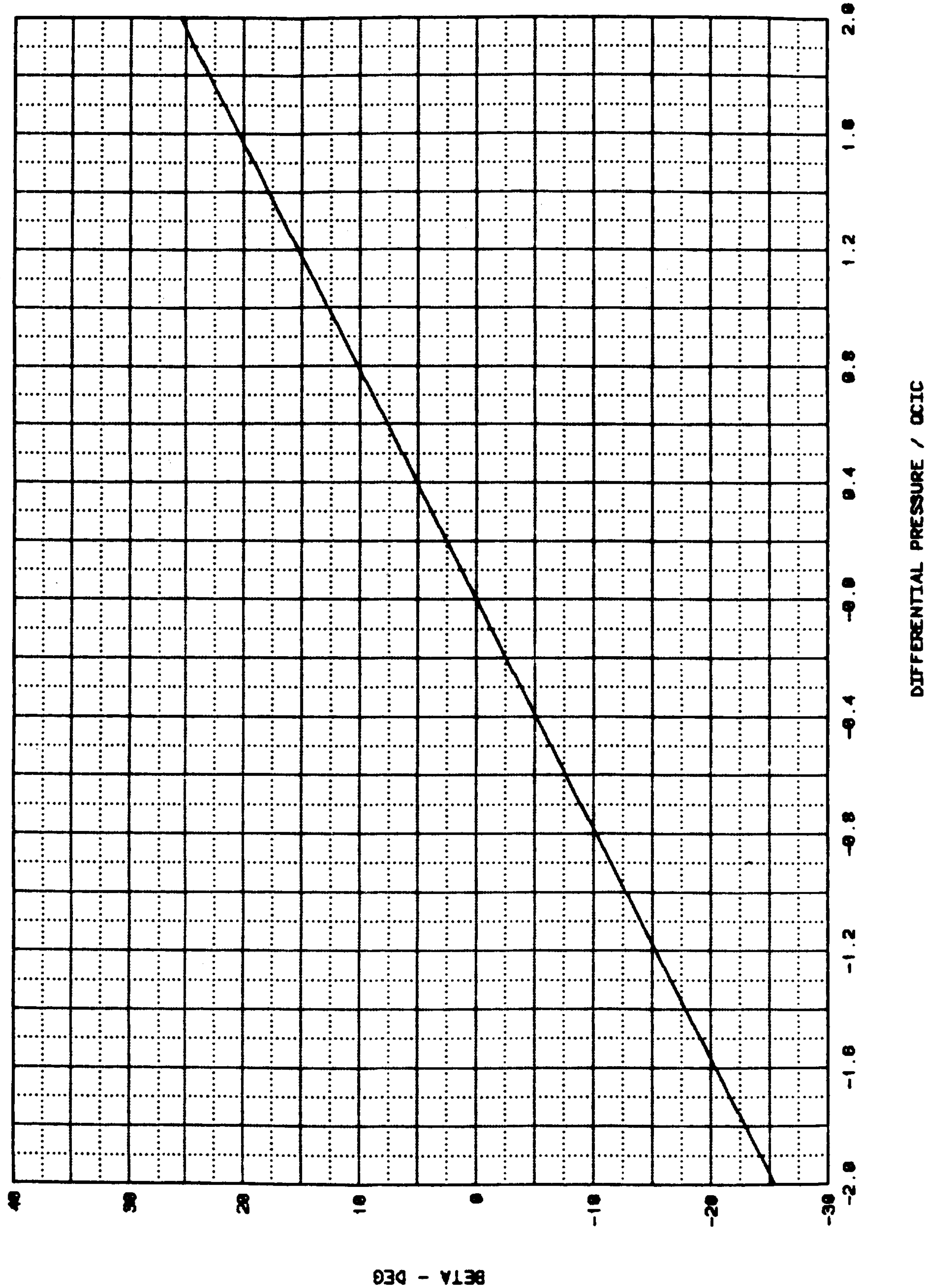

CALC		03/04/86	REVISED	DATE	ROSEMOUNT PROBE BETA CAL	Fig. 7.3.3
CHECK	3/14/86	JLJ				
APPD					DE HAVILLAND TWIN OTTER	DHC-6-004
APPD	JLJ					
TIME	10:30:22				KOHLMAN SYSTEMS RESEARCH	7.3.6

An additional boom bending calibration was performed to correct for errors caused by bending due to dynamic maneuvers. The calibration shown in Figure 7.3.4 was accomplished by loading the boom to represent the load experienced in dynamic maneuvers and then measuring the deflection of the boom. Since the boom is symmetrical in both axes, the beta boom bending correction shown in Figure 7.3.5 was derived from the alpha boom bending.

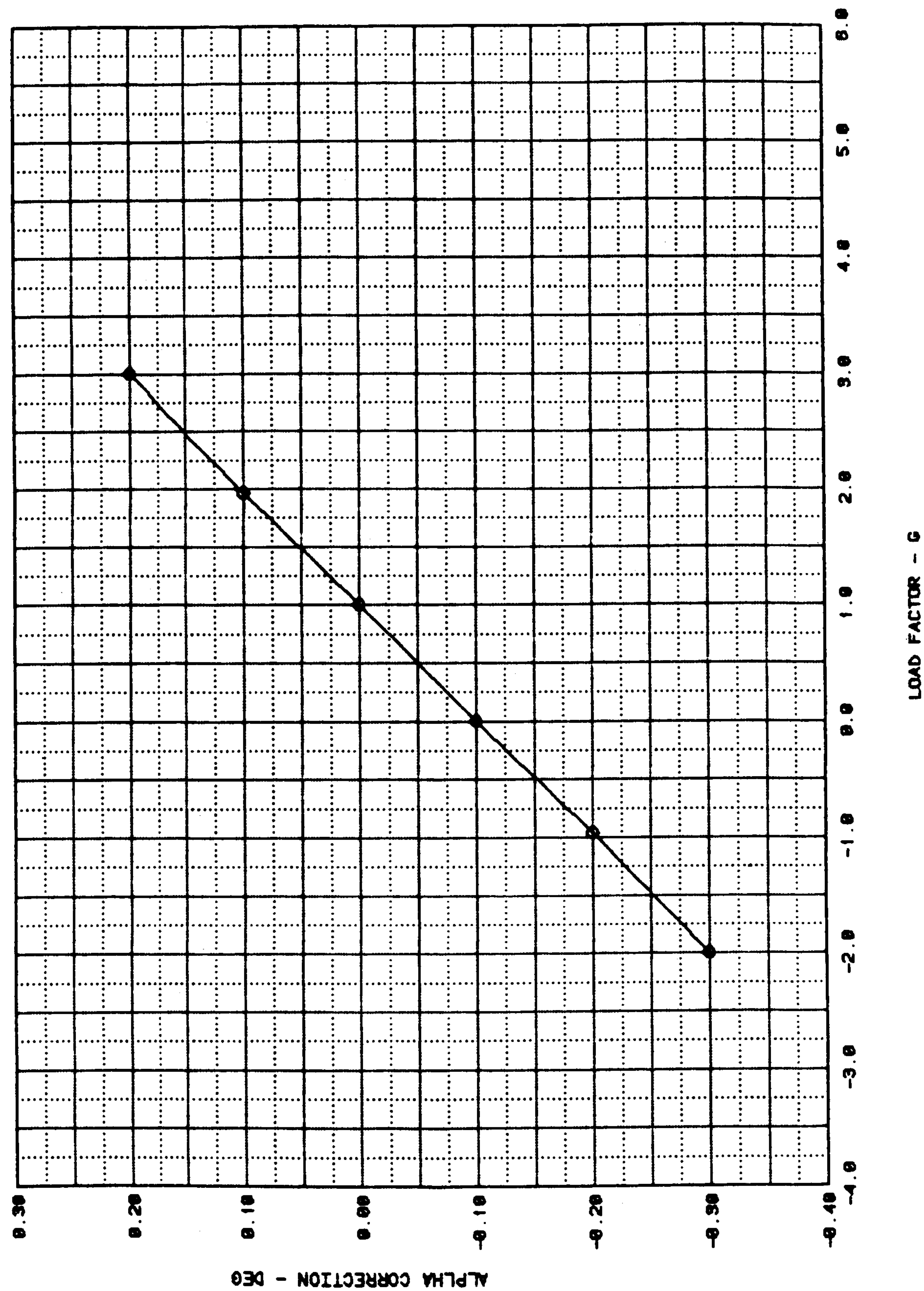

CALC		03/04/86	REVISED	DATE	ALPHA BOOM BENDING CORR.	Fig. 7.3.4
CHECK	JLJ	3/14/86				
APPD					DE HAVILLAND TWIN OTTER	DHC-6-004
APPD	JLJ					
TIME	10:08:27				KOHLMAN SYSTEMS RESEARCH	7.3.8

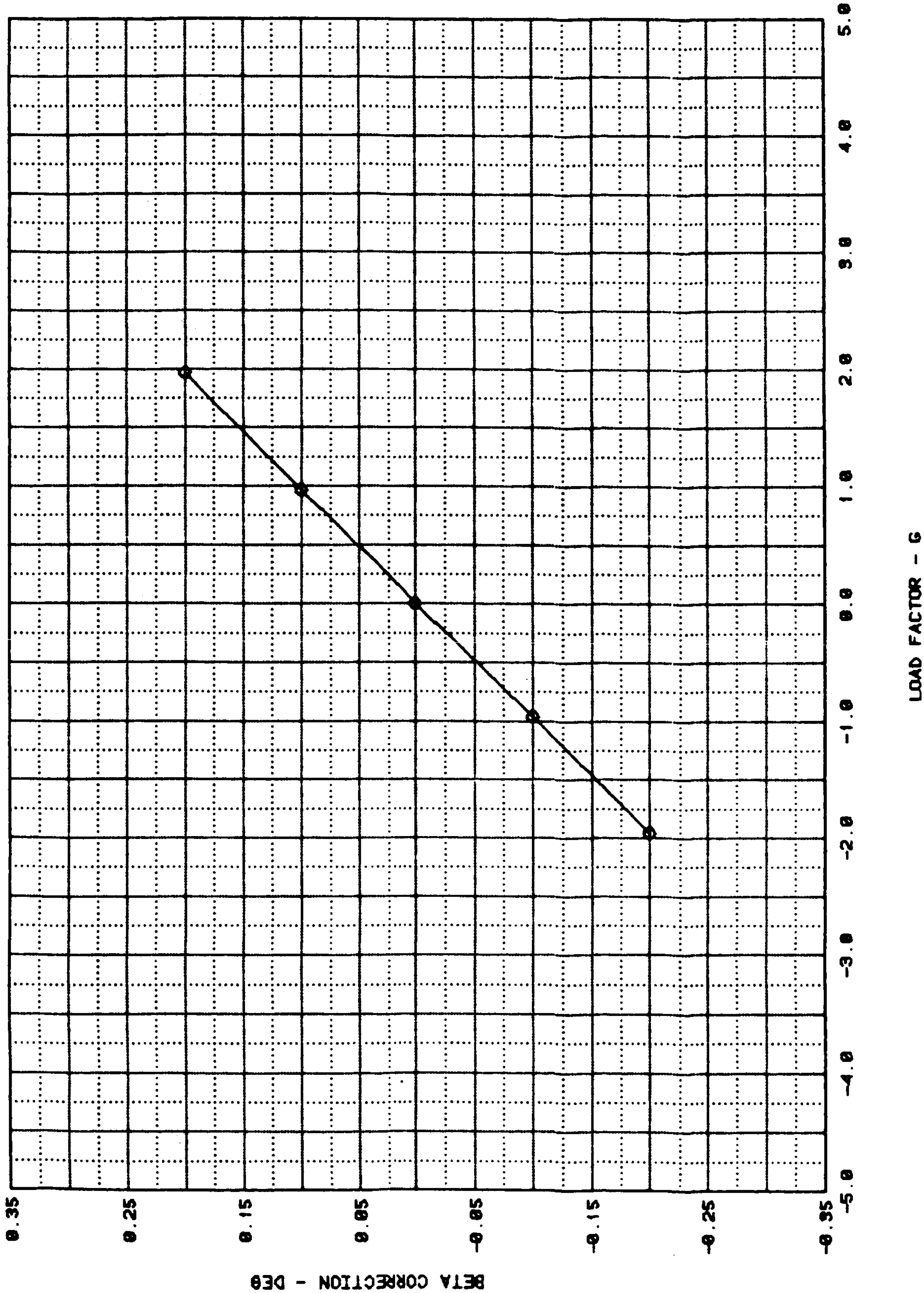

CALC		03/04/86	REVISED	DATE	BETA BOOM BENDING CORR.	Fig. 7.3.5
CHECK		3/14/86				
APPD					DE HAVILLAND TWIN OTTER	DHC-6-004
APPD	JLJ				KOHLMAN SYSTEMS RESEARCH	7.3.9
TIME	10:15:31					

THIS PAGE INTENTIONALLY LEFT BLANK

8. RESULTS OF FLIGHT TEST

This section contains the results of all analyzed flight test data. This includes stability and control, performance, and special tests and calibrations.

All flight test data in this report assume a center of gravity position of 26% MAC. Standard transformations can be used for other c.g. positions. The coefficients and derivatives in this report are based on the stability axis system.

Flights 20 and 21 were selected for performance analysis. Flight 20 represented a moderate to heavy mixed icing condition and 21 represented a moderate glaze icing condition. Flights 16 and 17 represented mixed icing conditions and were used to analyze the longitudinal stability. Flight 16 compared between the baseline and all iced, and then baseline and wing only iced. Flight 17 compared the baseline with all iced, and then the baseline with the tail only iced. Flight 23 represented rime ice conditions and provided an analysis of the directional derivative ratio $C_{h_{\delta_r}} / C_{h_\beta}$ for the baseline the vertical tail iced configuration. Icing cloud data by NASA during natural icing test is shown in Table 8.1.

8.1. Longitudinal Coefficients and Derivatives

The longitudinal derivatives and coefficients are in subsections representing lift, drag, and pitching moment.

8.1.1. Lift Coefficient, CL

The lift decrements that were broken out by selectively deicing the aircraft, remain relatively the same percentage-wise at both high and low power settings. The total degradation in lift coefficient at 6 degree angle of attack is approximately 7% with 40 psi torque and 8% with 15 psi torque. The individual contributions of each iced component are nearly the same at both power settings.

The elevator effectiveness, $C_{L_{\delta_e}}$ with the aircraft in the all-iced configuration showed an average 10% degradation. When the tail only was iced this degradation averaged around 8.5%, and when the wing only was iced a 2% degradation was found. When flaps were lowered to 10 degrees the all-iced degradation in these coefficients increased to 15-16% and the wing ice accounted for approximately 9% or nearly equivalent in magnitude to the tail ice contribution.

It was found that the state coefficient $(C_{L_q} + C_{L_{\dot{\alpha}}})$ showed no change due to ice in the flaps-up case, however, when the flaps were lowered 10 degrees and there was ice on the wings, tail, or both, this coefficient was degraded approximately 23 percent.

TABLE 8.1

SUMMARY OF AVERAGED ICING CLOUD DATA FOR PERFORMANCE AND STABILITY AND CONTROL

Flt No.	Start Time	End Time	Alt., PA, ft	TAS, Kts	AOA, deg	Static Temp °C	Dew Point °C	Average LWC $g \cdot m^{-3}$	Avg MVD μm
16	14:32:58	15:12:18	8060	138.6	1.4	-8.0	----	0.25	19
17	10:08:28	10:27:18	7309	135.0	1.6	-7.2	-8.1	.33	21
20	12:42:48	13:36:58	6163	127.3	1.8	-9.5	-10.1	.46	14
21	09:55:38	10:40:38	4315	130.8	1.6	-5.0	-4.8	-.20	15
23	10:13:38	11:11:48	4330	136.4	0.5	-10.7	-10.0	.33	10

THIS PAGE INTENTIONALLY LEFT BLANK

The aerodynamic lift force coefficients investigated for the NASA Twin Otter are presented below. The lines designated as "baseline" represent the dry air baseline testing. The iced configurations are defined using the letters E thru J, with multiple designations for a given curve indicating that there was no discernable difference between results for the different configurations.

Letter Code	Aircraft Configuration
E	Cruise configuration, aircraft all iced
F	Cruise configuration, aircraft complete tail and struts iced
G	Cruise configuration, aircraft vertical tail and struts iced
H	Cruise configuration, aircraft horizontal tail and struts iced
I	Cruise configuration, aircraft struts iced
J	Cruise configuration, residual ice only

	Figure #
$C_{L_{A/C}}$	8.1.1a - 8.1.1d
$(C_{L_q} + C_{L_{\dot{\alpha}}})$	8.1.2a - 8.1.2b
$C_{L_{\delta_e}}$	8.1.3a - 8.1.3d

PRECEDING PAGE BLANK NOT FILMED

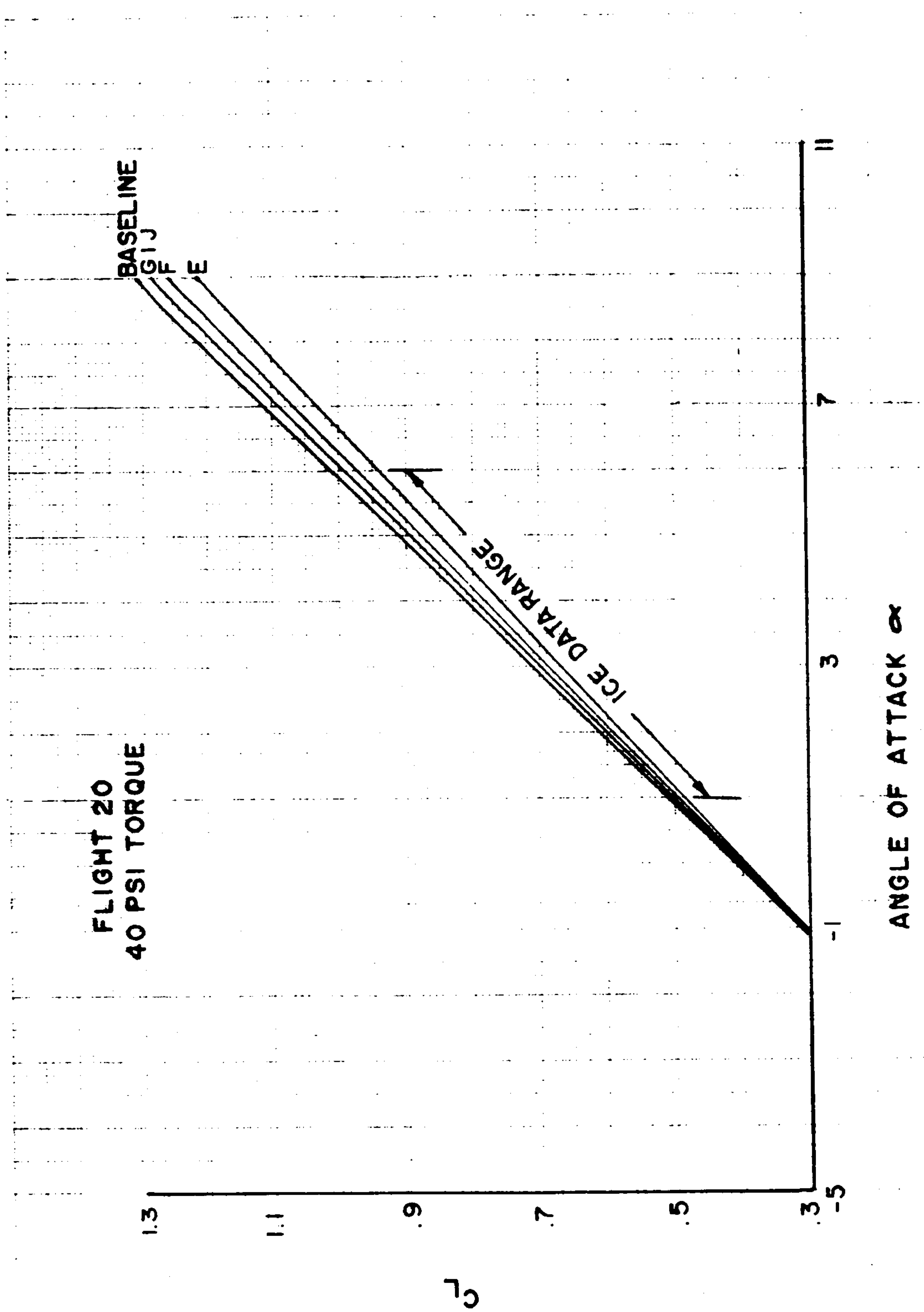

			REVISED	DATE		
CALC					CHANGE IN AIRCRAFT LIFT DUE TO ICE, TORQUE 40 PSI, FLIGHT 20	Fig. 8.1.1a
CHECK	JLJ	3/14/86				DHC-6-004
APPD						
APPD					KOHLMAN SYSTEMS RESEARCH - LAWRENCE KANSAS	8.1.4
DRAWN	26 FEB 86	KEB				

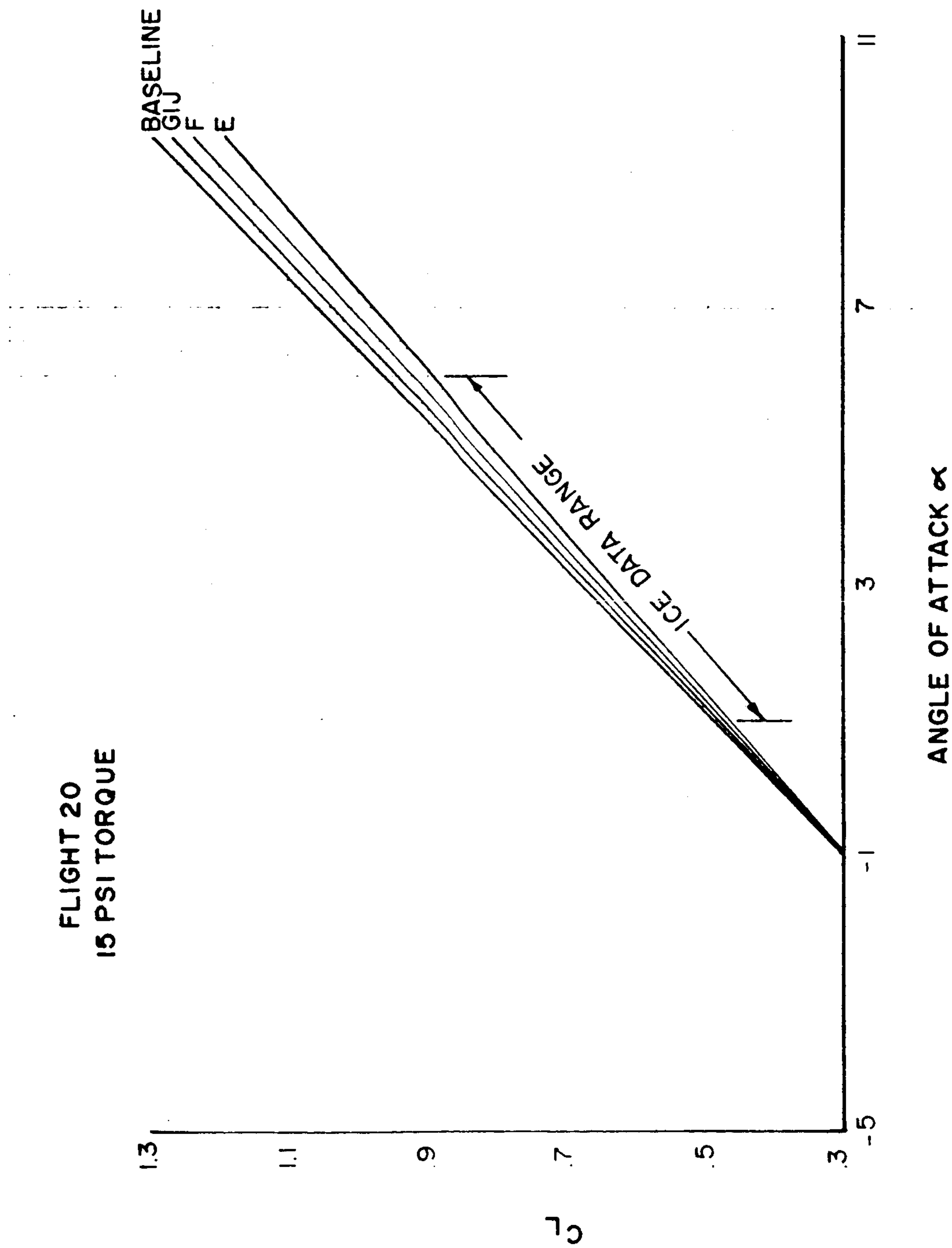

			REVISED	DATE		
CALC					CHANGE IN AIRCRAFT LIFT DUE TO ICE, TORQUE 15 PSI, FLIGHT 20	Fig. 8.1.1b
CHECK	JYJ	3/14/86				DHC-6-004
APPD						
APPD					KOHLMAN SYSTEMS RESEARCH LAWRENCE KANSAS	8.1.5
DRAWN	25 FEB 86	KEB				

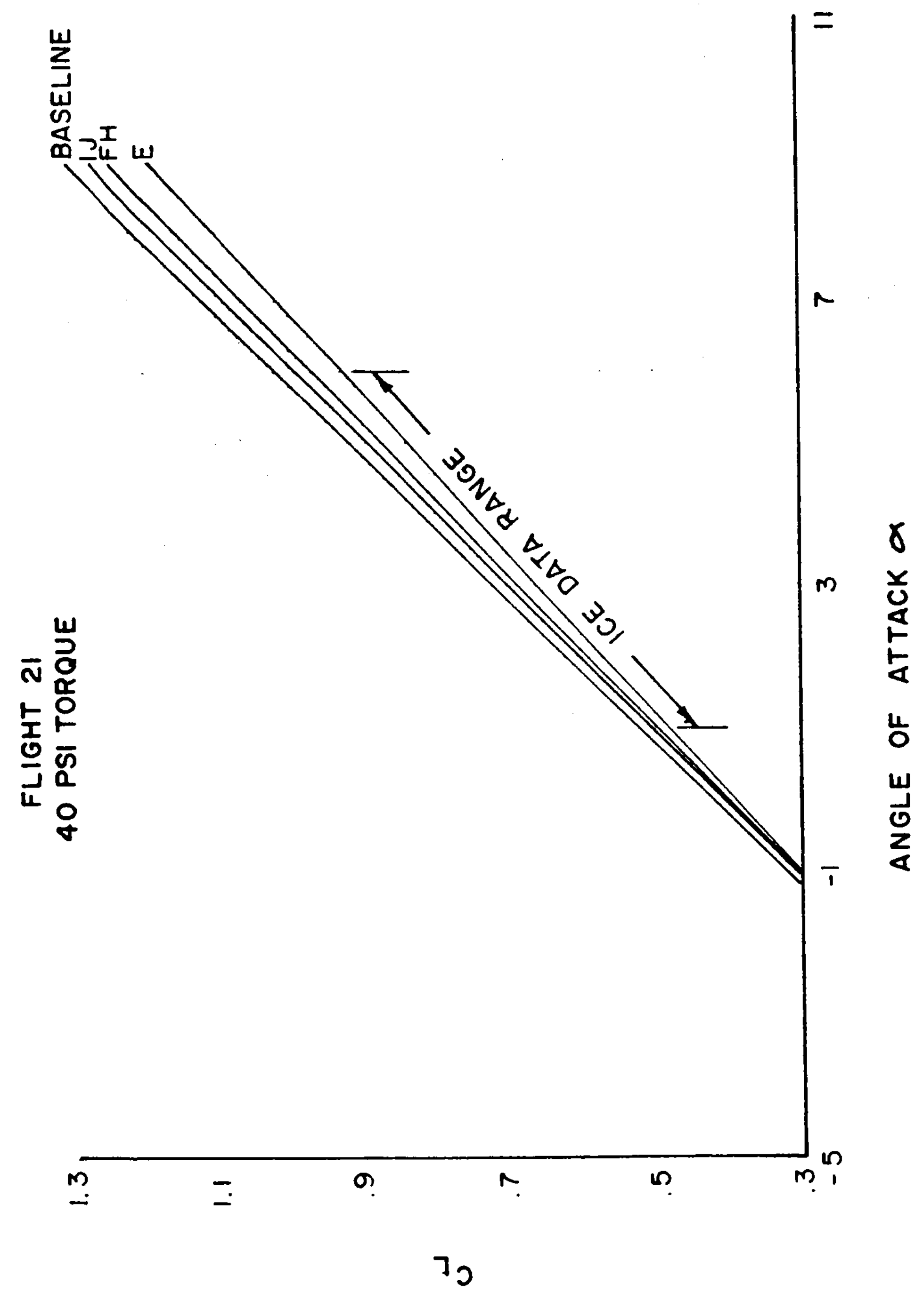

CALC		REVISED	DATE	CHANGE IN AIRCRAFT LIFT DUE TO ICE, TORQUE 40 PSI, FLIGHT 21	Fig. 8.1.1c
CHECK	JKJ 3/14/86				DHC-6-004
APPD					
APPD				KOHLMAN SYSTEMS RESEARCH LAWRENCE KANSAS	8.1.6
DRAWN	26 FEB 86 KEB				

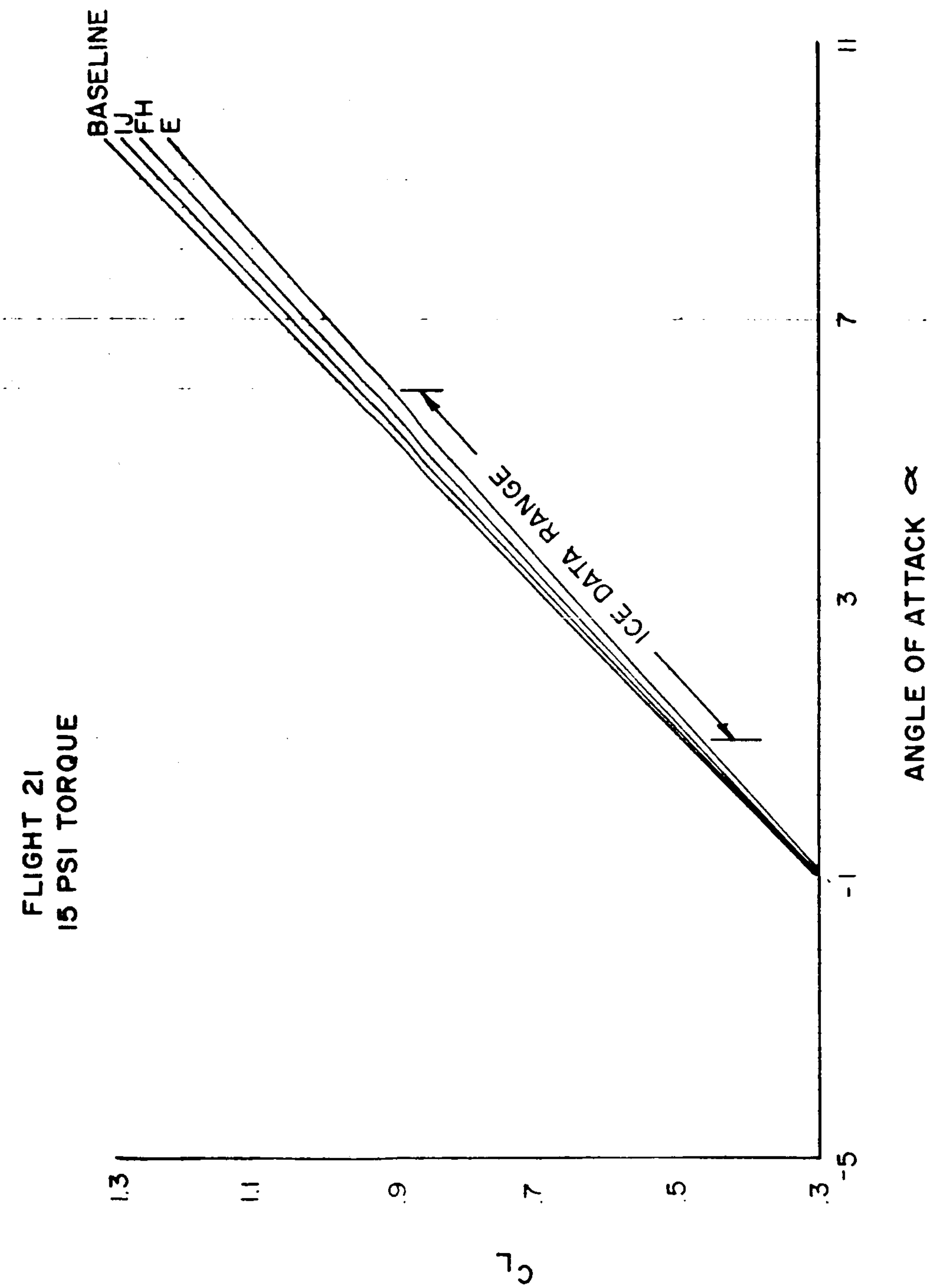

			REVISED	DATE		
CALC					CHANGE IN AIRCRAFT LIFT DUE TO ICE, TORQUE 15 PSI, FLIGHT 21	Fig. 8.1.1d
CHECK	JYJ	3/14/86				DHC-6-004
APPD						
APPD						
DRAWN	25 FEB 86				**KOHLMAN SYSTEMS RESEARCH** LAWRENCE KANSAS	8.1.7

FLIGHT 16 & 17

$C_T = .06 - .08$

$(C_{L_q} + C_{L_{\dot{\alpha}}})_{baseline} = 10.8\ rad^{-1}$

$\delta_F = 0°$

$\Delta(C_{L_q} + C_{L_{\dot{\alpha}}})_{ice} = 0$

CALC			REVISED	DATE	EFFECT OF ICE ON STATE COEFFICIENTS	Fig. 8.1.2a
CHECK	J.G.J.	3/14/86			$(C_{L_q} + C_{L_{\dot{\alpha}}})$, $\delta_F = 0°$	DHC-6-004
APPD					FLIGHTS 16 & 17	
APPD					KOHLMAN SYSTEMS RESEARCH LAWRENCE KANSAS	8.1.8
DRAWN	KEB	24 FEB 86				

$C_T = .05 - .07$

$(C_{L_q} + C_{L_{\dot\alpha}})_{baseline} = 5.9 \text{ rad}^{-1}$

$\delta_F = 10°$

FLIGHTS 16 & 17

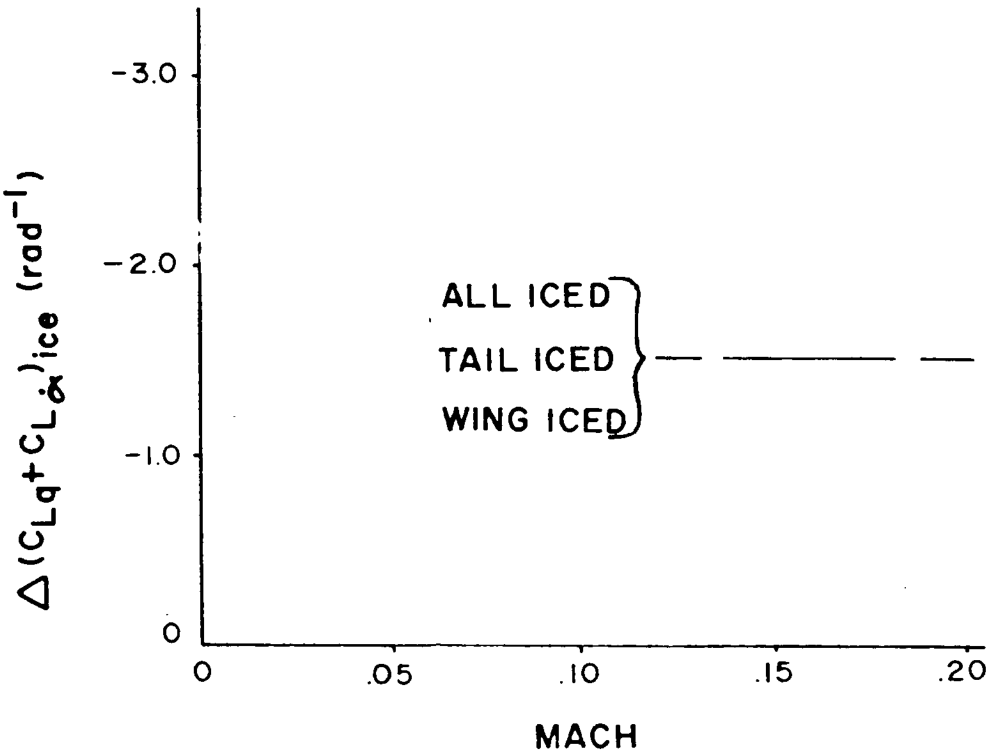

			REVISED	DATE		
CALC					EFFECT OF ICE ON STATE COEFFICIENT $(C_{L_q} + C_{L_{\dot\alpha}})$, $\delta_F = 10°$, FLIGHTS 16 & 17	Fig. 8.1.2b
CHECK	J.A.J.	3/14/86				DHC-6-004
APPD						
APPD					KOHLMAN SYSTEMS RESEARCH LAWRENCE KANSAS	8.1.9
DRAWN	KEB	24 FEB 86				

$C_T = .06 - .08$

$C_{L_{\delta e_{baseline}}} = .0069 \ deg^{-1}$

$\delta_F = 0°$

FLIGHT 16

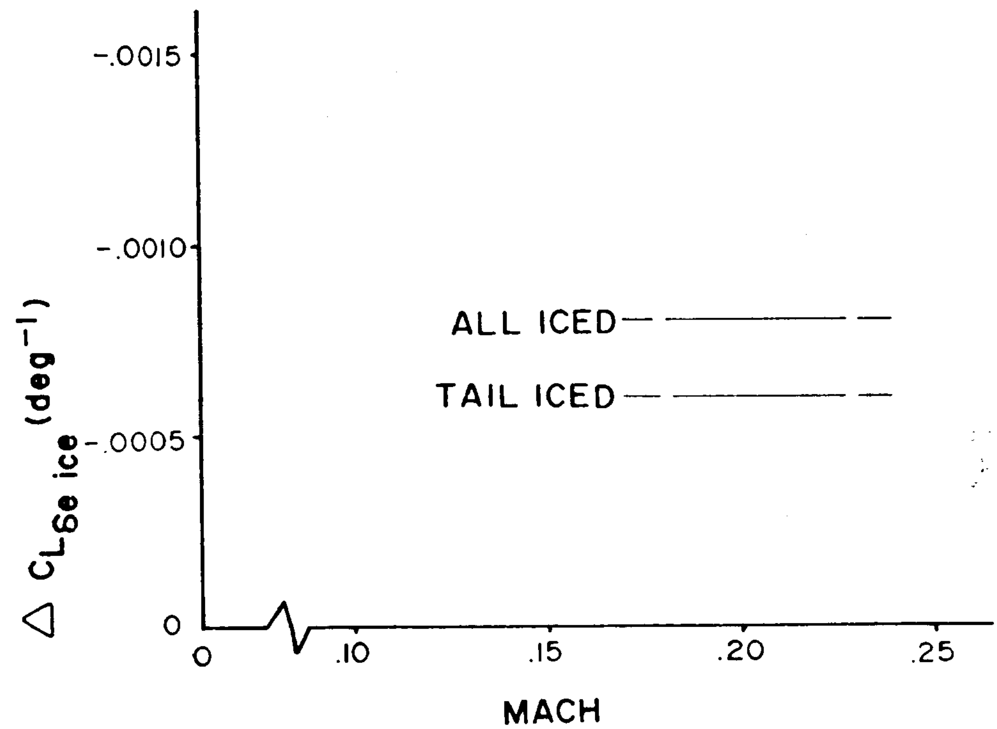

			REVISED	DATE		
CALC					CHANGE IN ELEVATOR LIFT DUE TO ICE, $\delta_F = 0°$, FLIGHT 16	Fig. 8.1.3a
CHECK	J.G.	3/14/86				DHC-6-004
APPD					KOHLMAN SYSTEMS RESEARCH. LAWRENCE KANSAS	8.1.10
APPD						
DRAWN	KEB	24 FEB 86				

$C_T = .06 - .08$

$C_{L_{\delta e}}{}_{baseline} = .0069 \ deg^{-1}$

$\delta_F = 0°$

FLIGHT 17

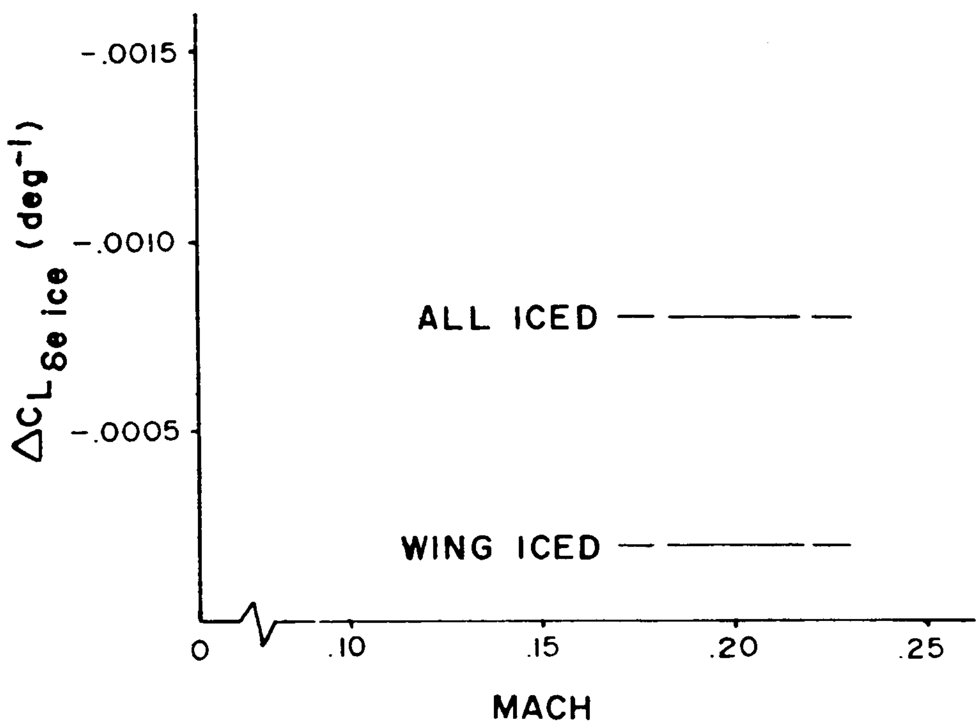

CALC			REVISED	DATE	CHANGE IN ELEVATOR LIFT DUE TO ICE, $\delta_F = 0°$, FLIGHT 17	Fig. 8.1.3b
CHECK	JYJ	3/14/86				DHC-6-004
APPD					KOHLMAN SYSTEMS RESEARCH LAWRENCE KANSAS	8.1.11
APPD						
DRAWN	KEB	24 FEB 86				

$C_T = .05 - .07$

$C_{L_{\delta e\,baseline}} = .0056\ deg^{-1}$

$\delta_F = 10°$

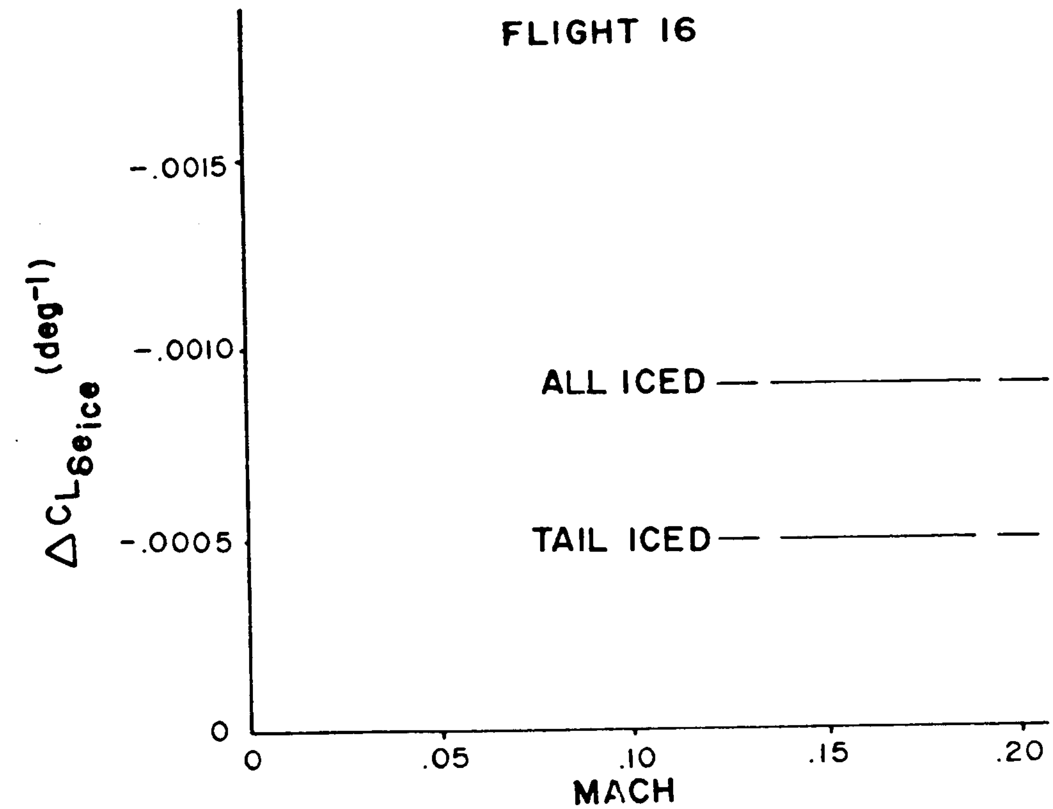

			REVISED	DATE		
CALC					CHANGE IN ELEVATOR LIFT DUE TO ICE, $\delta_F = 10°$, FLIGHT 16	Fig. 8.1.3c
CHECK	J.G.J.	3/14/86				DHC-6-004
APPD						
APPD					KOHLMAN SYSTEMS RESEARCH LAWRENCE KANSAS	8.1.12
DRAWN	KEB	25 FEB 86				

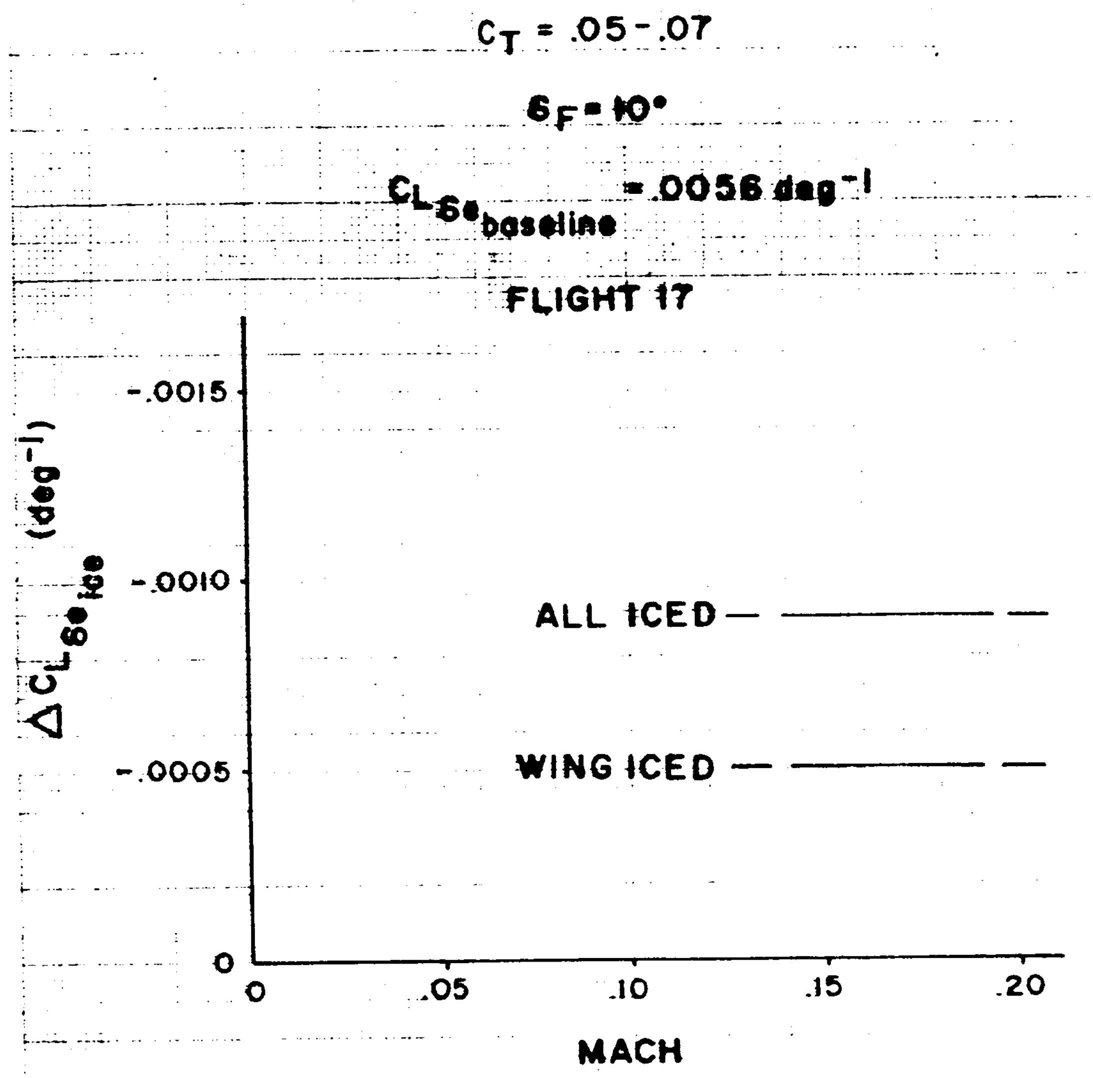

			REVISED	DATE		
CALC					CHANGE IN ELEVATOR LIFT DUE TO ICE, δ_F = 10°, FLIGHT 17	Fig. 8.1.3d
CHECK	JGJ.	3/14/86				DHC-6-004
APPD						
APPD					KOHLMAN SYSTEMS RESEARCH - LAWRENCE KANSAS	8.1.13
DRAWN	KEB	25 Feb 86				

8.1.2. Drag Coefficient, CD

As it was found with lift, the drag decrements remain relatively the same percentage-wise at both high and low power settings. Within the linear portion of the flight envelope the relative magnitude of lift and drag decrements due to ice appear independent of power. However, the absolute magnitude of these decrements are dependent on power effects.

Flight 21 points out that the shape of aircraft ice accretions on both lifting and nonlifting surfaces is the most important factor influencing performance. For example, the icing encounter on flight 20 lasted 54 minutes at an approximate average LWC of 0.20 gm/ 3. Though the average MVD on each flight was approximately 14 to 15 microns, the temperature differed by 4.5 degrees C. This difference in temperature resulted in a glazed-type ice formation on flight 21. The encounter on flight 21 was nine minutes less than on flight 20 and the LWC less by a factor of greater than two, yet the overall drag increase was about 15-20% more than that of flight 20.

The aerodynamic drag force coefficient investigated are presented below. The lines designated as "baseline" represent the dry air baseline testing. The iced configurations are defined using the letters E thru J, with multiple designations for a given curve indicating that there was no discernable difference between results for the different configurations.

Letter Code	Aircraft Configuration
E	Cruise configuration, aircraft all iced
F	Cruise configuration, aircraft complete tail and struts iced
G	Cruise configuration, aircraft vertical tail and struts iced
H	Cruise configuration, aircraft horizontal tail and struts iced
I	Cruise configuration, aircraft struts iced
J	Cruise configuration, residual ice only

	Figure #
C_D	8.1.4a - 8.1.4d

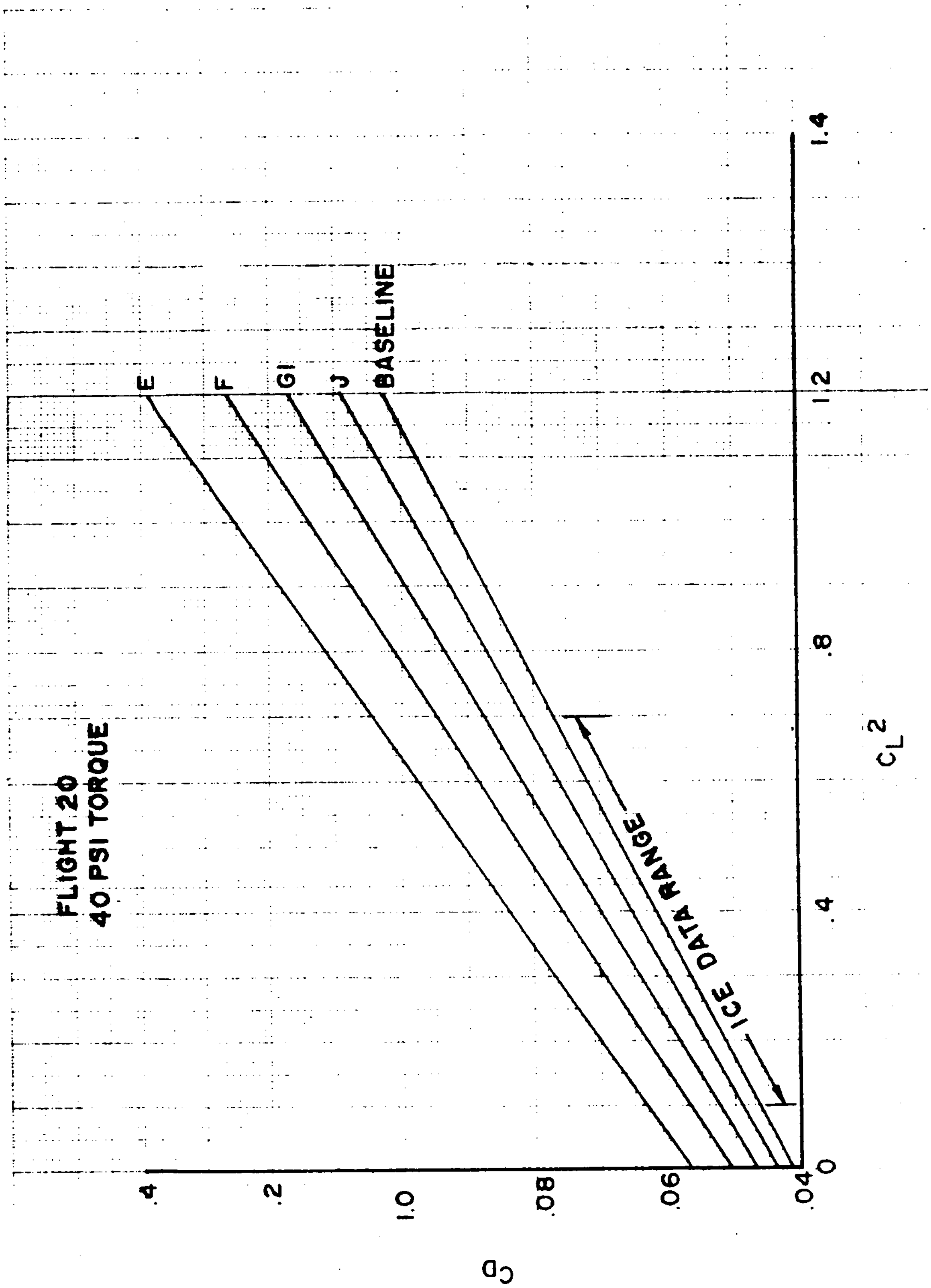

			REVISED	DATE		
CALC					CHANGE IN AIRCRAFT DRAG DUE TO ICE, TORQUE 40 PSI, FLIGHT 20	Fig. 8.1.4a
CHECK	J.Y.J.	3/14/86				DHC-6-004
APPD						
APPD					KOHLMAN SYSTEMS RESEARCH - LAWRENCE KANSAS	8.1.16
DRAWN	25 FEB 86	KEB				

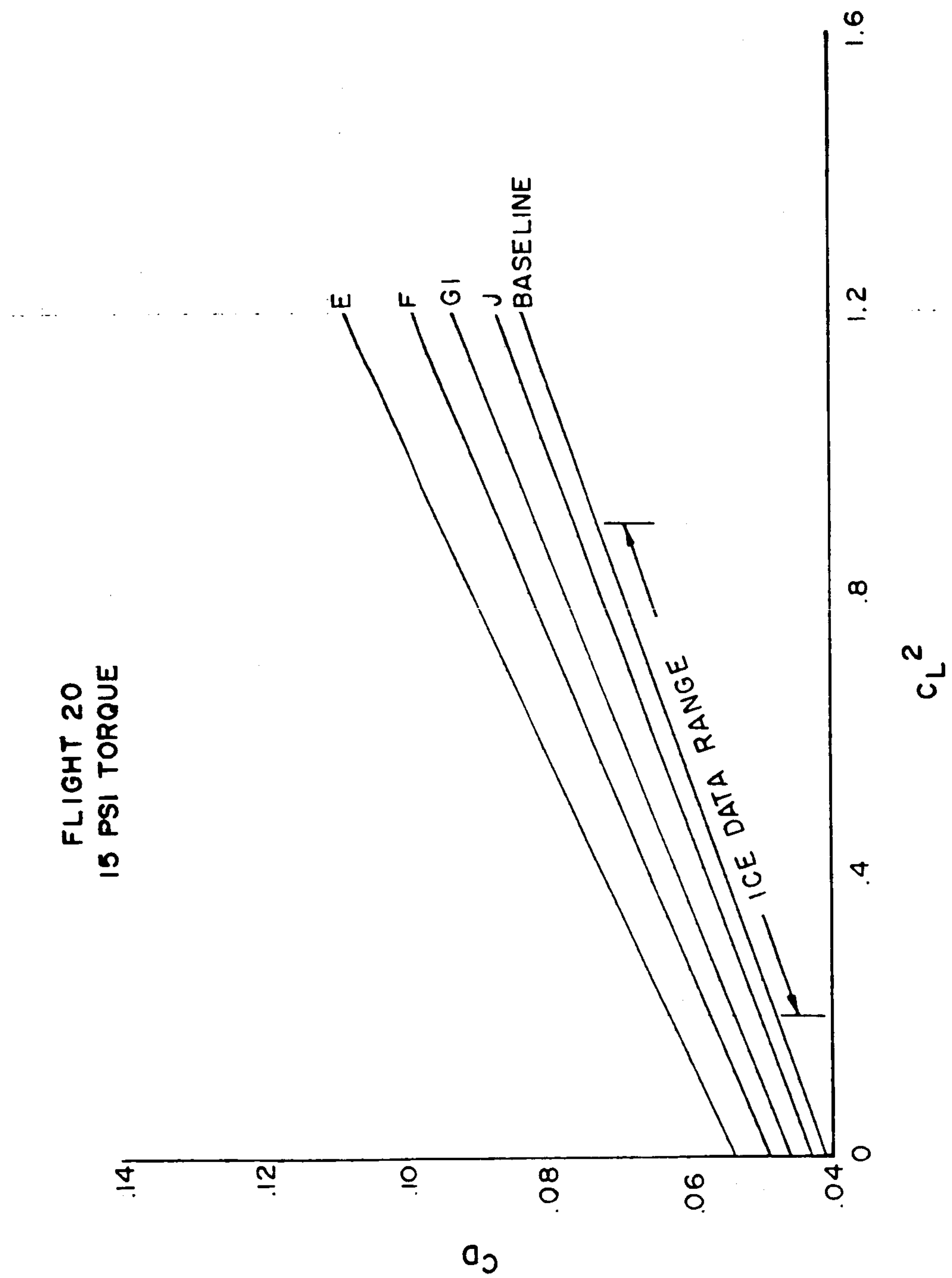

			REVISED	DATE
CALC				
CHECK	J.Z.J	3/14/86		
APPD				
APPD				
DRAWN	25 FEB 86	KEB		

CHANGE IN AIRCRAFT DRAG DUE TO ICE, TORQUE 15 PSI, FLIGHT 20

Fig. 8.1.4b

DHC-6-004

KOHLMAN SYSTEMS RESEARCH
LAWRENCE KANSAS

8.1.17

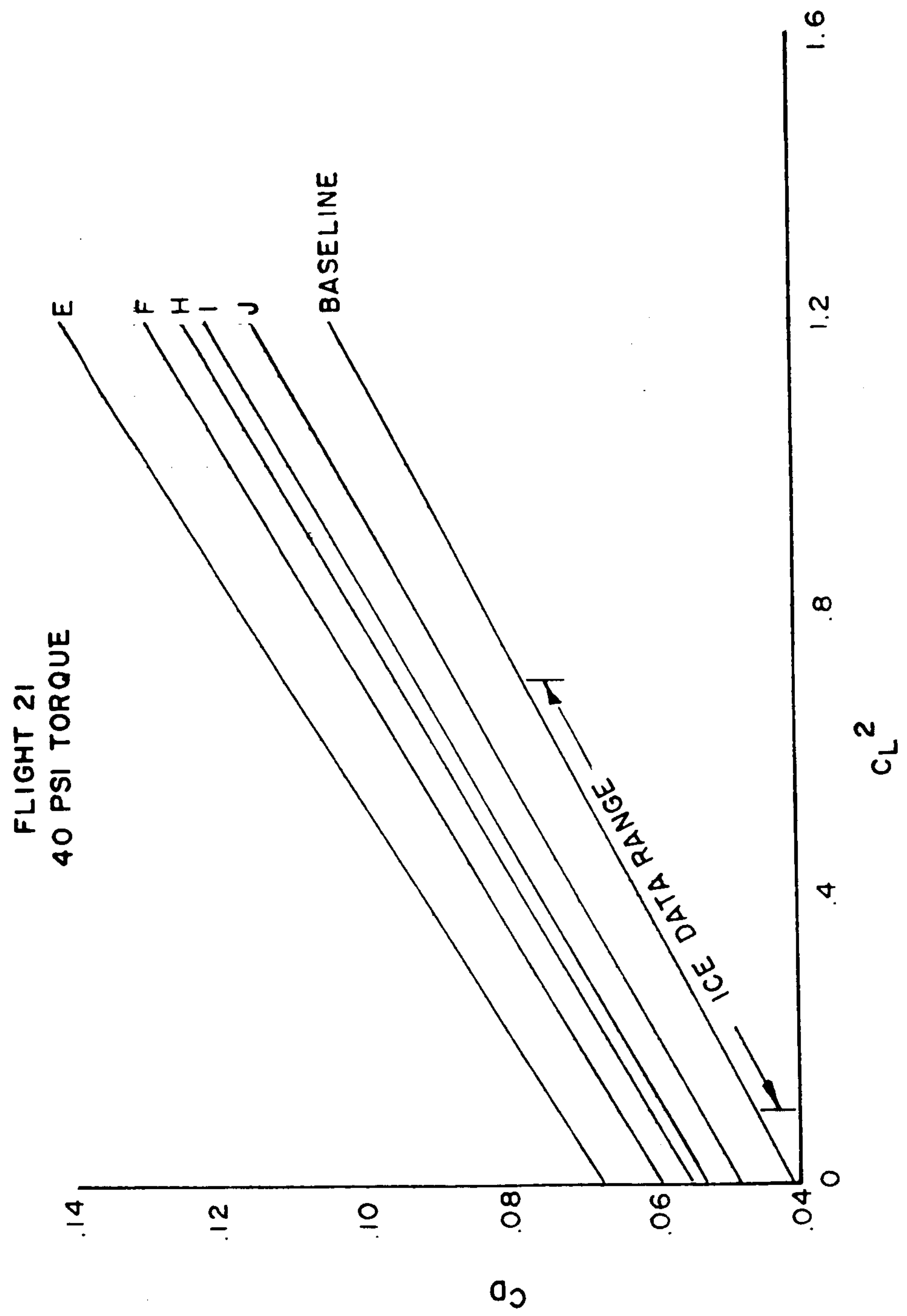

			REVISED	DATE		
CALC					CHANGE IN AIRCRAFT DRAG DUE TO ICE, TORQUE 40 PSI, FLIGHT 21	Fig. 8.1.4c
CHECK	J.L.J.	3/14/86				DHC-6-004
APPD						
APPD					KOHLMAN SYSTEMS RESEARCH. LAWRENCE KANSAS	8.1.18
DRAWN	26 FEB 86	KEB				

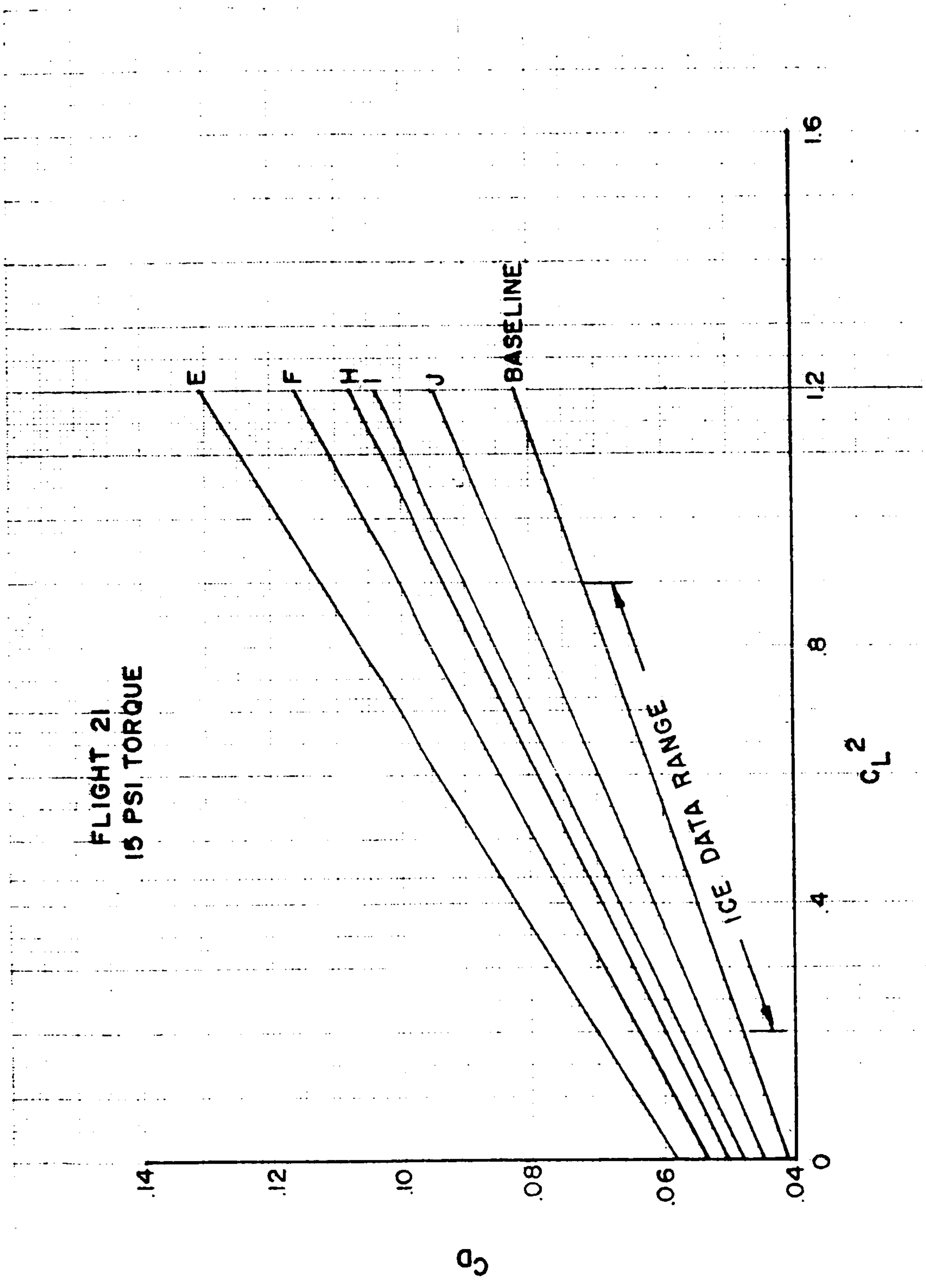

			REVISED	DATE	
CALC					CHANGE IN AIRCRAFT DRAG DUE TO ICE, TORQUE 15 PSI, FLIGHT 21
CHECK	JJJ.	3/14/86			
APPD					
APPD					KOHLMAN SYSTEMS RESEARCH - LAWRENCE KANSAS
DRAWN	25 FEB 86	KEB			

Fig. 8.1.4d

DHC-6-004

8.1.3. Pitching Moment Coefficient, CM

The effect of aircraft icing on pitching moment at the 15 psi torque setting was not seen in data from either flight 20 or 21. At the 40 psi torque setting small reductions were measured in pitching moment on both flights. However, both the glazed and mixed type ice shape gave the same results.

The elevator power, $C_{m_{\delta_e}}$ with the aircraft in the all-iced configuration showed an 10% degradation. When the tail only was iced this degradation averaged around 8.5%, and when the wing only was iced a 2% degradation was found. When flaps were lowered to 10 degrees the all-iced degradation in these coefficients increased to 15-16% and the wing ice accounted for approximately 9% or nearly equivalent in magnitude to the tail ice contribution.

It was found that the pitch damping state coefficient showed no change due to ice in the flaps-up case, however when the flaps were lowered 10 degrees and there was ice on the wings, tail, or both this coefficient was degraded approximately 23%.

The aerodynamic pitching moment coefficients investigated are presented below. The lines designated as "baseline" represent the dry air baseline testing. The iced configurations are defined using the letters E thru J, with multiple designations for a given curve indicating that there was no discernable difference between results for the different configurations.

Letter Code	Aircraft Configuration
E	Cruise configuration, aircraft all iced
F	Cruise configuration, aircraft complete tail and struts iced
G	Cruise configuration, aircraft vertical tail and struts iced
H	Cruise configuration, aircraft horizontal tail and struts iced
I	Cruise configuration, aircraft struts iced
J	Cruise configuration, residual ice only

	Figure #
Cm	8.1.5a - 8.1.5b
$(Cm_q + Cm_{\dot{\alpha}})$	8.1.6a - 8.1.6b
Cm_{δ_e}	8.1.7a - 8.1.7d

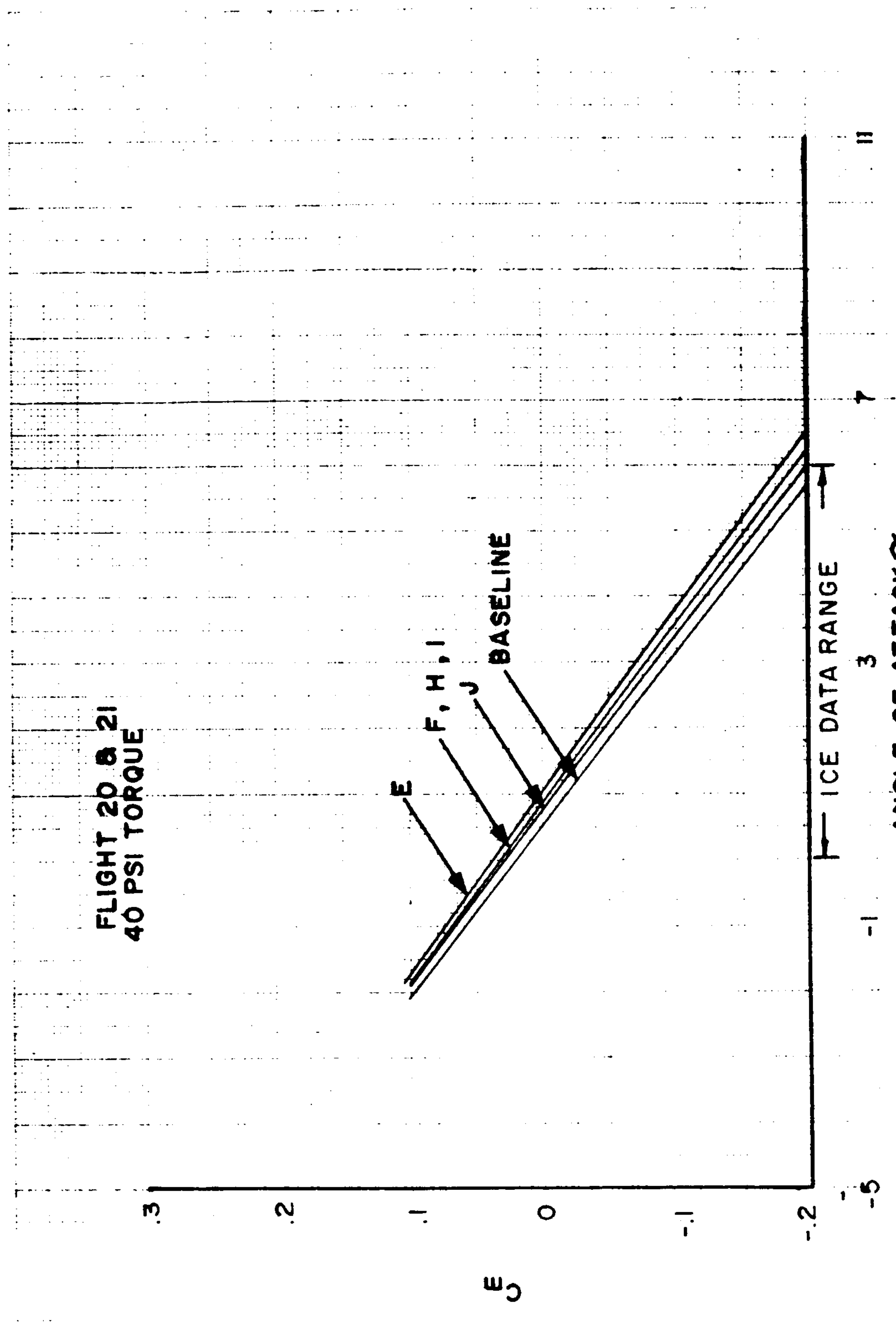

			REVISED	DATE	CHANGE IN AIRCRAFT PITCHING MOMENT DUE TO ICE, TORQUE 40 PSI, FLIGHTS 20 & 21	Fig. 8.1.5a
CALC						
CHECK	J.J.	3/14/86				DHC-6-004
APPD						
APPD					KOHLMAN SYSTEMS RESEARCH - LAWRENCE KANSAS	8.1.22
DRAWN	25 FEB 86	KEB				

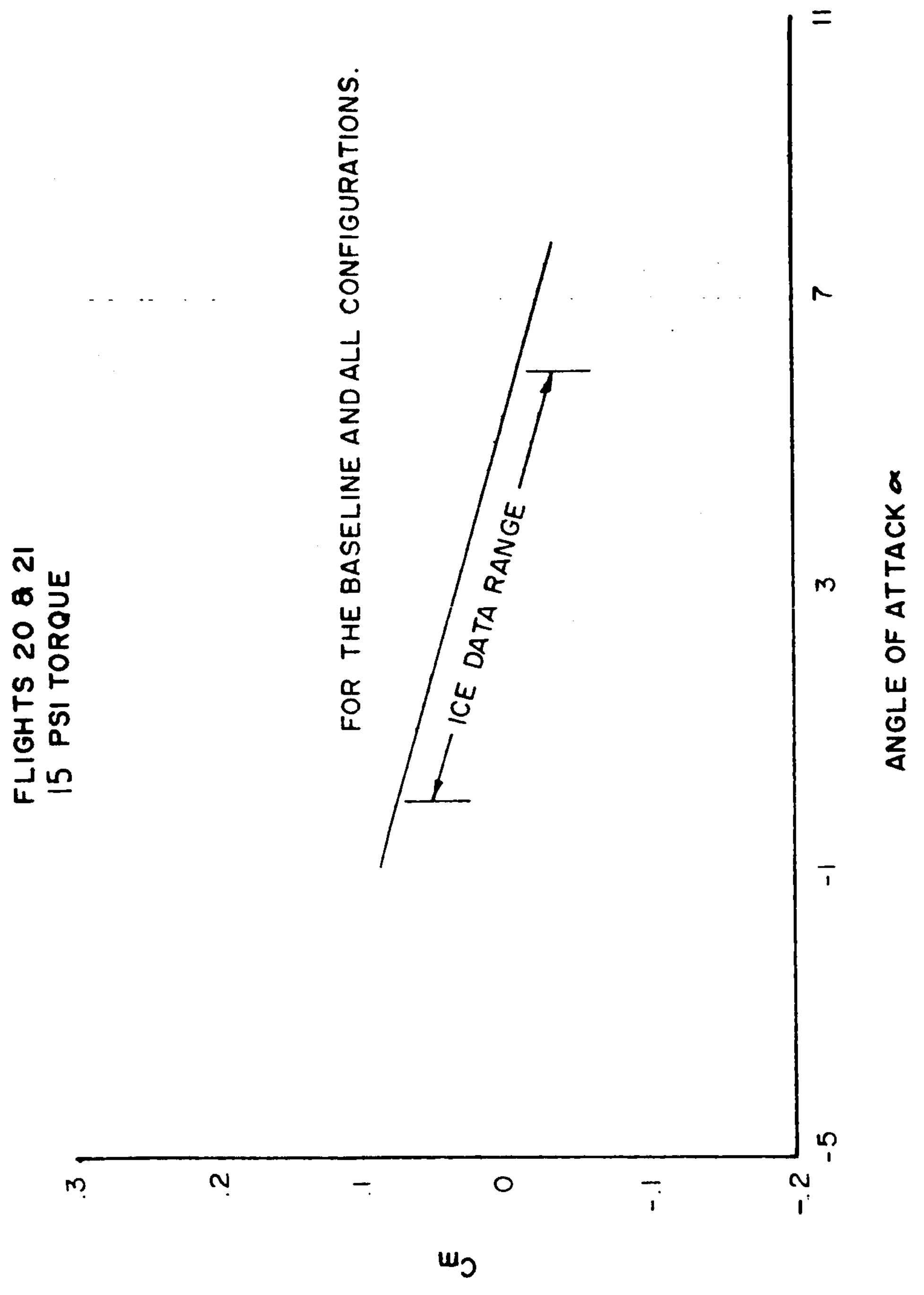

			REVISED	DATE		
CALC					CHANGE IN AIRCRAFT PITCHING MOMENT DUE TO ICE, TORQUE 15 PSI, FLIGHTS 20 & 21	Fig. 8.1.5b
CHECK	J.Y.J.	3/14/86				DHC-6-004
APPD						
APPD					KOHLMAN SYSTEMS RESEARCH. LAWRENCE KANSAS	8.1.23
DRAWN	25 FEB86	KEB				

FLIGHTS 16 & 17

$C_T = .06 - .08$

$(C_{m_q} + C_{m_{\dot\alpha}})_{baseline} = -48 \text{ rad}^{-1}$

$\delta_F = 0°$

$\Delta (C_{m_q} + C_{m_{\dot\alpha}})_{ice} = 0$

C-3

CALC			REVISED	DATE	EFFECT OF ICE ON STATE COEFFICIENTS $(C_{m_q} + C_{m_{\dot\alpha}})$, $\delta_F = 0°$ FLIGHTS 16 & 17	Fig. 8.1.6a
CHECK	C.Y.J.	3/14/86				DHC-6-004
APPD						
APPD					KOHLMAN SYSTEMS RESEARCH. LAWRENCE KANSAS	8.1.24
DRAWN	KEB	24 FEB 86				

$C_T = .05 - .07$

$(Cm_q + Cm_{\dot{\alpha}})_{baseline} = -26\ rad^{-1}$

$\delta_F = 10°$

FLIGHTS 16 & 17

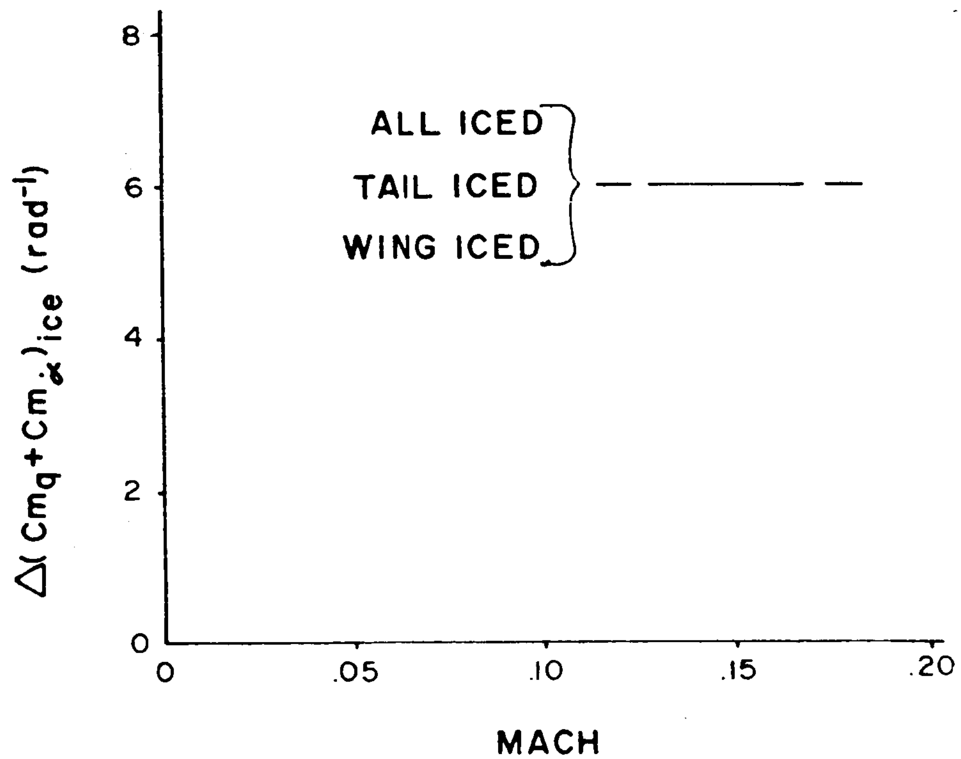

CALC			REVISED	DATE	CHANGE IN PITCH DAMPING STATE COEFFICIENT DUE TO ICE, δ_F 10°, FLIGHTS 16 & 17	Fig. 8.1.6b
CHECK	J.G.J.	3/14/86				DHC-6-004
APPD					KOHLMAN SYSTEMS RESEARCH LAWRENCE KANSAS	8.1.25
APPD						
DRAWN	KEB	24 FEB 86				

$C_T = .06 - .08$

$Cm_{\delta e_{baseline}} = -.0285 \text{ deg}^{-1}$

$\delta_F = 0°$

FLIGHT 16

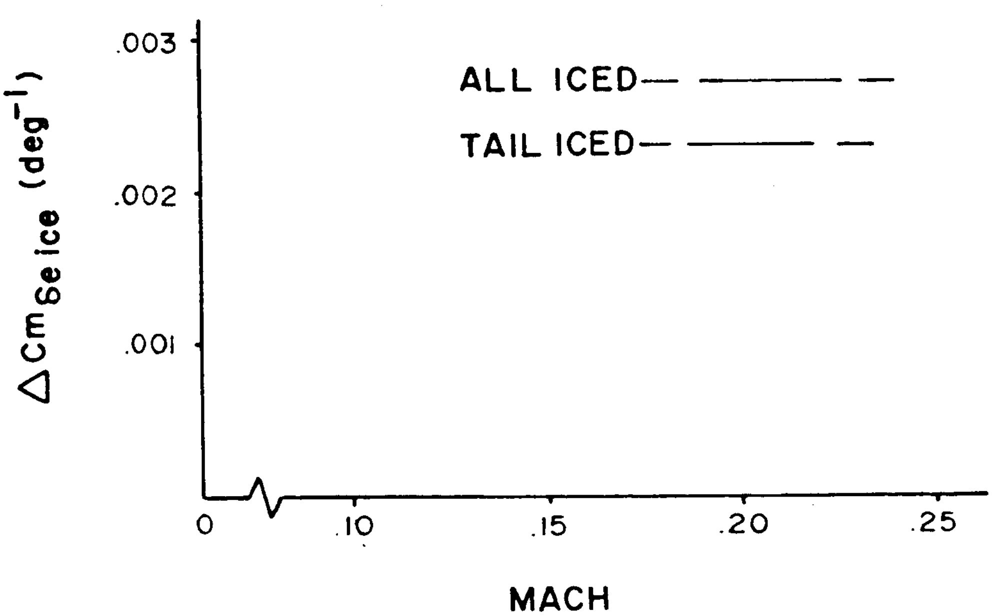

			REVISED	DATE		
CALC					CHANGE IN ELEVATOR CONTROL POWER DUE TO ICE, $\delta_F = 0°$ FLIGHT 16	Fig. 8.1.7a
CHECK	J.G.J.	3/14/86				DHC-6-004
APPD						
APPD					KOHLMAN SYSTEMS RESEARCH LAWRENCE KANSAS	8.1.26
DRAWN	KEB	24 FEB 86				

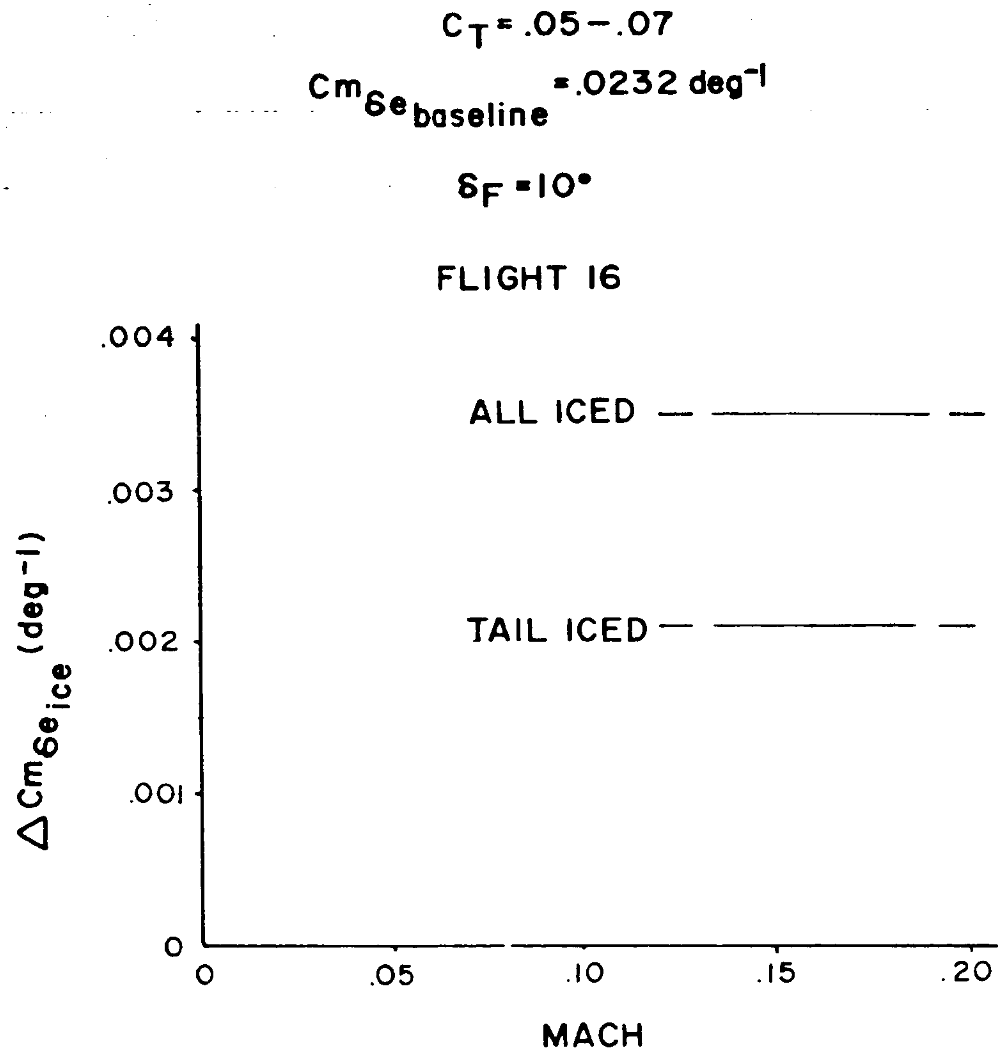

CALC			REVISED	DATE	CHANGE IN ELEVATOR CONTROL POWER DUE TO ICE, $\delta_F = 10°$, FLIGHT 16	Fig. 8.1.7b
CHECK	J.J.J.	3/14/86				DHC-6-004
APPD						
APPD					KOHLMAN SYSTEMS RESEARCH LAWRENCE KANSAS	8.1.27
DRAWN	KEB	24 FEB 86				

$C_T = .06 - .08$

$Cm_{\delta e_{baseline}} = -.0285 \text{ deg}^{-1}$

$\delta_F = 0°$

FLIGHT 17

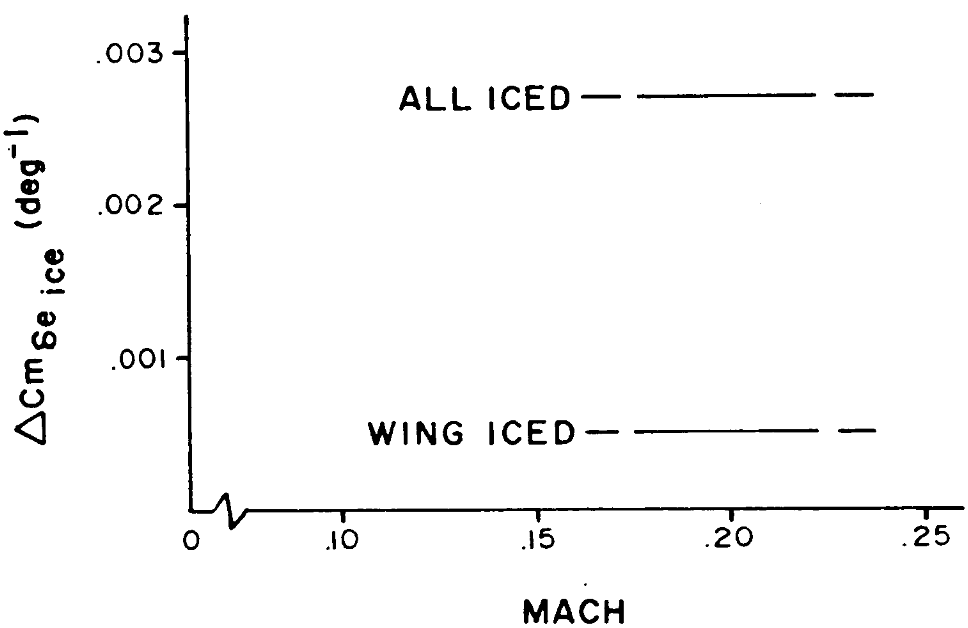

			REVISED	DATE		
CALC					CHANGE IN ELEVATOR CONTROL POWER DUE TO ICE, $\delta_F = 0°$, FLIGHT 17	Fig. 8.1.7c
CHECK	J.J.J.	3/14/86				DHC-6-004
APPD						
APPD					KOHLMAN SYSTEMS RESEARCH LAWRENCE KANSAS	8.1.28
DRAWN	21 Feb 86	KEB				

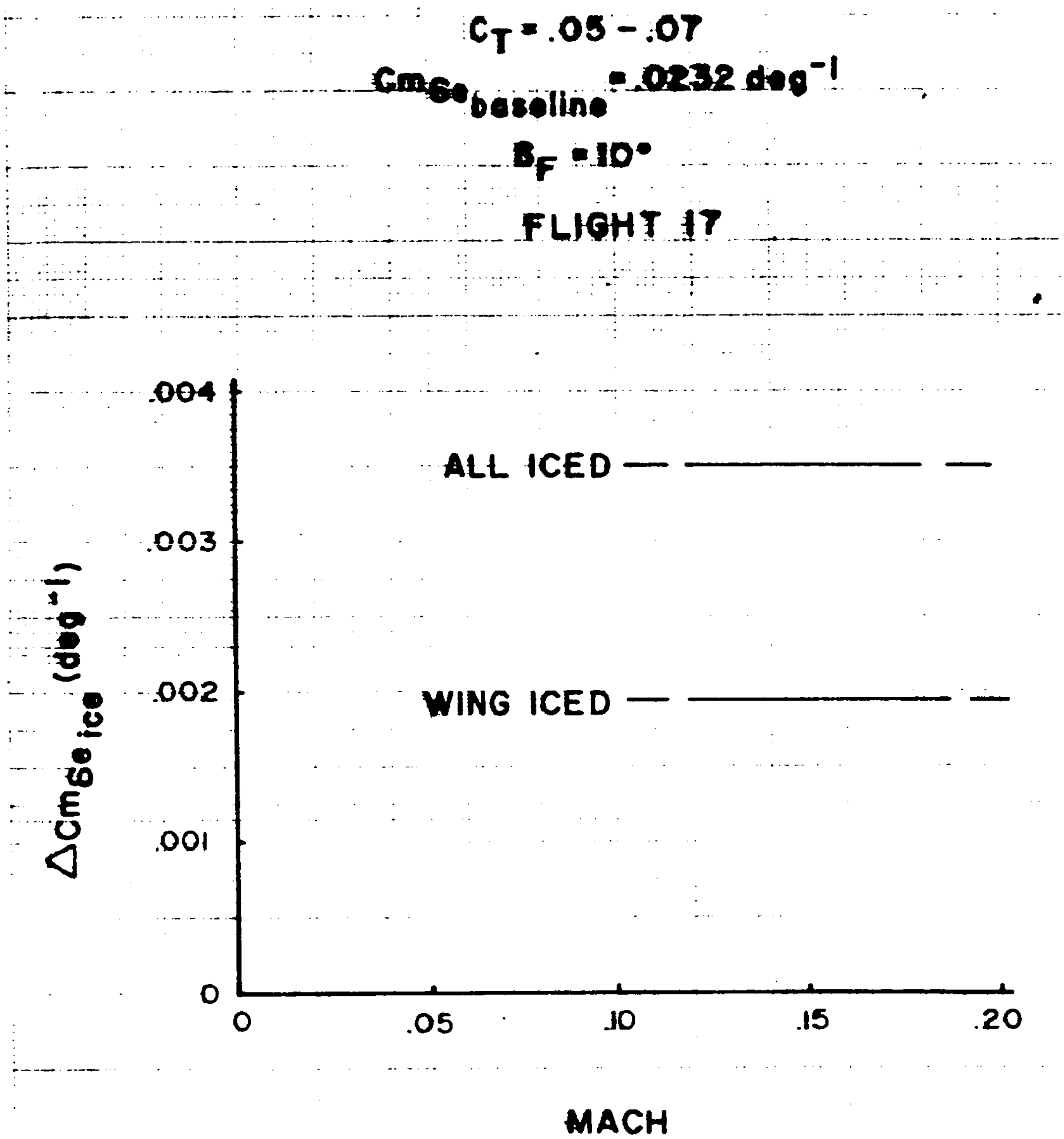

CALC			REVISED	DATE	CHANGE IN ELEVATOR CONTROL DUE TO ICE δ_F = 10°, FLIGHT 17	Fig. 8.1.7d
CHECK	J.Y.J.	3/14/86				DHC-6-004
APPD						
APPD					KOHLMAN SYSTEMS RESEARCH LAWRENCE KANSAS	8.1.29
DRAWN	KEB	21 Feb 86				

8.1.4 Stick Free Stability Rudder Float Ratio

An analysis was done on the stick free stability rudder float ratio. This ratio Ch_{δ_r}/Ch_{β} was measured by performing an a~~s~~symmetric power sideslip maneuver. The baseline test consisted of a slow deceleration from 95-72 KIAS and the hinge moment ratio was calculated at 7.5. With a small accretion of rime ice this ratio decreased to 4.8 as measured by a slow deceleration from 89-86 KIAS.

Time history plots are presented to show the effect of ice on the vertical fin. These are presented for six runs from two flights in Figures 8.1.8a thru 8.1.13g. Perhaps the most interesting time history of this series is run 25, flight 23, which shows a decrease in vertical fin power due to ice. For five selected runs the ratio of Ch_{δ_r}/Ch_{β} was calculated and plotted in Figures 8.1.14 and 8.1.15.

	Figure #
Time history for N111+36A	8.1.8a - 8.1.8g
Time history for N111+37A	8.1.9a - 8.1.9g
Time history for N123+23A	8.1.10a - 8.1.10g
Time history for N123+24A	8.1.11a - 8.1.11g
Time history for N123+25A	8.1.12a - 8.1.12g
Time history for N123-26A	8.1.13a - 8.1.13g
Ch_{δ_r}/Ch_{β} plot for runs N111+36A & N111+37A	- 8.1.14
$Ch_{\delta_r}/Ch_{\delta_r}$ plot for run N123+24A, N123+25A & N123+26A	- 8.1.15

SIDELSLIP WITH VERT. FIN ICED

INITIAL CONDITIONS FOR TEST NUMBER:

FLIGHT: 11
RUN: 36
AIRCRAFT TYPE: LaRC Twin Otter Icing Flts
SERIAL NUMBER: DHC-6-004

ALT_CAL (FEET)	= 6796.6	N1_L (%)	= 74.9
AIRSPD_CAL (KNOT)	= 85.6	N1_R (%)	= 98.2
AIRSPD_TRU (KNOT)	= 96.1	PROP_RPM_L (%)	= 84.3
MACH_CAL	= 0.150	PROP_RPM_R (%)	= 84.6
DYN_PRS_CA (PSF)	= 26.1	TORQUE_L (ft-lb)	= 243.4
NCLT	= 0.9	TORQUE_R (ft-lb)	= 1201.8
ALPHA_ROS2 (DEG)	= 0.1	FUEL_FLO_L (LB/HR)	= 125.
AMB_PRESS (PSF)	= 1645.6	FUEL_FLO_R (LB/HR)	= 305.
TEMP_AMB (DEGK)	= 269.7	FUELTEMP_L (DEG_K)	= 256.5
AC_WEIGHT (LB)	= 10037.	FUELTEMP_R (DEG_K)	= 257.3
CG_PCT_MAC (%)	= 26.73		
IXX_BODY (SLG-SQFT)	= 15996.		
IYY_BODY (SLG-SQFT)	= 22813.		
IZZ_BODY (SLG-SQFT)	= 35852.		
IXZ_BODY (SLG-SQFT)	= 1103.		
FLAP (DEG)	= 0.0		
DELTA_E (DEG)	= -6.0		
DELTA_A_L (DEG)	= 7.8		
DELTA_R (DEG)	= 2.6		

APPD	J.E.J.	3/4/86	CONV	02/05/86	KOHLMAN SYSTEMS RESEARCH	FIG. 8.1.8a
DRAWN	17 22 16	03/06/86				8.1.31

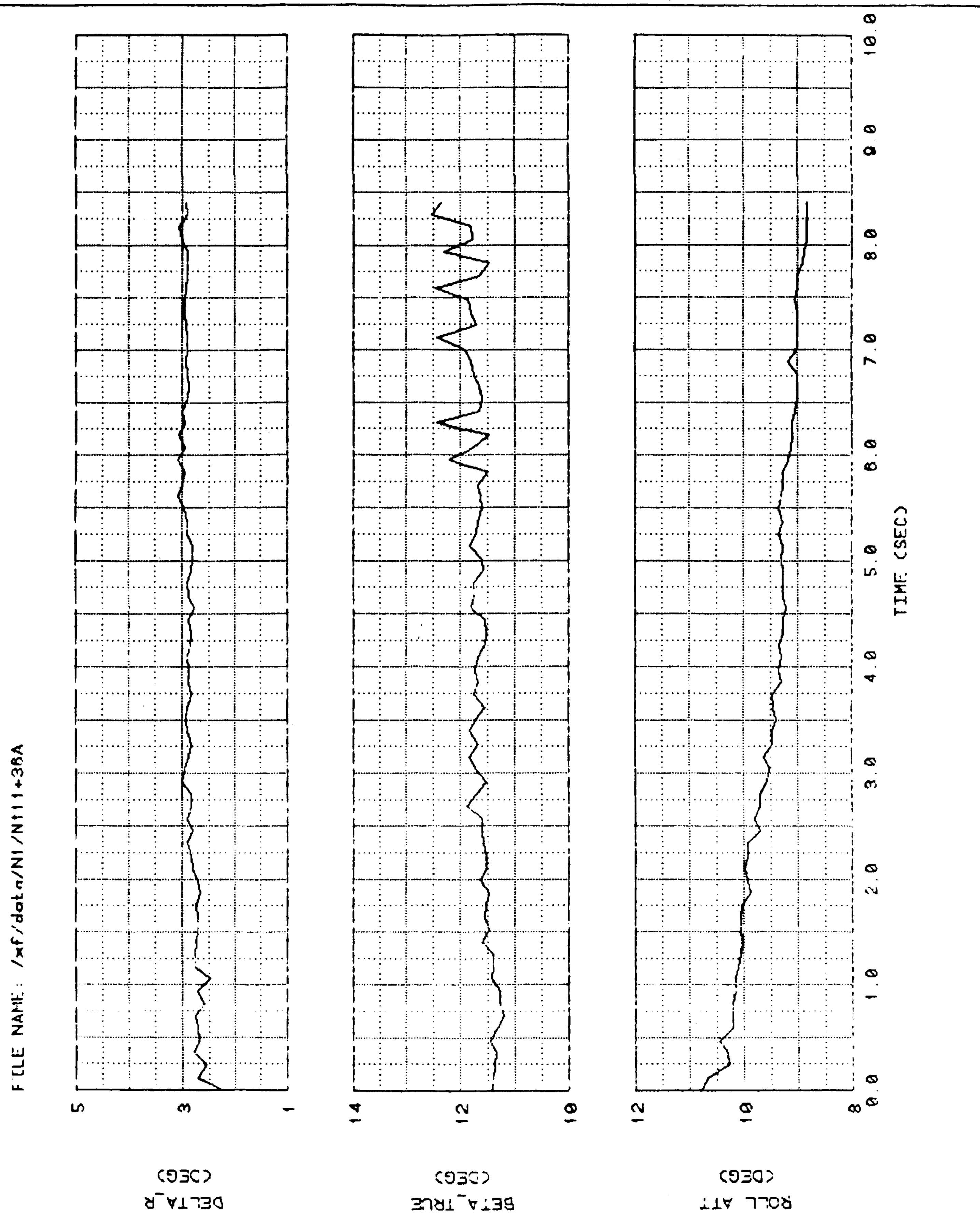

CONV		02/05/86	REVISED	DATE	SIDELSLIP WITH VERT. FIN ICED	DHC-6-004
CHECK					FLT# '' RUN 36	
CHECK	[signature]	3/14/86				Fig. 8.1.8b
APPD						
DRAWN	17:23:20	03/06/86			KOHLMAN SYSTEMS RESEARCH	8.1.32

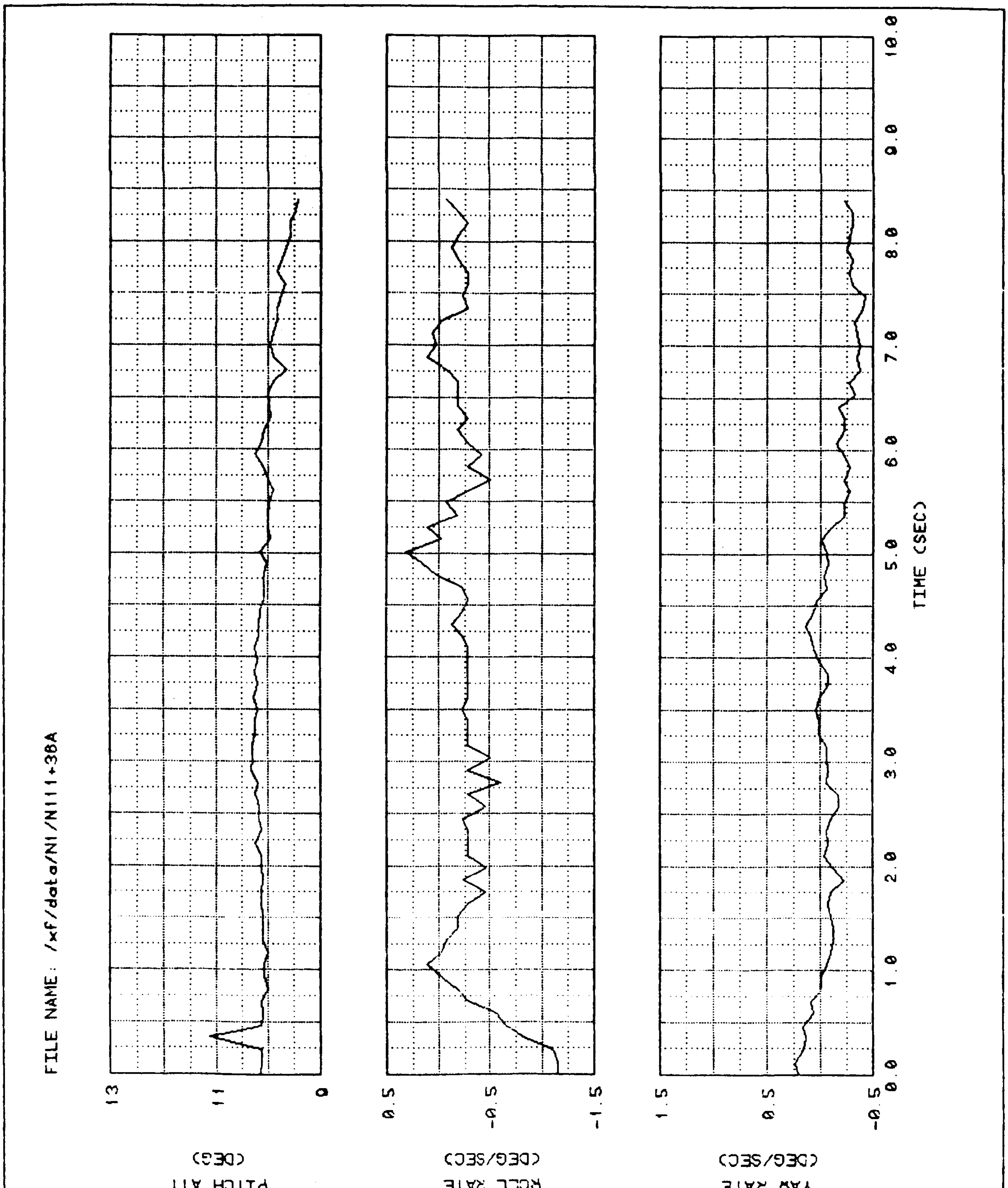

CC		02/05/85	REVISED	DATE	SIDELSLIP WITH VERT. FIN ICED	DHC-6-004
CHECK					FLT# 11 RUN 36	
CHECK	G.G.	3/11/96				Fig. 8.1.8c
APPD						
DRAWN	17 25 20	03/06/85			KOHLMAN SYSTEMS RESEARCH	8.1.33

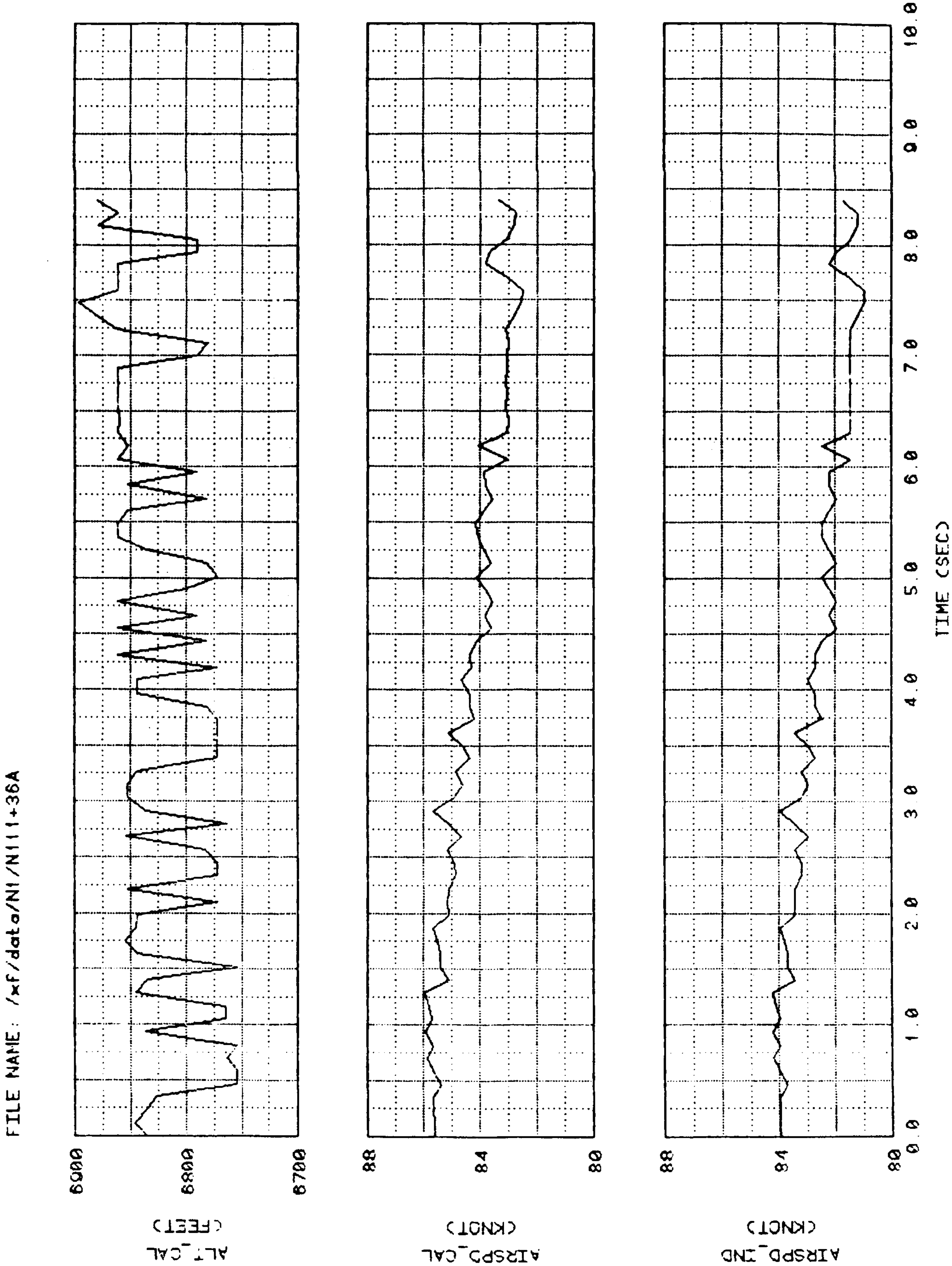

CONV		02/05/85	REVISED	DATE	SIDELSLIP WITH VERT. FIN ICED FLT# 11 RUN 36	DHC-6-004
CHECK						
CHECK	[signature]	3/14/96				Fig. 8.1.8d
APPD						
DRAWN	'7 28 18	03/08/85			KOHLMAN SYSTEMS RESEARCH	8.1.34

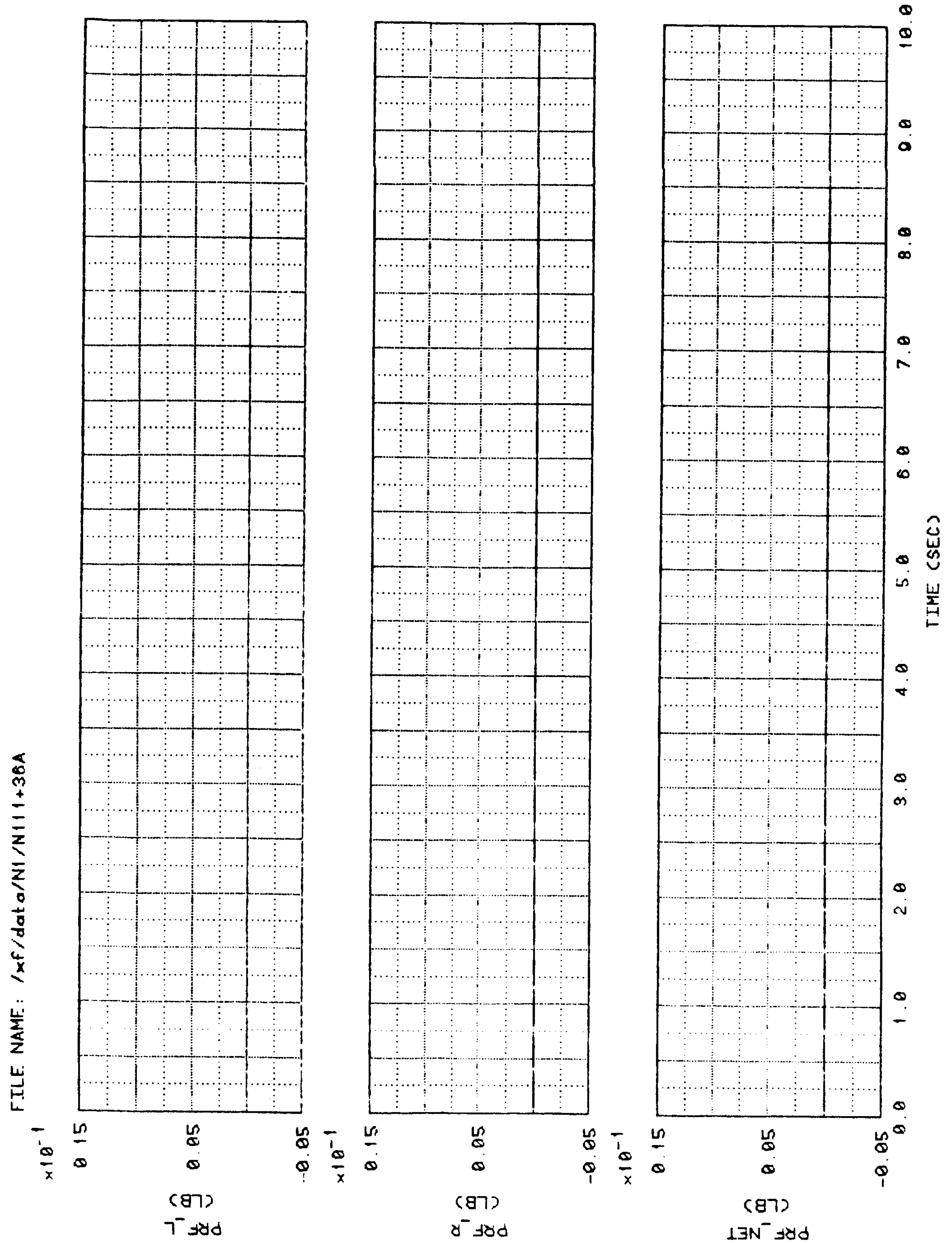

CO		02/05/86	REVISED	DATE		DHC-6-004
CHECK					SIDELSLIP WITH VERT. FIN ICED FLT# 11 RUN 36	
CHECK	[signature]	3/14/86				
APPD						Fig. 8.1.8d
DRAWN	17 30 00	03/06/86			KOHLMAN SYSTEMS RESEARCH	8.1.35

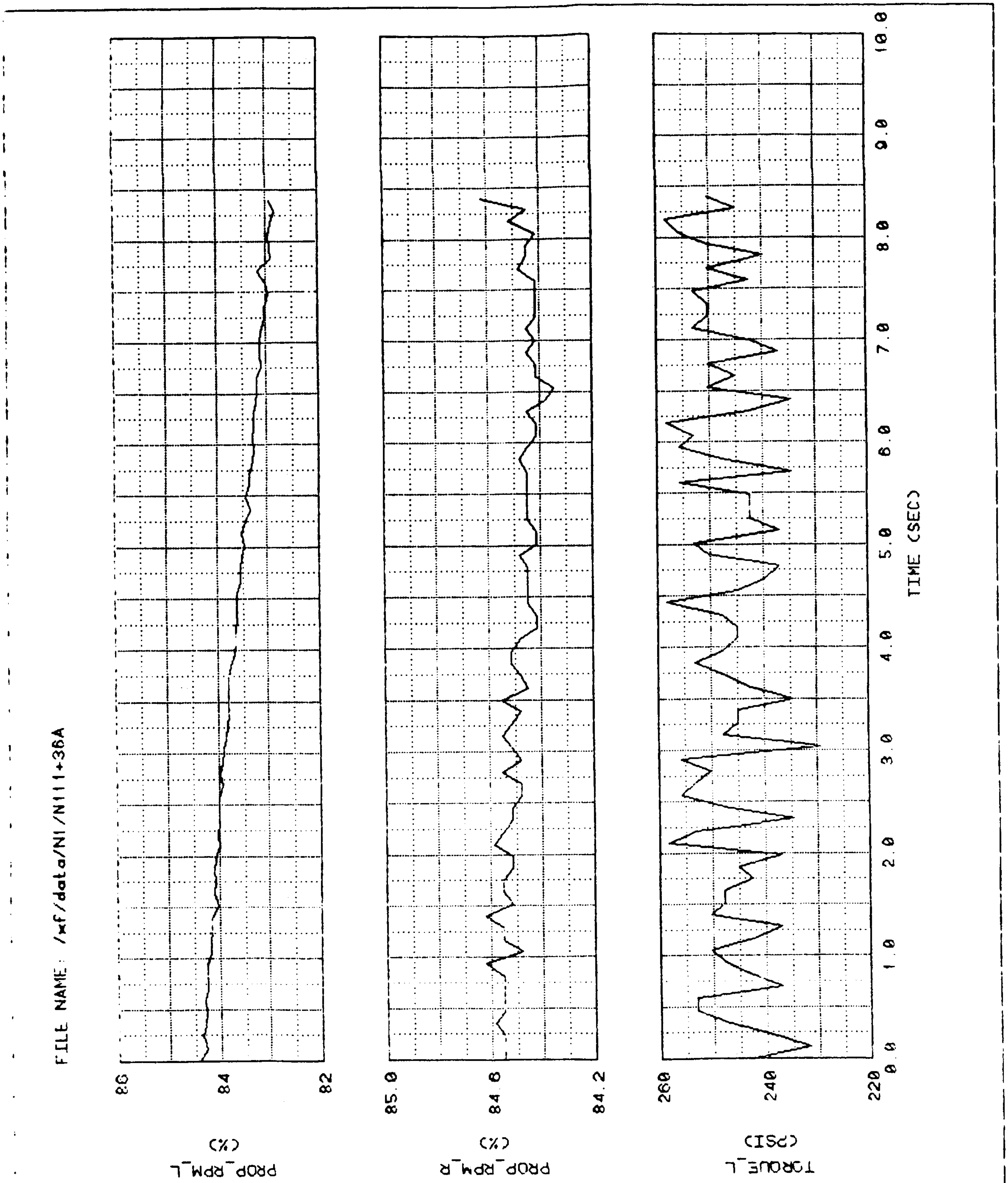

CONV		02/05/86	REVISED	DATE	SIDELSLIP WITH VERT FIN ICED	DHC-6-004
CHECK						
CHECK	G.B.J.	3/14/86			FLT# 11 RUN 36	Fig. 8.1.8f
APPD					KOHLMAN SYSTEMS RESEARCH	8.1.36
DRAWN	17:31:44	03/06/86				

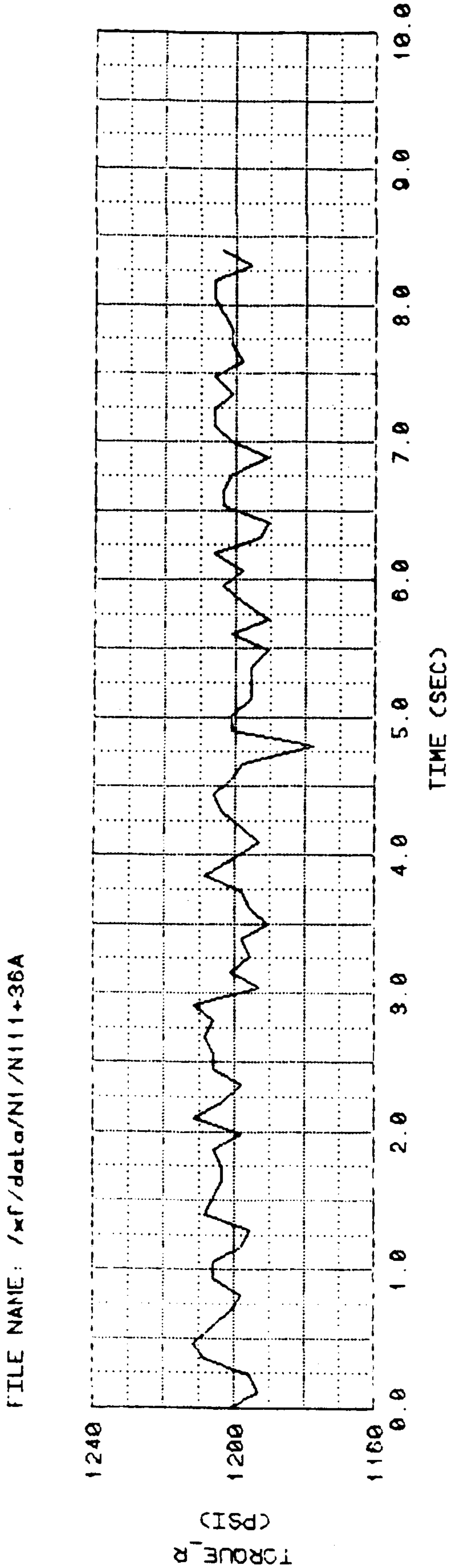

CO		02/05/86	REVISED	DATE	SIDELSLIP WITH VERT. FIN ICED FLT# 11 RUN 36	DHC-6-004
CHECK						
CHECK	D.G.J.	3/14/86				Fig. 8.1.8g
APPD					KOHLMAN SYSTEMS RESEARCH	8.1.37
DRAWN	17:33:22	03/06/86				

SIDESLIP WITH VERT. FIN ICED

INITIAL CONDITIONS FOR TEST NUMBER:

FLIGHT: 11
RUN: 37
AIRCRAFT TYPE: LeRC Twin Otter Icing Flts
SERIAL NUMBER: DHC-6-004

ALT_CAL (FEET)	= 6839.2	N1_L (%)	= 74.9
AIRSPD_CAL (KNOT)	= 84.2	N1_R (%)	= 98.4
AIRSPD_TRU (KNOT)	= 92.4	PROP_RPM_L (%)	= 83.2
MACH_CAL	= 0.144	PROP_RPM_R (%)	= 84.5
DYN_PRS_CA (PSF)	= 24.0	TORQUE_L (ft-lb)	= 258.0
NCLT	= 1.0	TORQUE_R (ft-lb)	= 1204.4
ALPHA_ROS2 (DEG)	= 0.1	FUEL_FLO_L (LB/HR)	= 128.
AMB_PRESS (PSF)	= 1642.9	FUEL_FLO_R (LB/HR)	= 301.
TEMP_AMB (DEGK)	= 269.2	FUELTEMP_L (DEG_K)	= 258.3
AC_WEIGHT (LB)	= 10031.	FUELTEMP_R (DEG_K)	= 257.3
CG_PCT_MAC (%)	= 26.74		
IXX_BODY (SLG-SOFT)	= 15995.		
IYY_BODY (SLG-SOFT)	= 22809.		
IZZ_BODY (SLG-SOFT)	= 35850.		
IXZ_BODY (SLG-SOFT)	= 1102.		
FLAP (DEG)	= 0.0		
DELTA_E (DEG)	= -6.3		
DELTA_A_L (DEG)	= 8.5		
DELTA_R (DEG)	= 2.9		

APPD	QJJ.	3/4/86	CONV	02/05/86
DRAWN	17:33:48	03/06/86		

KOHLMAN SYSTEMS RESEARCH

Fig. 8.1.9a
8.1.38

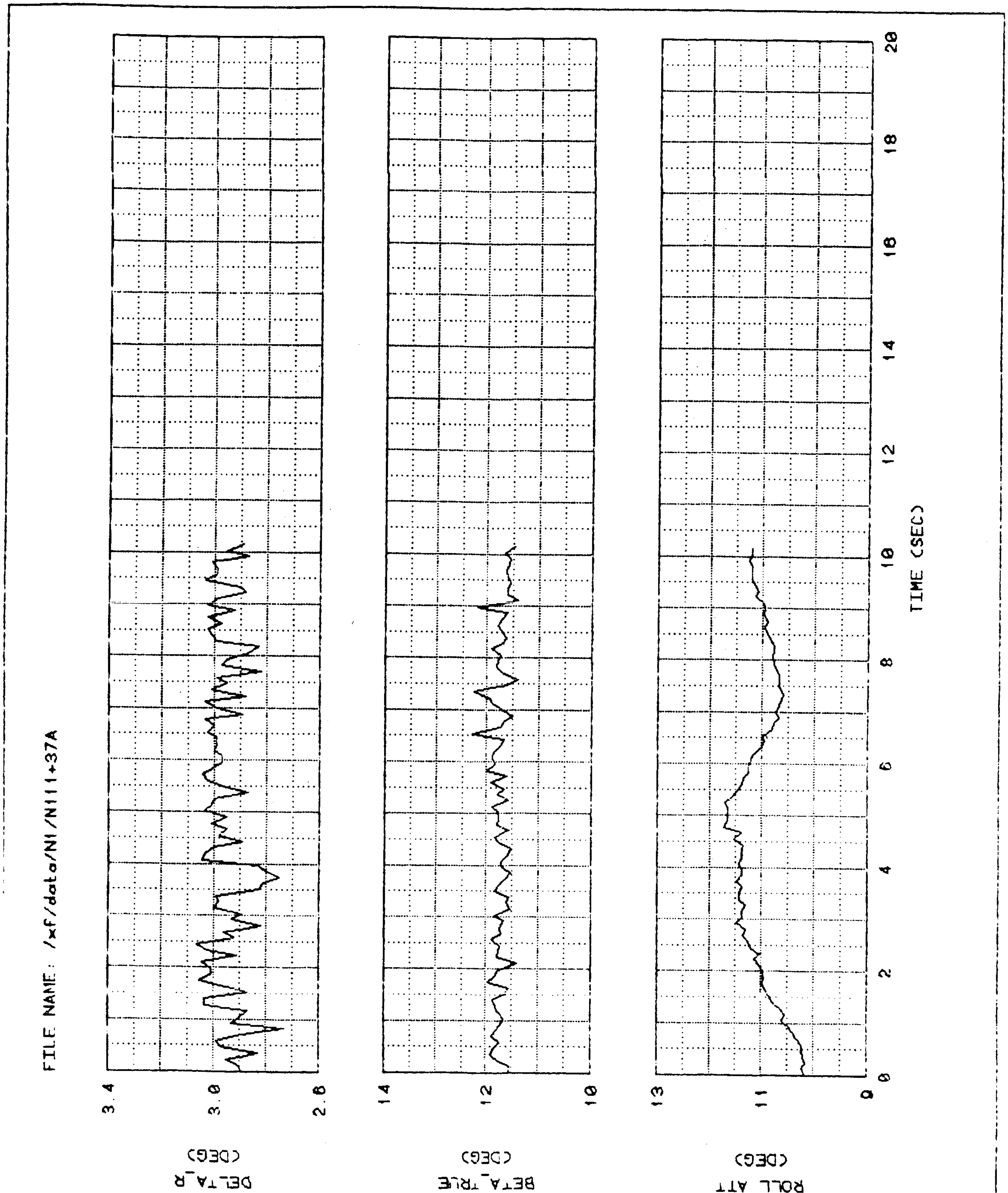

COI		02/05/86	REVISED	DATE	SIDESLIP WITH VERT. FIN ICED	DHC-6-004
CHECK					FLT# 11 RUN 37	
CHECK	J.G.J.	3/14/86				
APPD					KOHLMAN SYSTEMS RESEARCH	Fig. 8.1.9b
DRAWN	17:37:01	03/06/86				8.1.39

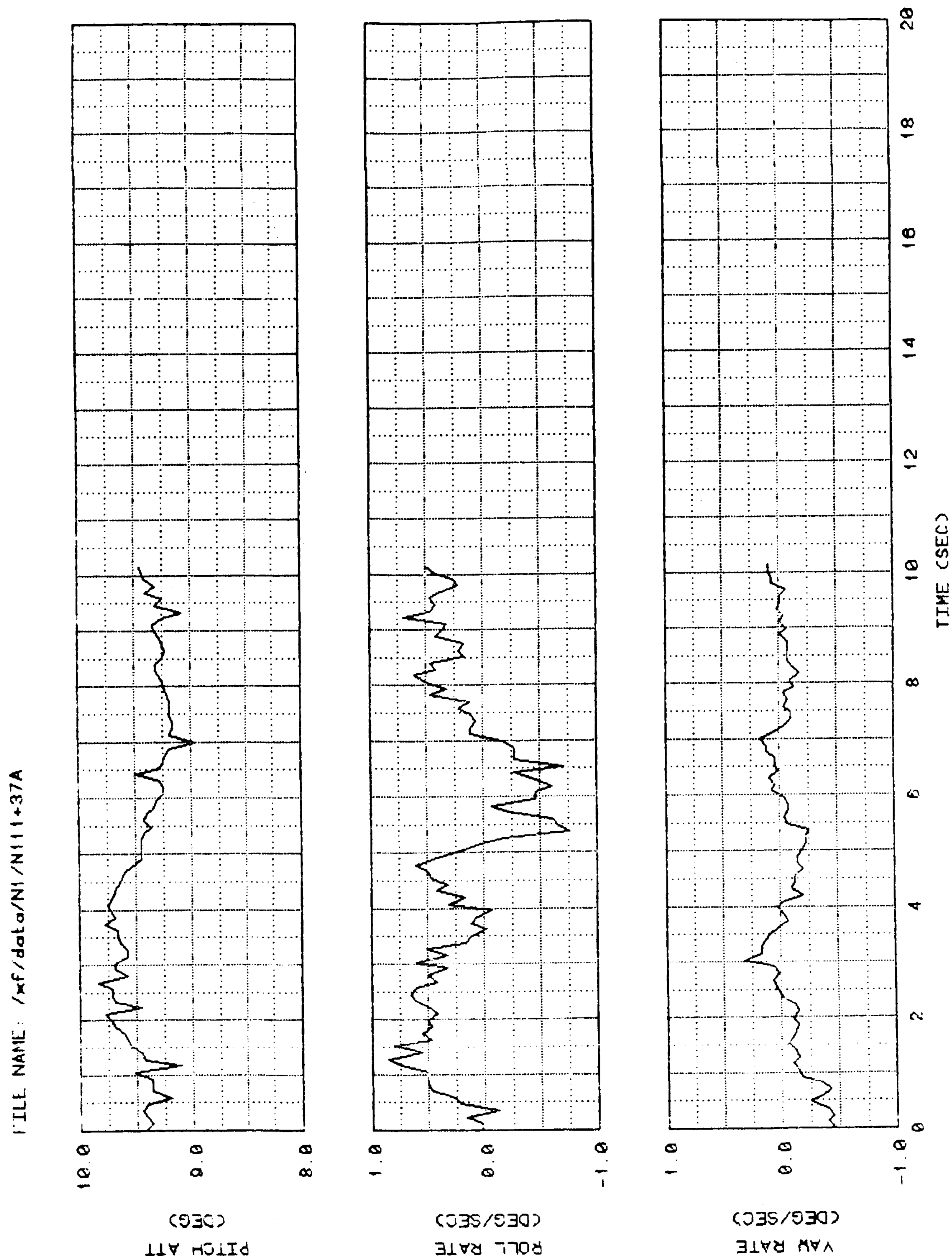

CONV		02/05/86	REVISED	DATE	SIDESLIP WITH VERT. FIN ICED	DHC-6-004
CHECK					FLT# 11 RUN 37	
CHECK	J.L.J.	3/14/86				Fig. 8.1.9c
APPD					KOHLMAN SYSTEMS RESEARCH	8.1.40
DRAWN	17:38:43	03/06/86				

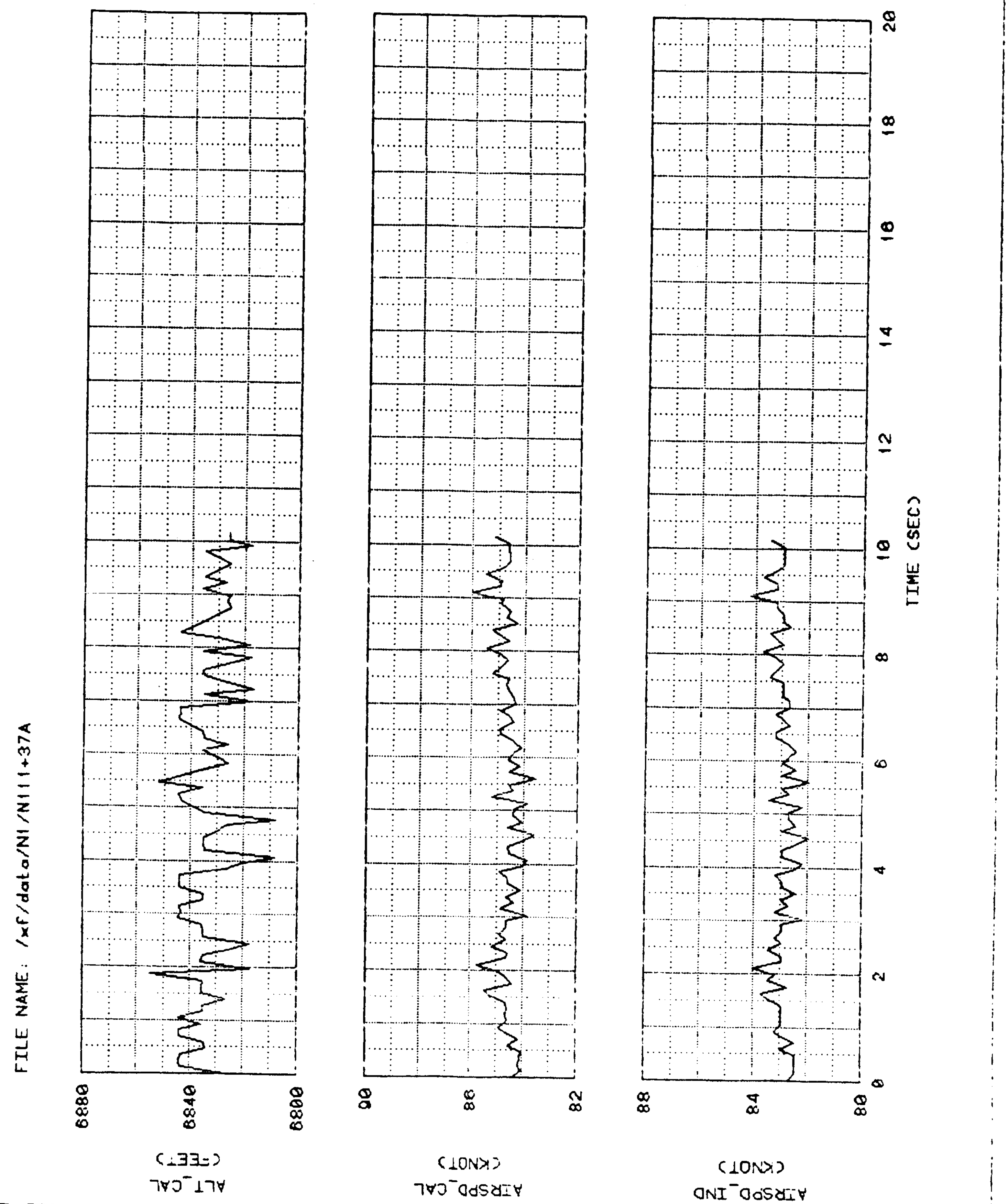

COI		02/05/86	REVISED	DATE	SIDESLIP WITH VERT. FIN ICED	DHC-6-004
CHECK					FLT# 11 RUN 37	
CHECK	J.J.J.	3/14/86				
APPD						Fig. 8.1.9d
DRAWN	17:40:27	03/06/86			KOHLMAN SYSTEMS RESEARCH	8.1.41

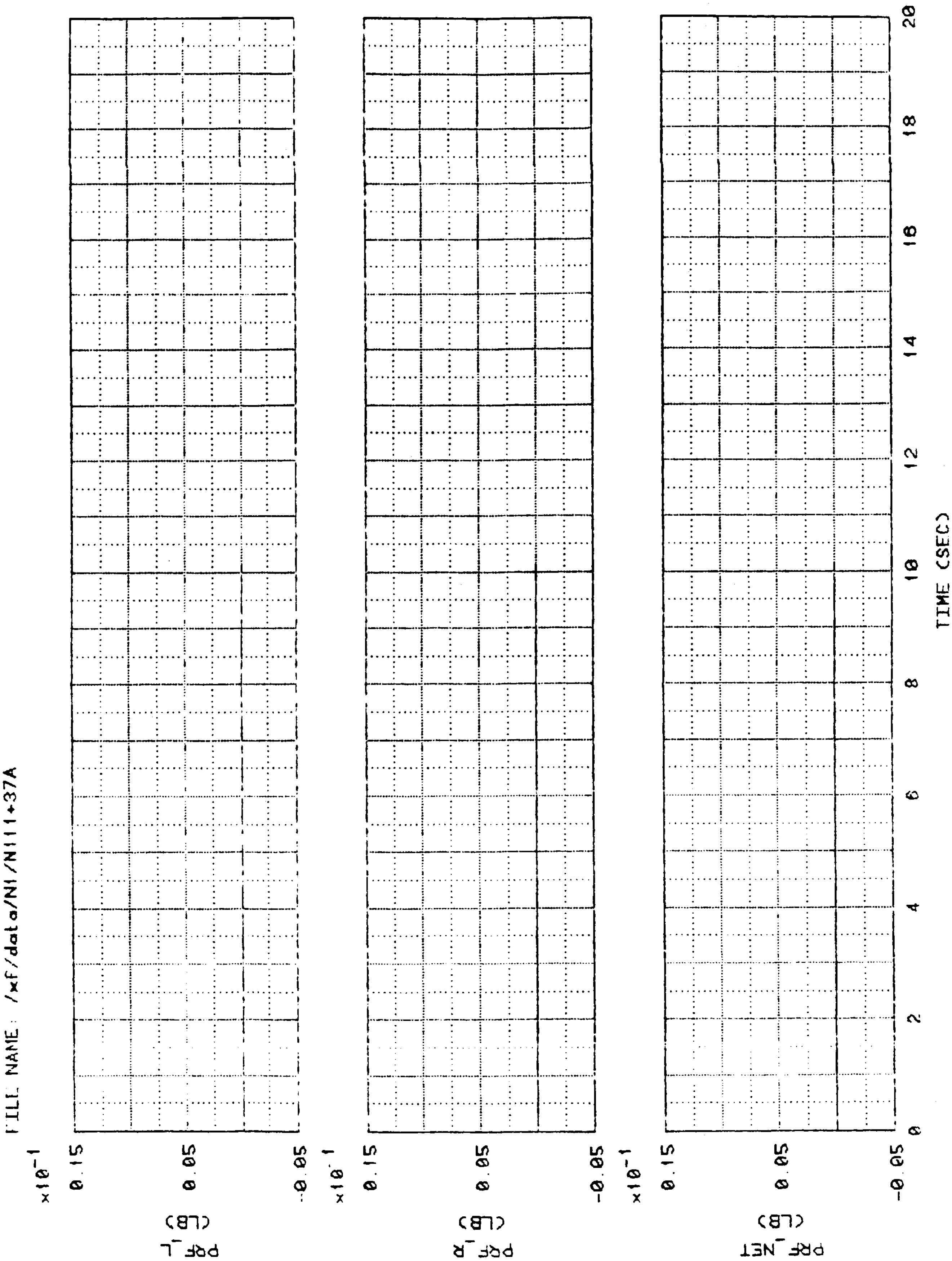

CONV		02/05/86	REVISED	DATE	SIDESLIP WITH VERT. FIN ICED	DHC-6-004
CHECK					FLT# 11 RUN 37	8.1.42
CHECK	[illegible]	3/14/86				
APPD						
DRAWN	17:42:08	03/06/86			KOHLMAN SYSTEMS RESEARCH	Fig. 8.1.9e

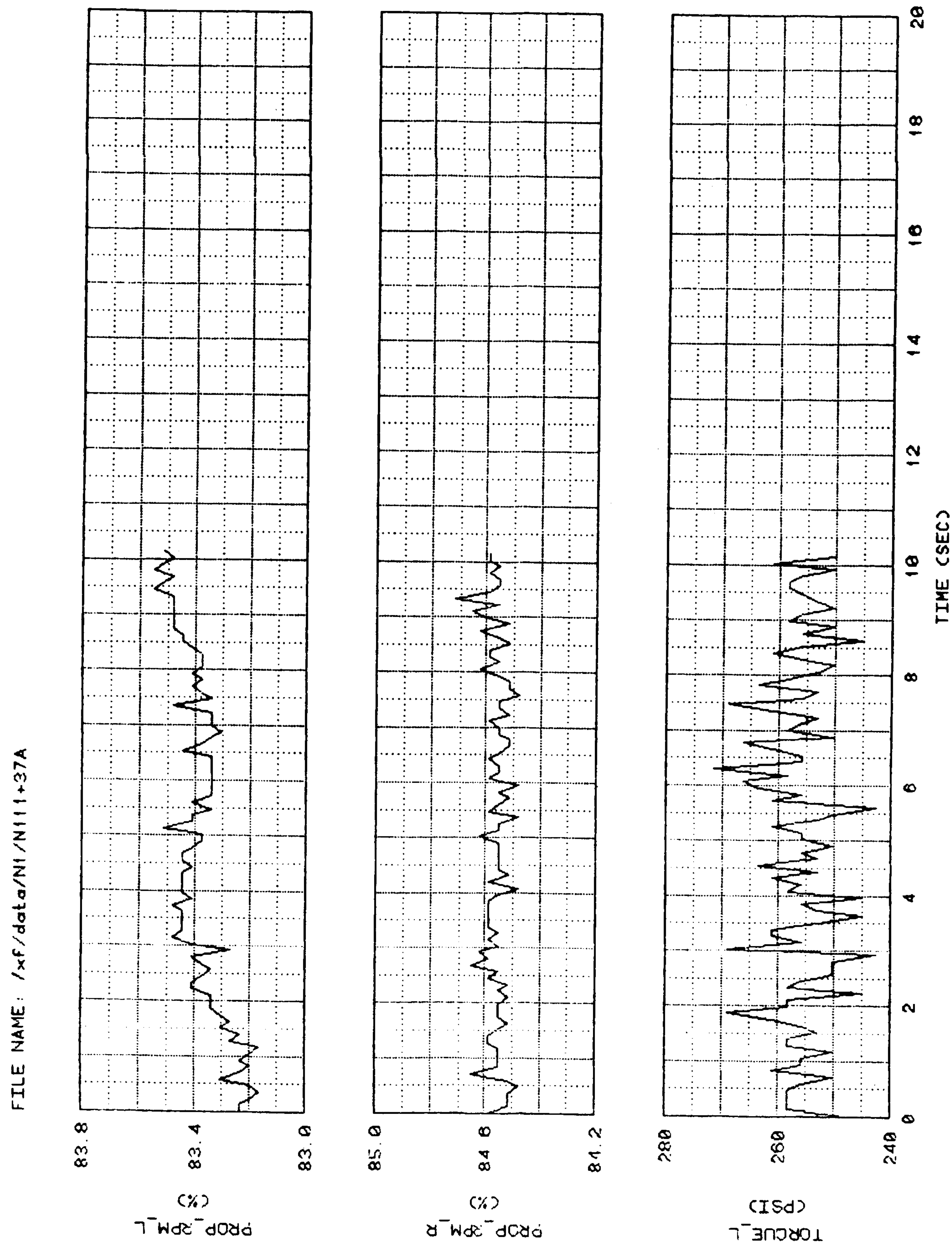

CON		02/05/86	REVISED	DATE	SIDESLIP WITH VERT. FIN ICED FLT# 11 RUN 37	DHC-6-004
CHECK						
CHECK	J.G.J.	3/14/86				
APPD						Fig. 8.1.9f
DRAWN	17:43:52	03/06/86			KOHLMAN SYSTEMS RESEARCH	8.1.43

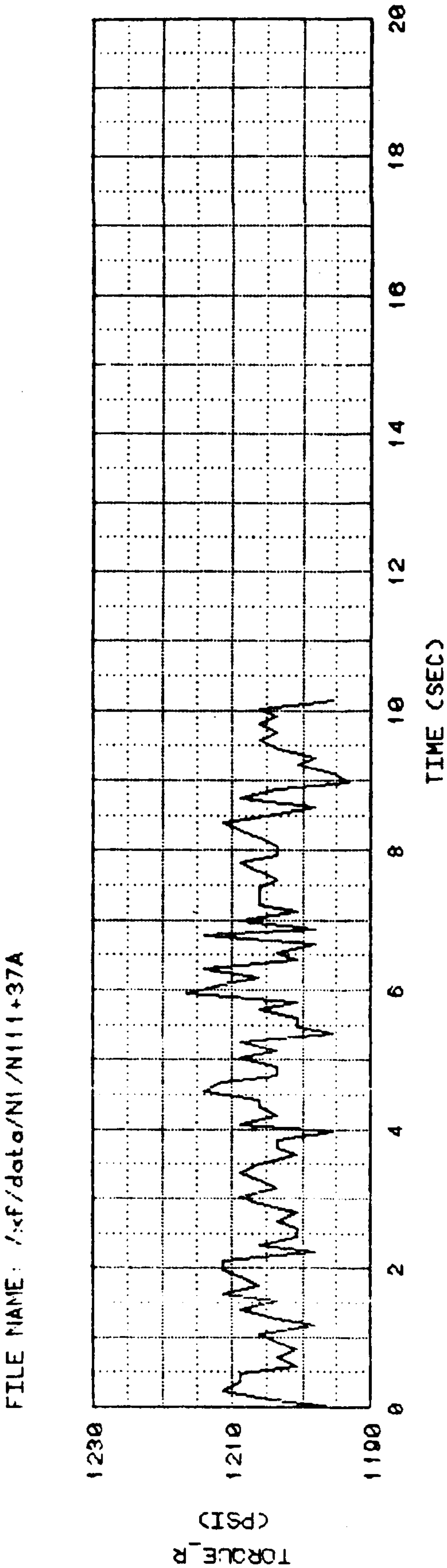

ƆNV		02/05/85	REVISED	DATE	SIDESLIP WITH VERT. FIN ICED	DHC-6-004
ECK					FLT# 11 RUN 37	
ECK	J.L.J.	3/14/86				
D						Fig. 8.1.9g
AWN	17 45 30	03/06/85			KOHLMAN SYSTEMS RESEARCH	8.1.44

SIDELSLIP WITH VERT. FIN ICED

INITIAL CONDITIONS FOR TEST NUMBER:
FLIGHT: 23
RUN: 23
AIRCRAFT TYPE: LaRC Twin Otter Icing Flts
SERIAL NUMBER: DHC-6-004

ALT_CAL (FEET)	= 5781.6	N1_L (%)	= 78.6
AIRSPD_CAL (KNOT)	= 94.5	N1_R (%)	= 90.3
AIRSPD_TRU (KNOT)	= 101.1	PROP_RPM_L (%)	= 94.0
MACH_CAL	= 0.159	PROP_RPM_R (%)	= 95.0
DYN_PRS_CA (PSF)	= 30.2	TORQUE_L (ft-lb)	= 290.9
NCLT	= 0.8	TORQUE_R (ft-lb)	= 1175.0
ALPHA_ROS2 (DEG)	= 0.0	FUEL_FLO_L (LB/HR)	= 147.
AMB_PRESS (PSF)	= 1709.9	FUEL_FLO_R (LB/HR)	= 335.
TEMP_AMB (DEGK)	= 266.5	FUELTEMP_L (DEG_K)	= 257.6
AC_WEIGHT (LB)	= 9920.	FUELTEMP_R (DEG_K)	= 257.7
CG_PCT_MAC (%)	= 26.84		
IXX_BODY (SLG-SQFT)	= 15957.		
IYY_BODY (SLG-SQFT)	= 22728.		
IZZ_BODY (SLG-SQFT)	= 35798.		
IXZ_BODY (SLG-SQFT)	= 1096.		
FLAP (DEG)	= 11.5		
DELTA_E (DEG)	= 2.8		
DELTA_A_L (DEG)	= 5.6		
DELTA_R (DEG)	= 1.1		

APPD	J.G.J.	3/14/86	CONV	02/10/86	KOHLMAN SYSTEMS RESEARCH	Fig. 8.1.10a
DRAWN	17:45:53	03/06/86				8.1.45

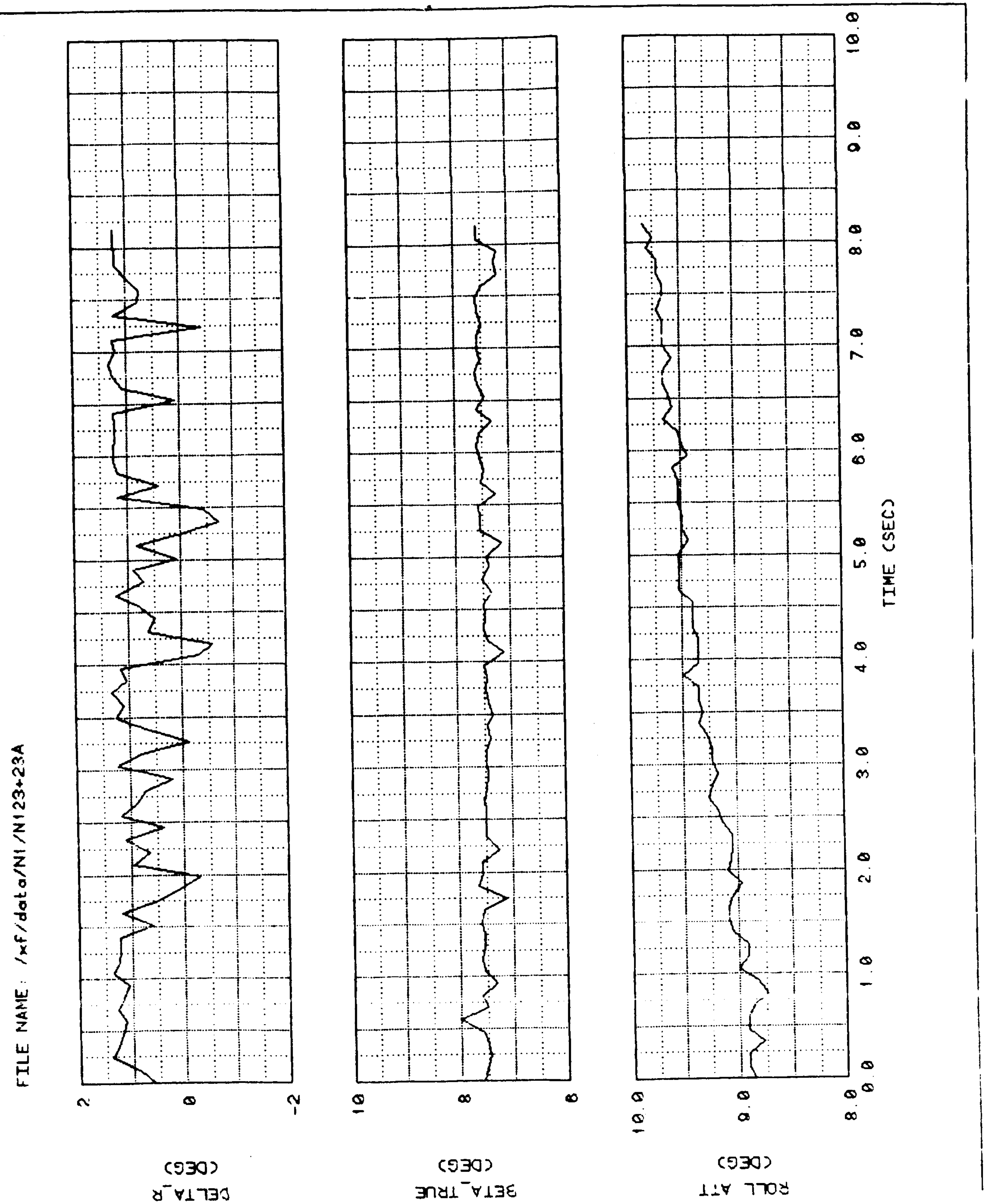

CONV		02/10/86	REVISED	DATE
CHECK				
CHECK		3/14/86		
APPD				
DRAWN	17:49:07	03/08/86		

SIDELSLIP WITH VERT. FIN ICED

FLT# 23 RUN 23

KOHLMAN SYSTEMS RESEARCH

DHC-6-004

Fig. 8.1.10b

8.1.46

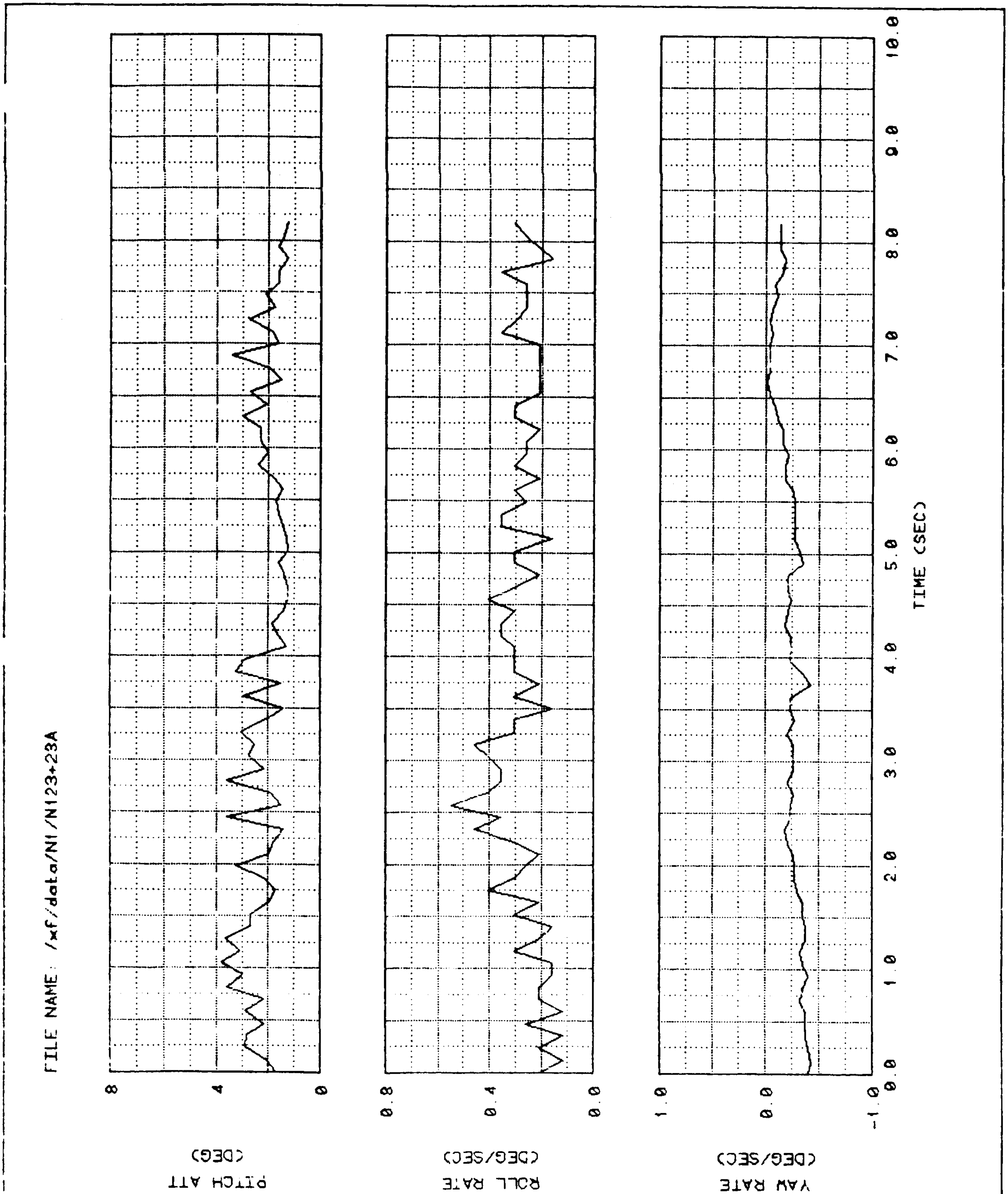

NV		02/10/86	REVISED	DATE	SIDELSLIP WITH VERT FIN ICED	DHC-6-004
CHECK					FLT# 23 RUN 23	
CHECK	J.J.J.	3/14/86				
APPD						Fig. 8.1.10
DRAWN	19:08:22	03/06/86			KOHLMAN SYSTEMS RESEARCH	8.1.47

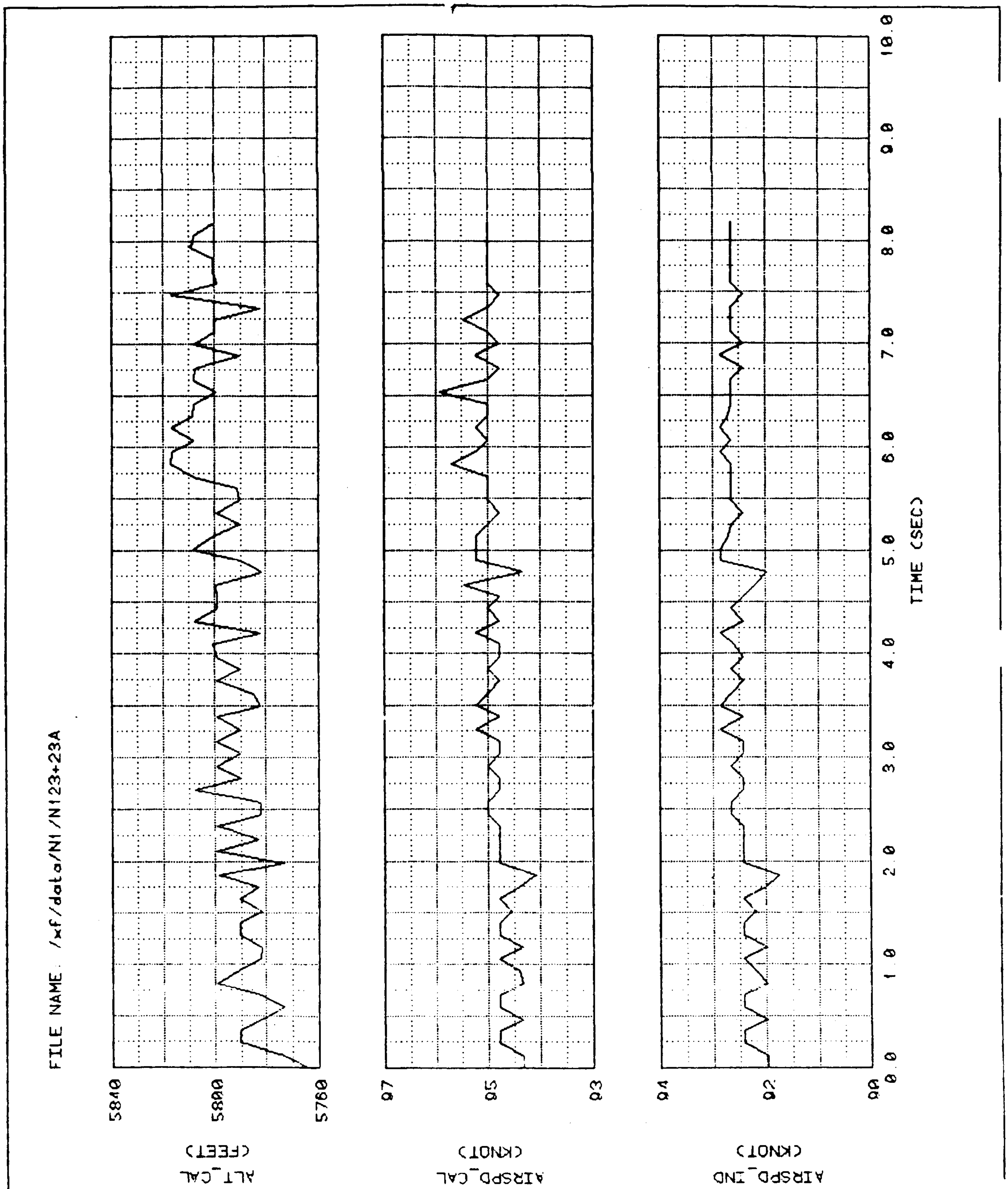

CONV		02/10/86	REVISED	DATE	SIDELSLIP WITH VERT FIN ICED	DHC-6-004
CHECK					FLT# 23 RUN 23	
CHECK		3/14/86				Fig. 8.1.10d
APPD						
DRAWN	19:10:06	03/06/86			KOHLMAN SYSTEMS RESEARCH	8.1.48

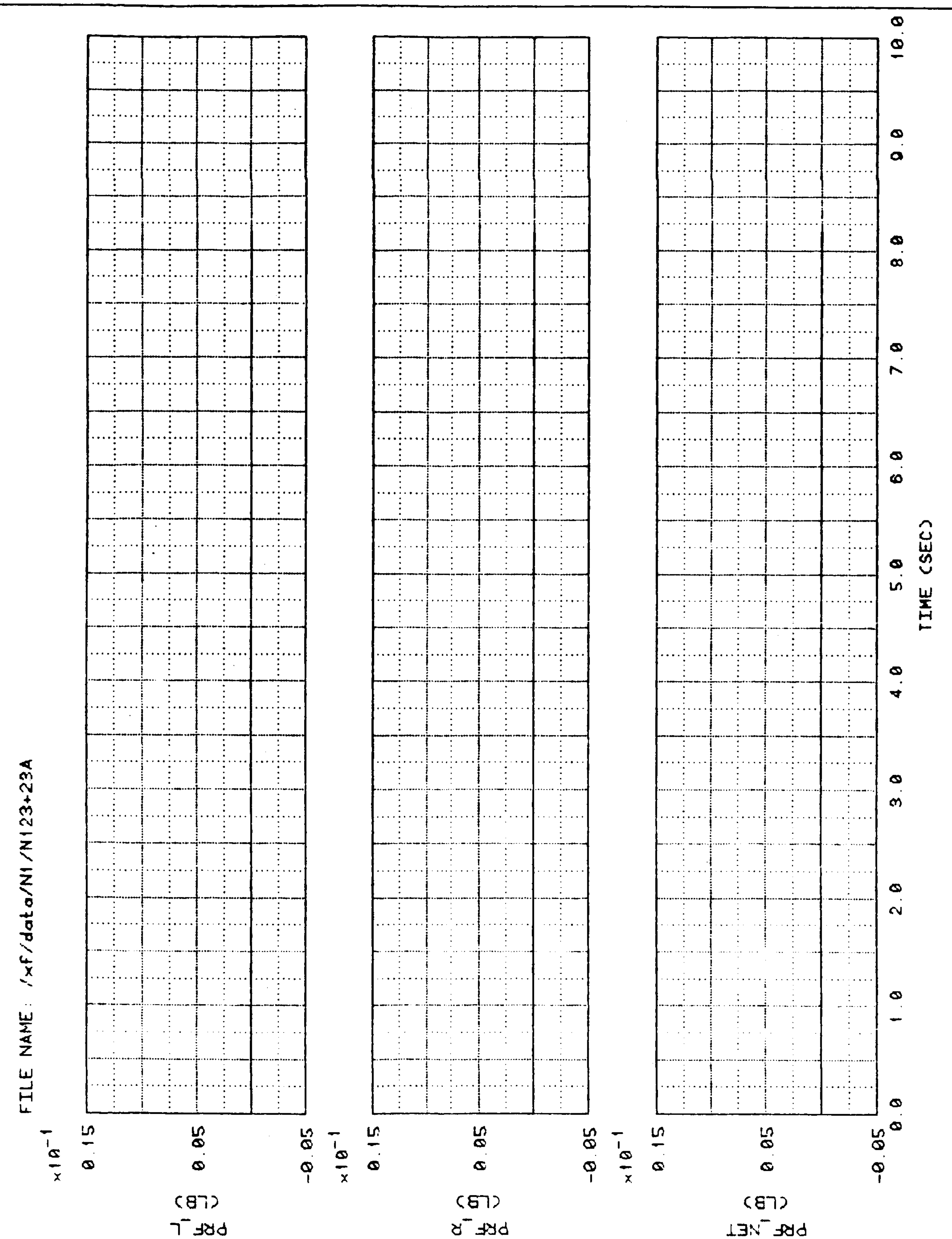

ENV		02/10/86	REVISED	DATE	SIDELSLIP WITH VERT. FIN ICED	DHC-6-004
CHECK					FLT# 23 RUN 23	
CHECK	J.J.J.	3/14/86				Fig. 8.1.10e
APPD						
DRAWN	19:11:47	03/05/85			KOHLMAN SYSTEMS RESEARCH	8.1.49

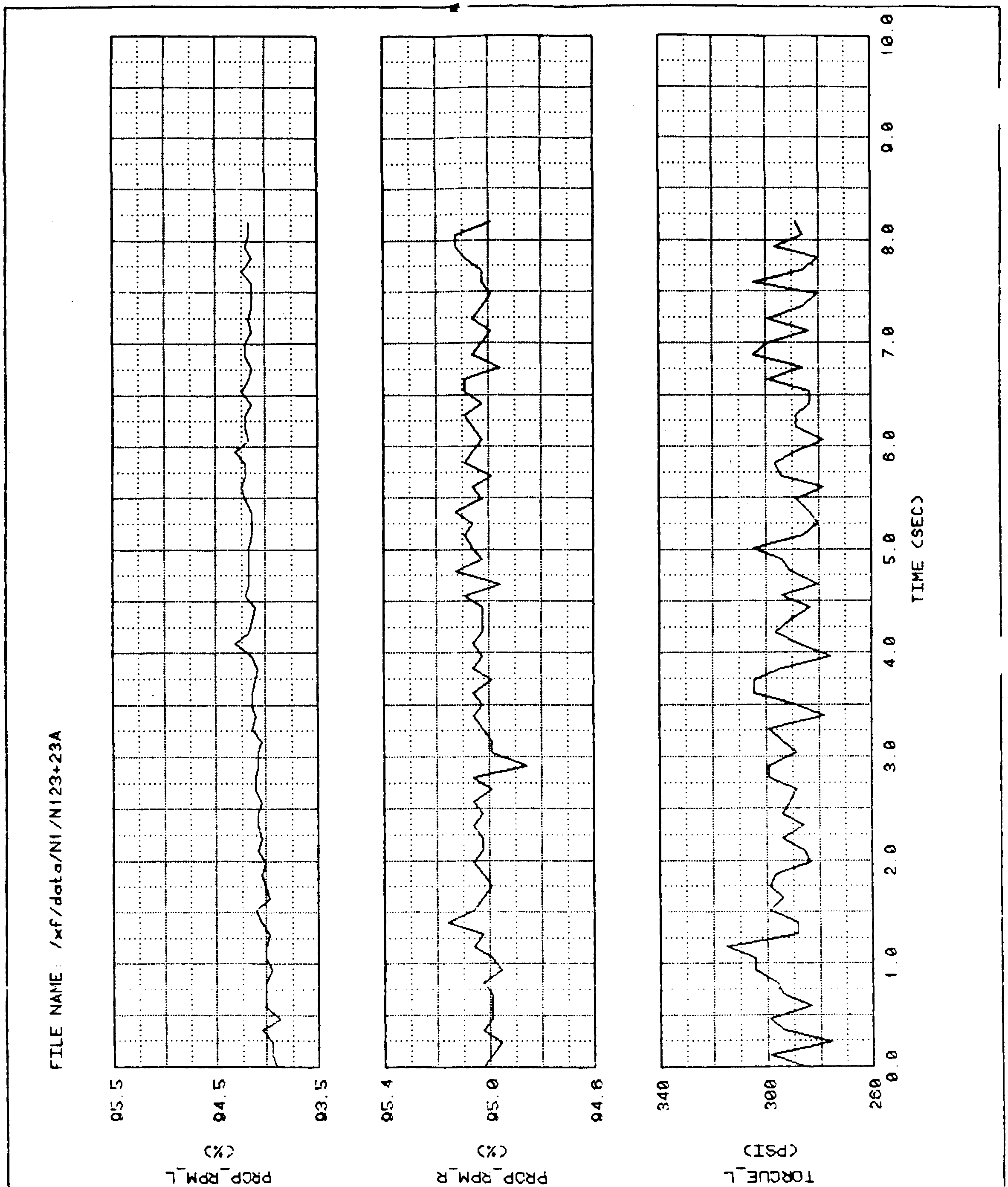

CONV		02/10/85	REVISED	DATE	SIDELSLIP WITH VERT. FIN ICED	DHC-6-004
CHECK					FLT# 23 RUN 23	
CHECK	J.C.J.	3/14/86				
APPD						Fig. 8.1.10f
DRAWN	19:13:30	03/05/85			KOHLMAN SYSTEMS RESEARCH	8.1.50

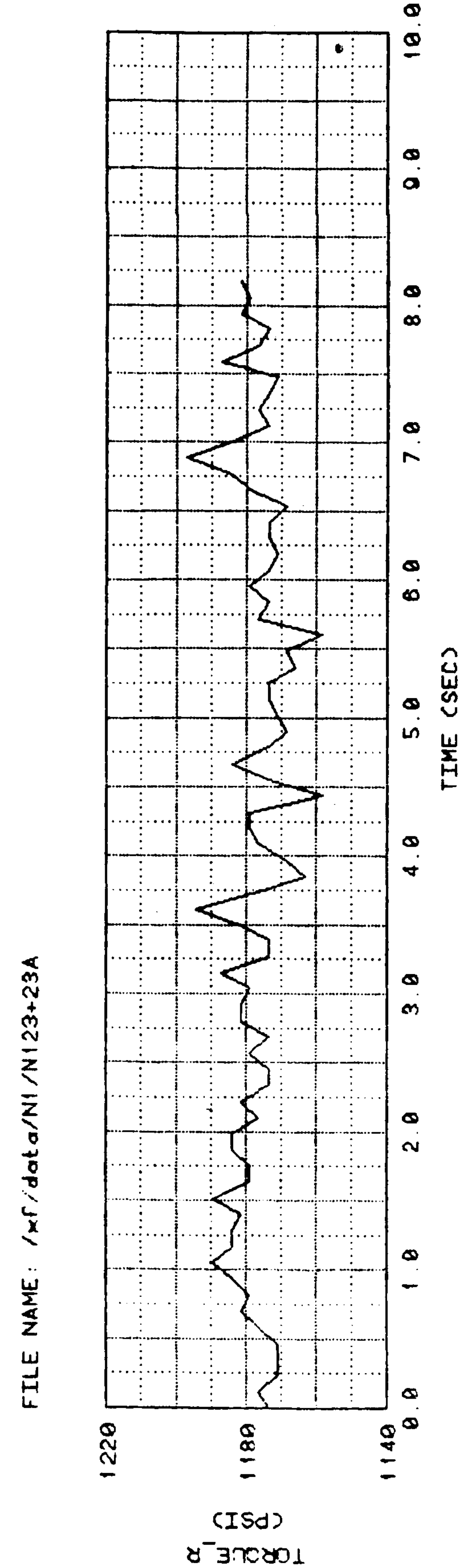

NV		02/10/86	REVISED	DATE	SIDELSLIP WITH VERT. FIN ICED	DHC-6-004
CHECK					FLT# 23 RUN 23	
CHECK	J.J.J.	3/4/86				
APPD						Fig. 8.1.10j
DRAWN	10:15:08	03/08/85			KOHLMAN SYSTEMS RESEARCH	8.1.51

SIDELSLIP WITH VERT. FIN ICED

INITIAL CONDITIONS FOR TEST NUMBER:

FLIGHT: 23
RUN: 24
AIRCRAFT TYPE: LaRC Twin Otter Icing Flts
SERIAL NUMBER: DHC-6-004

ALT_CAL (FEET)	= 5482.2	N1_L (%)	= 78.5
AIRSPD_CAL (KNOT)	= 88.8	N1_R (%)	= 90.3
AIRSPD_TRU (KNOT)	= 94.7	PROP_RPM_L (%)	= 90.9
MACH_CAL	= 0.140	PROP_RPM_R (%)	= 95.0
DYN_PRS_CA (PSF)	= 26.7	TORQUE_L (ft-lb)	= 310.8
NCLT	= 0.9	TORQUE_R (ft-lb)	= 1173.7
ALPHA_ROS2 (DEG)	= 0.0	FUEL_FLO_L (LB/HR)	= 150.
AMB_PRESS (PSF)	= 1720.2	FUEL_FLO_R (LB/HR)	= 338.
TEMP_AMB (DEGK)	= 288.0	FUELTEMP_L (DEG_K)	= 257.5
AC_WEIGHT (LB)	= 9910.	FUELTEMP_R (DEG_K)	= 257.6
CG_PCT_MAC (%)	= 26.85		
IXX_BODY (SLG-SQFT)	= 15953.		
IYY_BODY (SLG-SQFT)	= 22719.		
IZZ_BODY (SLG-SQFT)	= 35793.		
IXZ_BODY (SLG-SQFT)	= 1096.		
FLAP (DEG)	= 11.5		
DELTA_E (DEG)	= 1.3		
DELTA_A_L (DEG)	= 7.1		
DELTA_R (DEG)	= 1.8		

APPD	J.J.J.	3/14/86	CONV	02/10/86
DRAWN	19 15:34	03/06/86		

KOHLMAN SYSTEMS RESEARCH

Fig. 8.1.11a

8.1.52

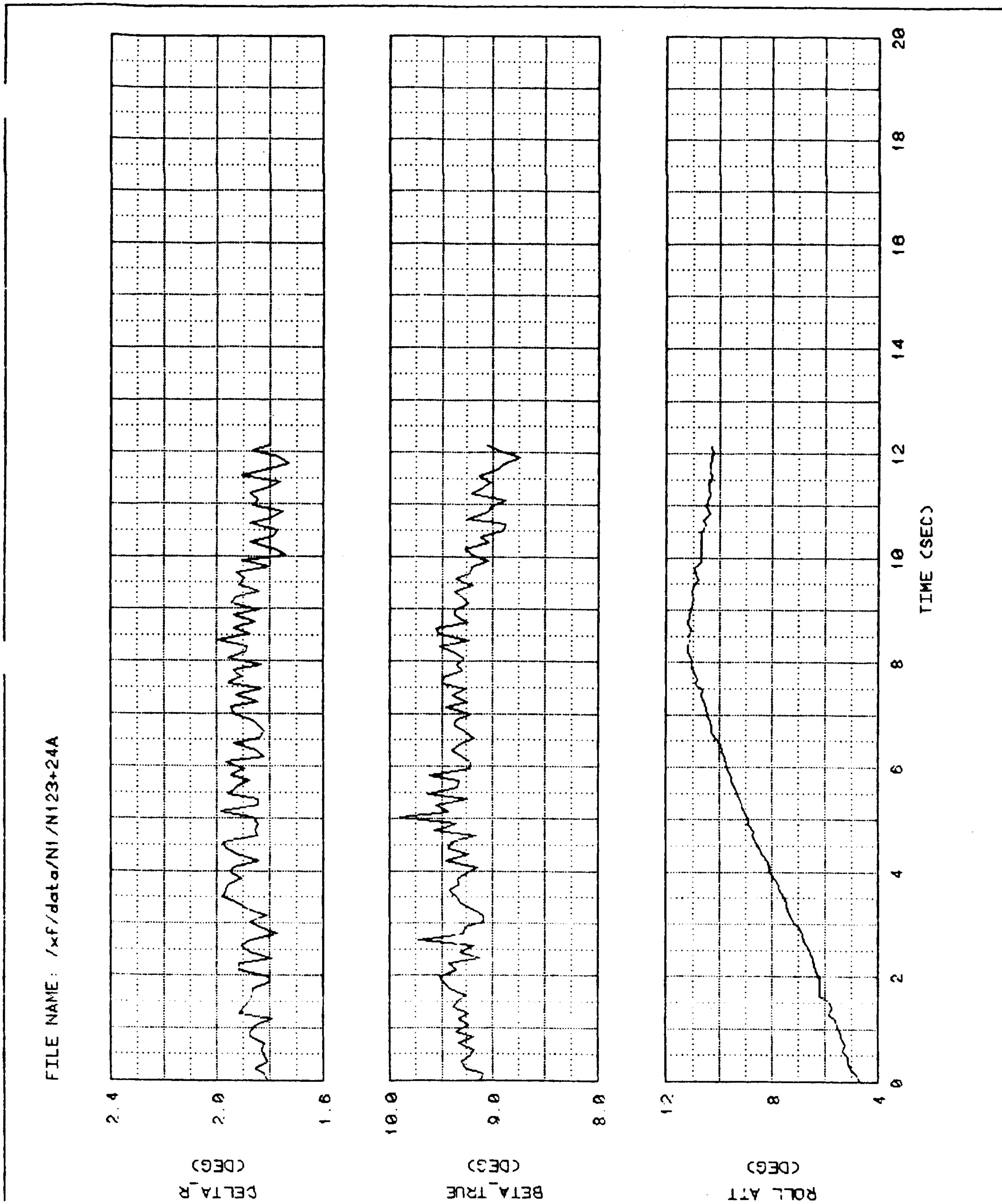

NV		02/10/85	REVISED	DATE	SIDELSLIP WITH VERT FIN ICED	DHC-6-004
CHECK					FLT# 23 RUN 24	
CHECK	[signature]	3/14/86				
APPD						Fig. 8.1.11b
DRAWN	10 18 43	03/06/86			KOHLMAN SYSTEMS RESEARCH	8.1.53

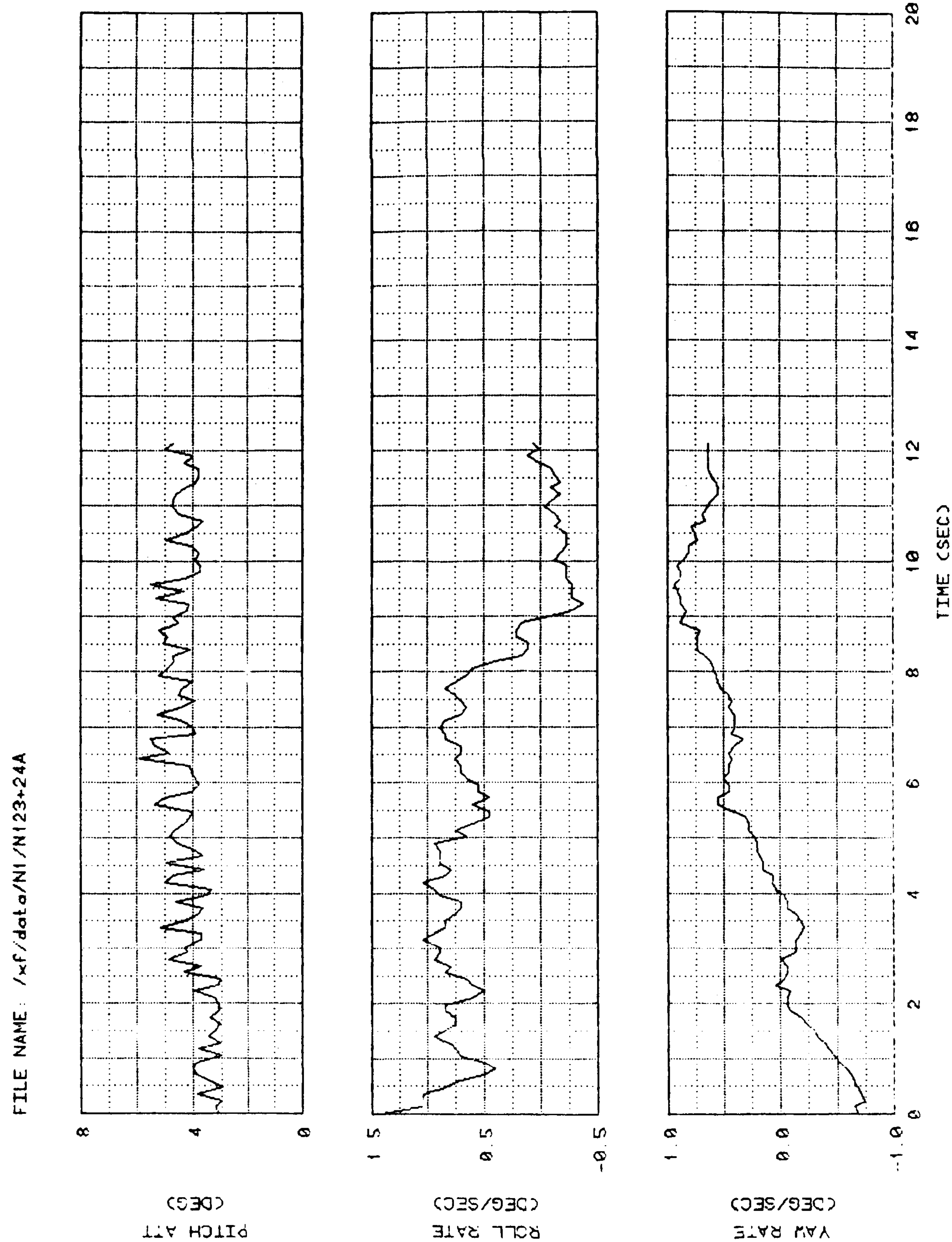

CONV		02/10/86	REVISED	DATE	SIDELSLIP WITH VERT FIN ICED	DHC-6-004
CHECK					FLT# 23 RUN 24	
CHECK	J.T.J.	3/4/86				Fig. 8.1.11c
APPD					KOHLMAN SYSTEMS RESEARCH	8.1.54
DRAWN	10:22:34	03/05/86				

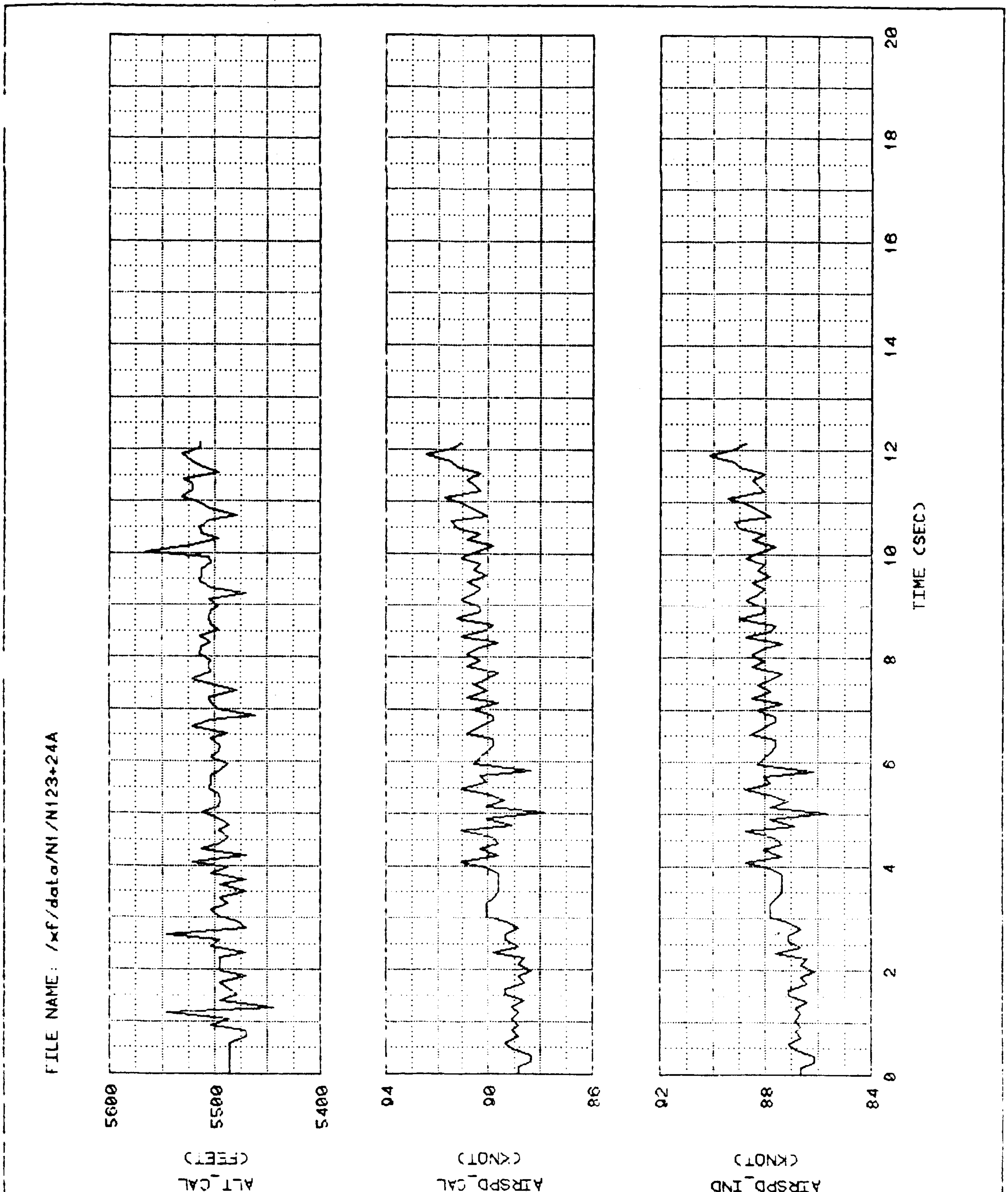

IV		02/10/86	REVISED	DATE
CHECK				
CHECK	J.J.J.	3/14/86		
APPD				
DRAWN	19:33:58	03/06/86		

SIDESLIP WITH VERT. FIN ICED

FLT# 23 RUN 24

KOHLMAN SYSTEMS RESEARCH

DHC-6-004

Fig. 8.1.11d

8.1.55

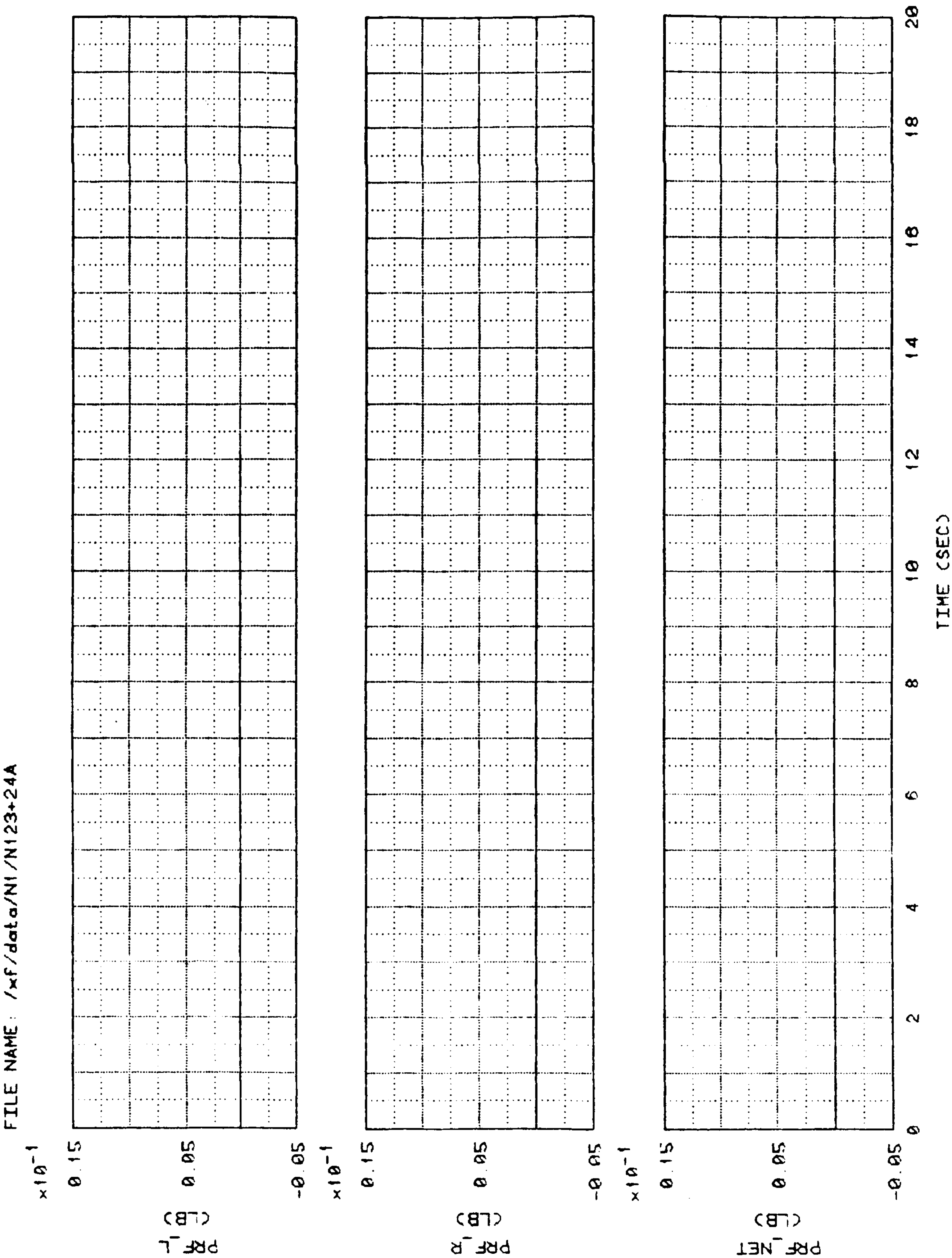

CONV		02/10/85	REVISED	DATE	SIDELSLIP WITH VERT. FIN ICED	DHC-6-004
CHECK					FLT# 23 RUN 24	
CHECK	J.Y.G.	3/14/86				
APPD						Fig. 8.1.11e
DRAWN	19:35:46	03/06/86			KOHLMAN SYSTEMS RESEARCH	B.1.56

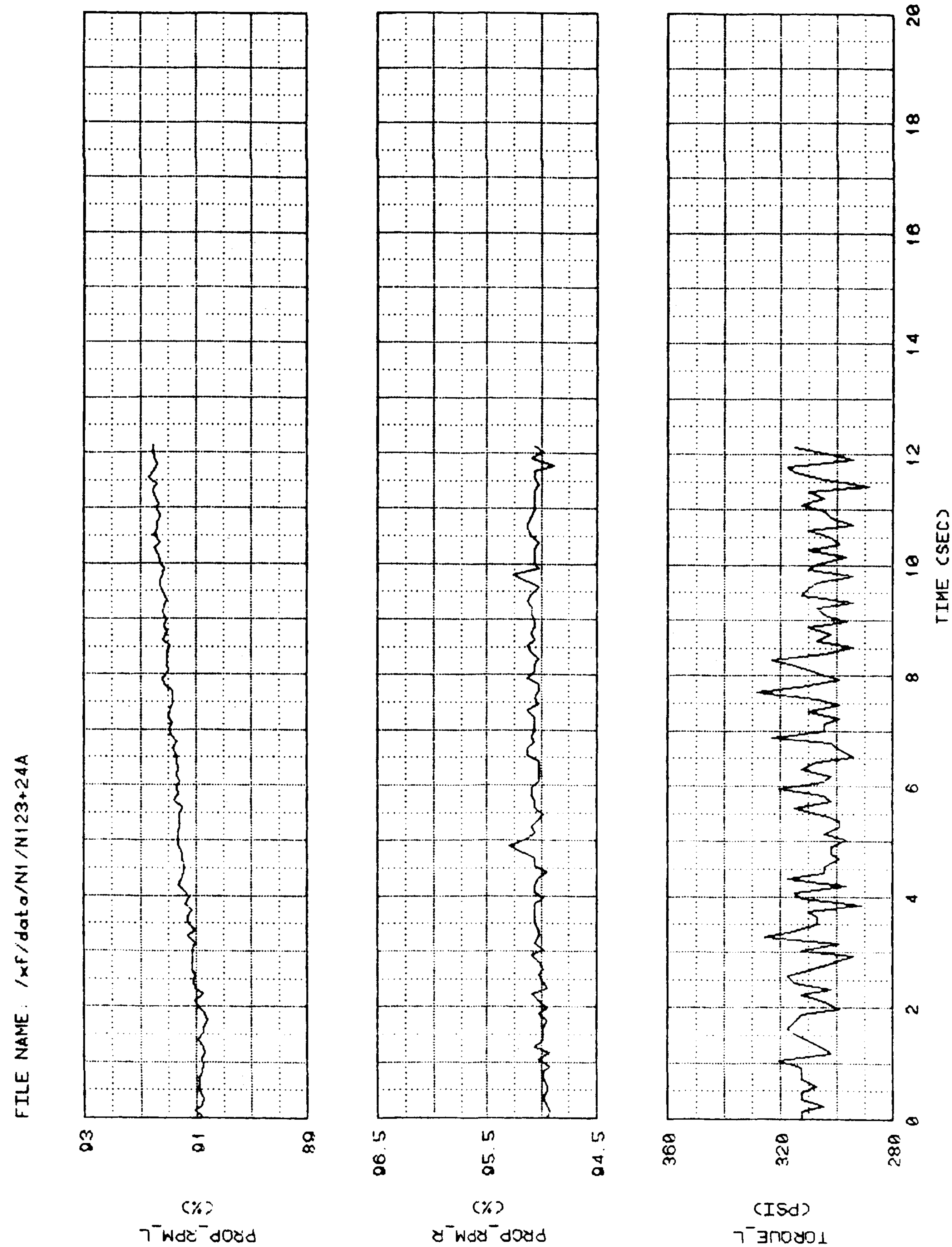

NV		02/10/86	REVISED	DATE	SIDELSLIP WITH VERT FIN ICED	DHC-6-004
CHECK					FLT# 23 RUN 24	
CHECK	[illegible]	3/14/86				Fig. 8.1.11f
APPD					KOHLMAN SYSTEMS RESEARCH	
DRAWN	10:37:20	03/06/86				8.1.57

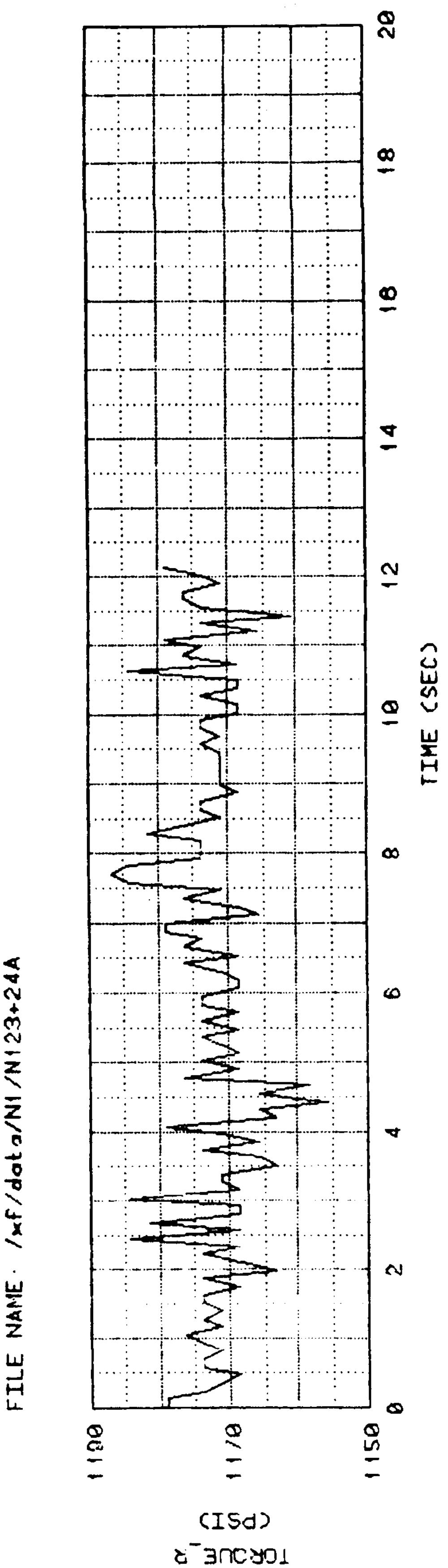

CONV		02/10/86	REVISED	DATE
CHECK				
CHECK	J.J.J.	3/14/86		
APPD				
DRAWN	19 39 08	03/05/86		

SIDELSLIP WITH VERT. FIN ICED

FLT# 23 RUN 24

KOHLMAN SYSTEMS RESEARCH

DHC-6-004

Fig. 8.1.11g

8.1.58

SIDESLIP WITH VERTICAL FIN ICED

INITIAL CONDITIONS FOR TEST NUMBER:

FLIGHT: 23

RUN: 25

AIRCRAFT TYPE: LeRC Twin Otter Icing Flts

SERIAL NUMBER: DHC-6-004

ALT_CAL (FEET)	=	5083.6	N1_L (%)	=	77.3
AIRSPD_CAL (KNOT)	=	88.9	N1_R (%)	=	99.3
AIRSPD_TRU (KNOT)	=	92.0	PROP_RPM_L (%)	=	88.7
MACH_CAL	=	0.144	PROP_RPM_R (%)	=	94.7
DYN_PRS_CA (PSF)	=	25.5	TORQUE_L (ft-lb)	=	268.1
NCLT	=	0.9	TORQUE_R (ft-lb)	=	1181.5
ALPHA_ROS2 (DEG)	=	0.0	FUEL_FLO_L (LB/HR)	=	144.
AMB_PRESS (PSF)	=	1755.3	FUEL_FLO_R (LB/HR)	=	341.
TEMP_AMB (DEGK)	=	268.0	FUELTEMP_L (DEG_K)	=	257.4
AC_WEIGHT (LB)	=	9809.	FUELTEMP_R (DEG_K)	=	257.4
CG_PCT_MAC (%)	=	28.86			
IXX_BODY (SLG-SQFT)	=	15949.			
IYY_BODY (SLG-SQFT)	=	22710.			
IZZ_BODY (SLG-SQFT)	=	35788.			
IXZ_BODY (SLG-SQFT)	=	1095.			
FLAP (DEG)	=	11.6			
DELTA_E (DEG)	=	1.2			
DELTA_A_L (DEG)	=	7.4			
DELTA_R (DEG)	=	2.2			

APPD	J.G.G.	3/14/86	CONV	02/10/86
DRAWN	10:30:34	03/06/86		

KOHLMAN SYSTEMS RESEARCH

REV A
Fig. 8.1.12a
8.1.59

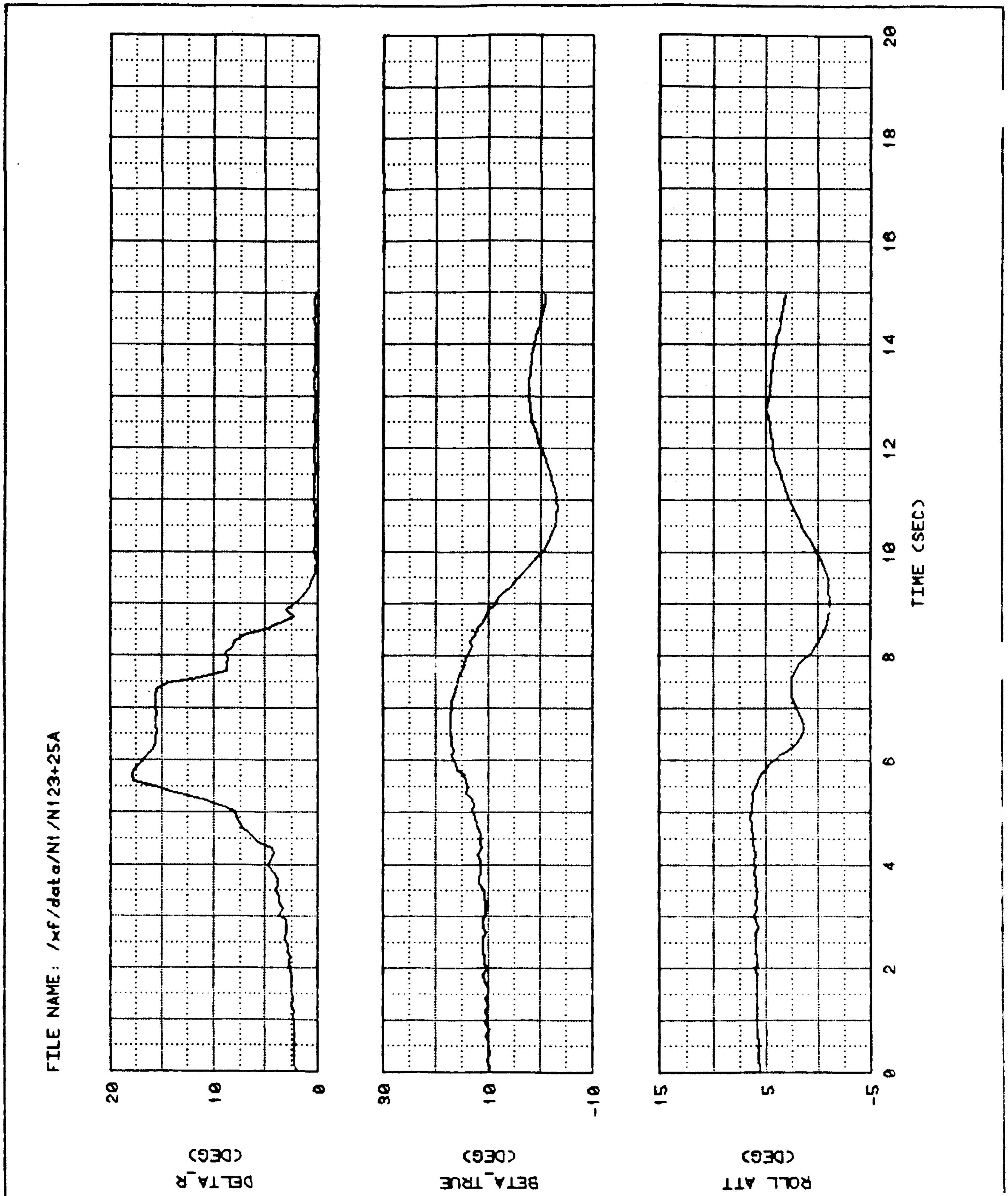

CONV		02/10/86	REVISED	DATE	SIDESLIP WITH VERTICAL FIN ICED	DHC-6-004
CHECK					FLT# 23 RUN 25	
CHECK	J.J.J.	3/14/86				REV A Fig. 8.1.12b
APPD						
DRAWN	20:45:00	03/06/86			KOHLMAN SYSTEMS RESEARCH	8.1.60

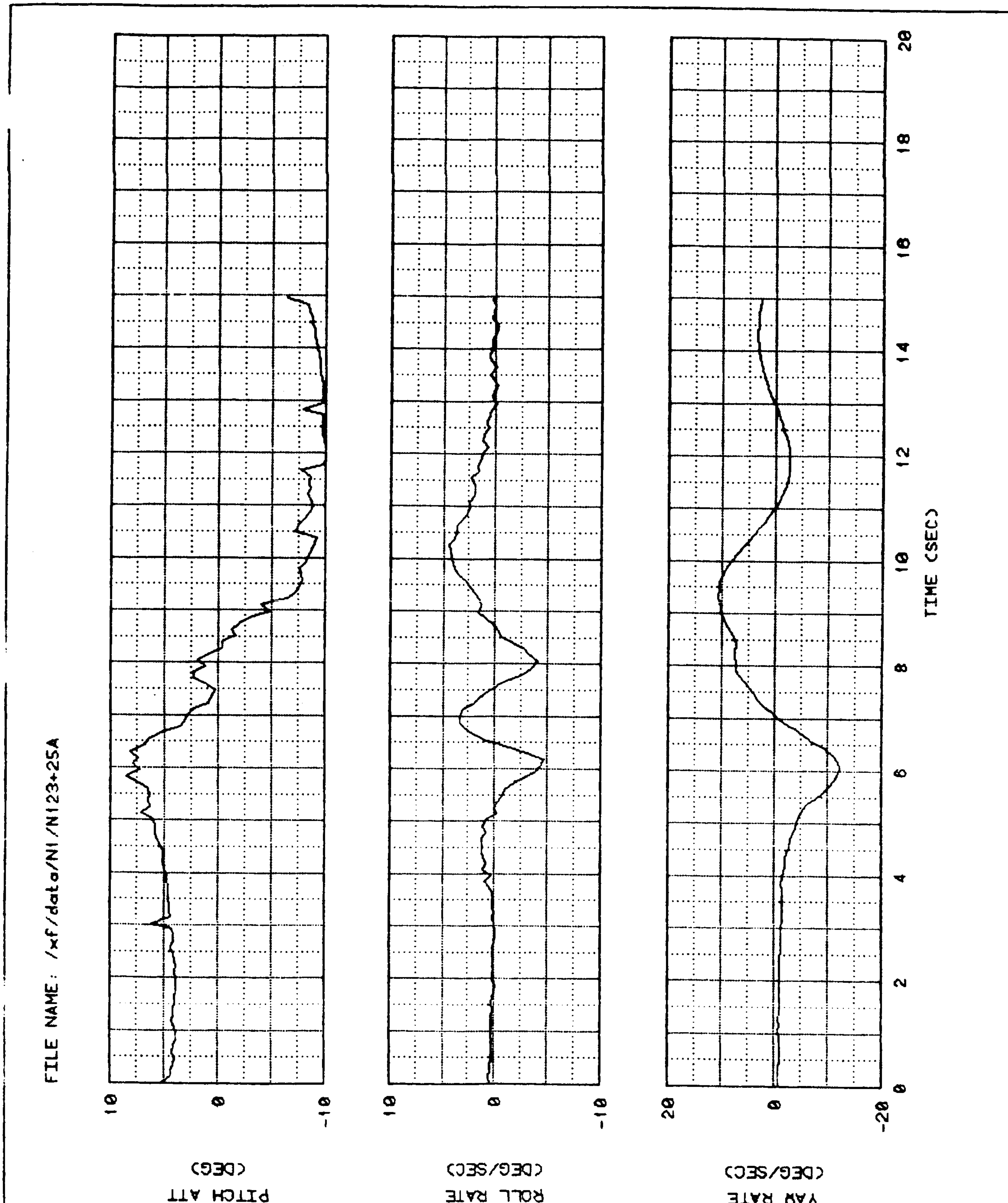

IV		02/10/85	REVISED	DATE	SIDESLIP WITH VERTICAL FIN ICED	DHC-6-004
CHECK					FLT# 23 RUN 25	
CHECK	JGJ.	3/14/86				REV A
APPD						Fig. 8.1.12c
DRAWN	21:01:54	03/06/86			KOHLMAN SYSTEMS RESEARCH	8.1.61

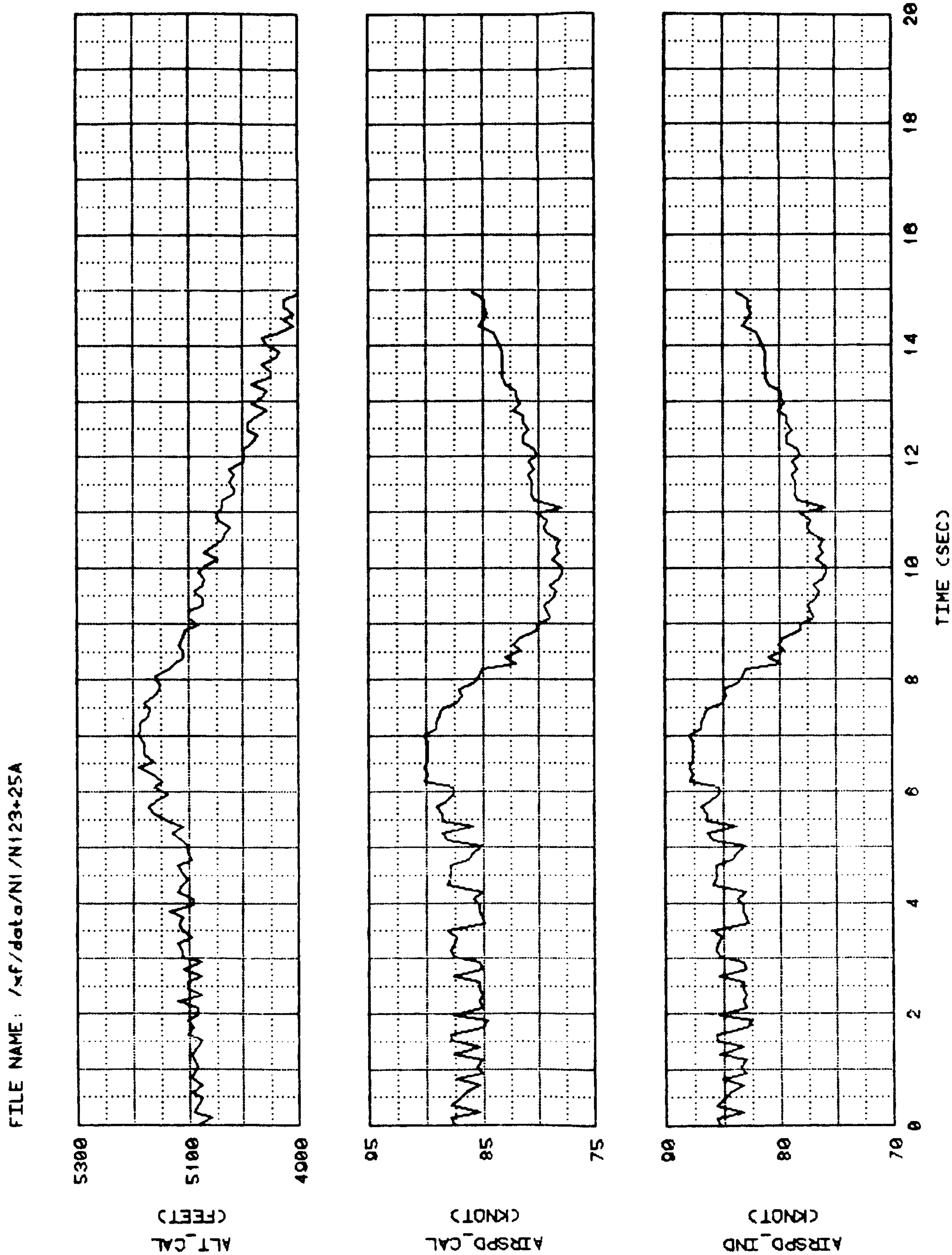

CONV		02/10/86	REVISED	DATE	SIDESLIP WITH VERTICAL FIN ICED	DHC-6-004
CHECK					FLT# 23 RUN 25	
CHECK	J.Y.J.	3/14/86				REV A
APPD						Fig. 8.1.12d
DRAWN	21:03:37	03/06/86			KOHLMAN SYSTEMS RESEARCH	8.1.62

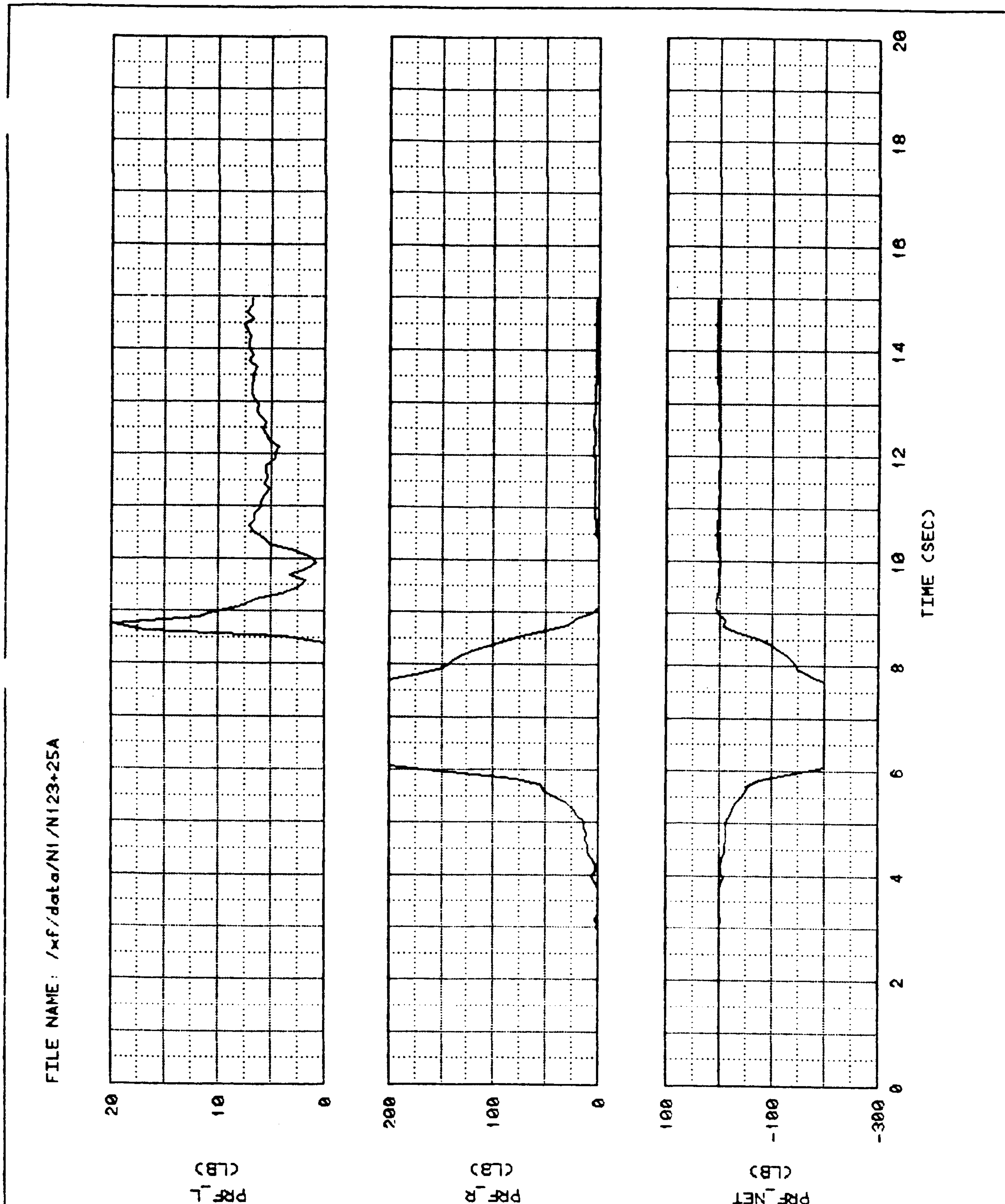

IV		02/10/86	REVISED	DATE	SIDESLIP WITH VERTICAL FIN ICED	DHC-6-004
CHECK					FLT# 23 RUN 25	
CHECK	J.Y.Q.	3/14/86				REV A
APPD						Fig. 8.1.12e
DRAWN	21:05:18	03/06/86			KOHLMAN SYSTEMS RESEARCH	8.1.63

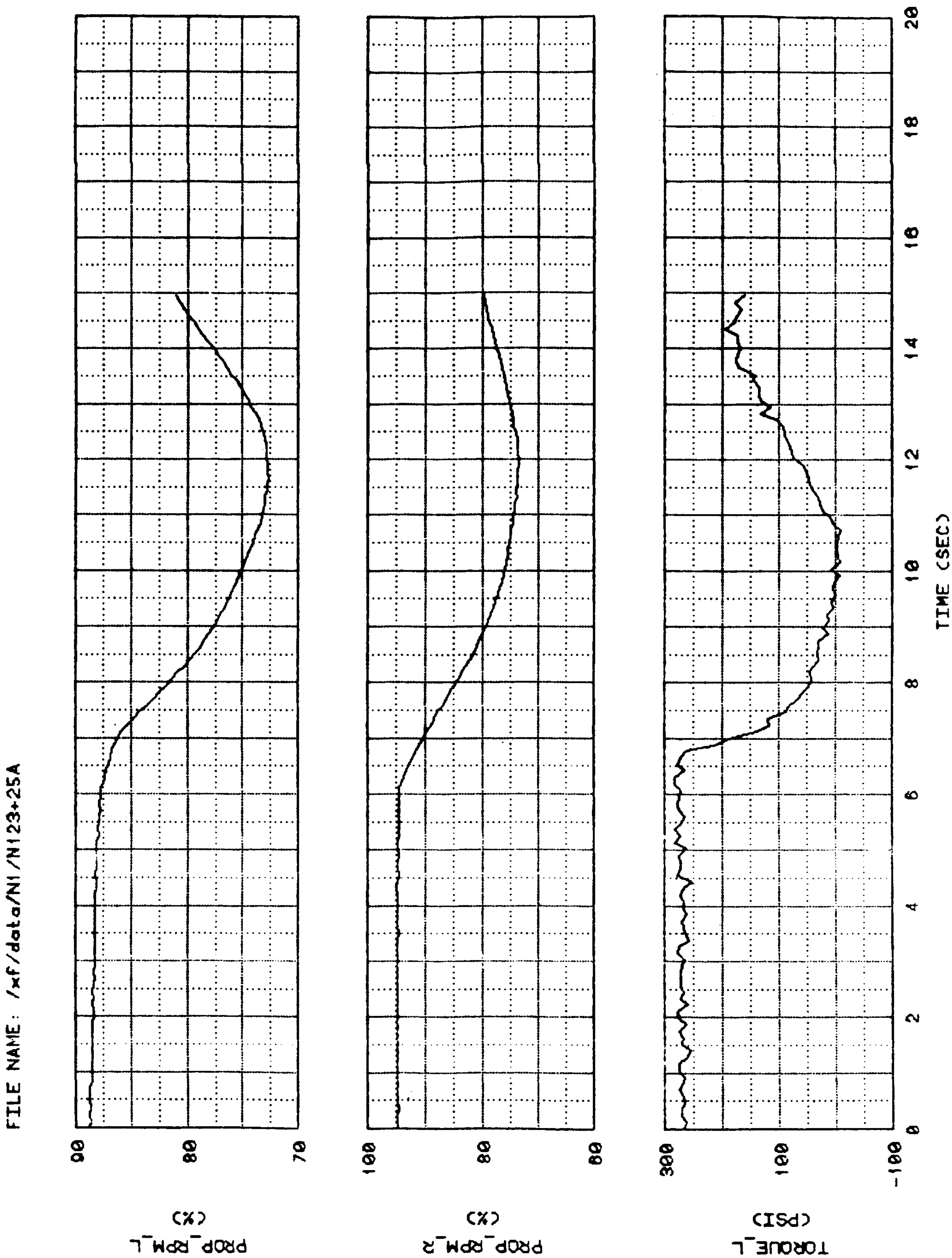

CONV		02/10/85	REVISED	DATE
CHECK				
CHECK	J.Z.J.	3/14/86		
APPD				
DRAWN	21:07:00	03/06/86		

SIDESLIP WITH VERTICAL FIN ICED

FLT# 23 RUN 25

KOHLMAN SYSTEMS RESEARCH

DHC-6-004

REV A

Fig. 8.1.12f

8.1.64

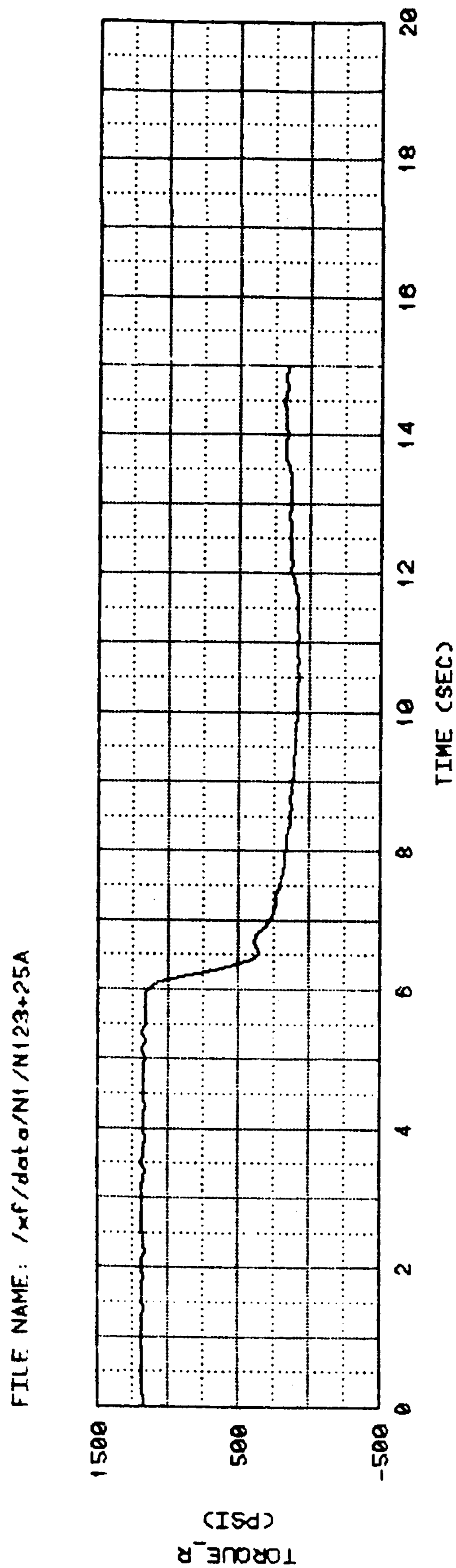

V		02/10/86	REVISED	DATE	SIDESLIP WITH VERTICAL FIN ICED FLT# 23 RUN 25	DHC-6-004
CHECK						
CHECK	J.Z.J.	3/14/86				REV A Fig. 8.1.12g
APPD						
DRAWN	21:08:11	03/06/86			KOHLMAN SYSTEMS RESEARCH	8.1.65

SIDELSLIP VERT. FIN DE-ICED

INITIAL CONDITIONS FOR TEST NUMBER:

FLIGHT: 23
RUN: 26
AIRCRAFT TYPE: LeRC Twin Otter Icing Flts
SERIAL NUMBER: DHC-6-004

ALT_CAL (FEET)	= 5000.6	N1_L (%)	= 78.3
AIRSPD_CAL (KNOT)	= 97.2	N1_R (%)	= 90.6
AIRSPD_TRU (KNOT)	= 103.6	PROP_RPM_L (%)	= 94.7
MACH_CAL	= 0.163	PROP_RPM_R (%)	= 95.2
DYN_PRS_CA (PSF)	= 31.9	TORQUE_L (ft-lb)	= 294.9
NCLT	= 0.8	TORQUE_R (ft-lb)	= 1177.6
ALPHA_ROS2 (DEG)	= 0.0	FUEL_FLO_L (LB/HR)	= 147.
AMB_PRESS (PSF)	= 1721.0	FUEL_FLO_R (LB/HR)	= 398.
TEMP_AMB (DEGK)	= 266.9	FUELTEMP_L (DEG_K)	= 257.7
AC_WEIGHT (LB)	= 9878.	FUELTEMP_R (DEG_K)	= 257.8
CG_PCT_MAC (%)	= 26.88		
IXX_BODY (SLG-SOFT)	= 15941.		
IYY_BODY (SLG-SOFT)	= 22603.		
IZZ_BODY (SLG-SOFT)	= 35778.		
IXZ_BODY (SLG-SOFT)	= 1094.		
FLAP (DEG)	= 11.5		
DELTA_E (DEG)	= 1.9		
DELTA_A_L (DEG)	= 5.5		
DELTA_R (DEG)	= 0.7		

APPD	J.G.G.	3/14/86	CONV	02/10/86
DRAWN	21:10:22	03/06/86		

KOHLMAN SYSTEMS RESEARCH

Fig. 8.1.13a
8.1.66

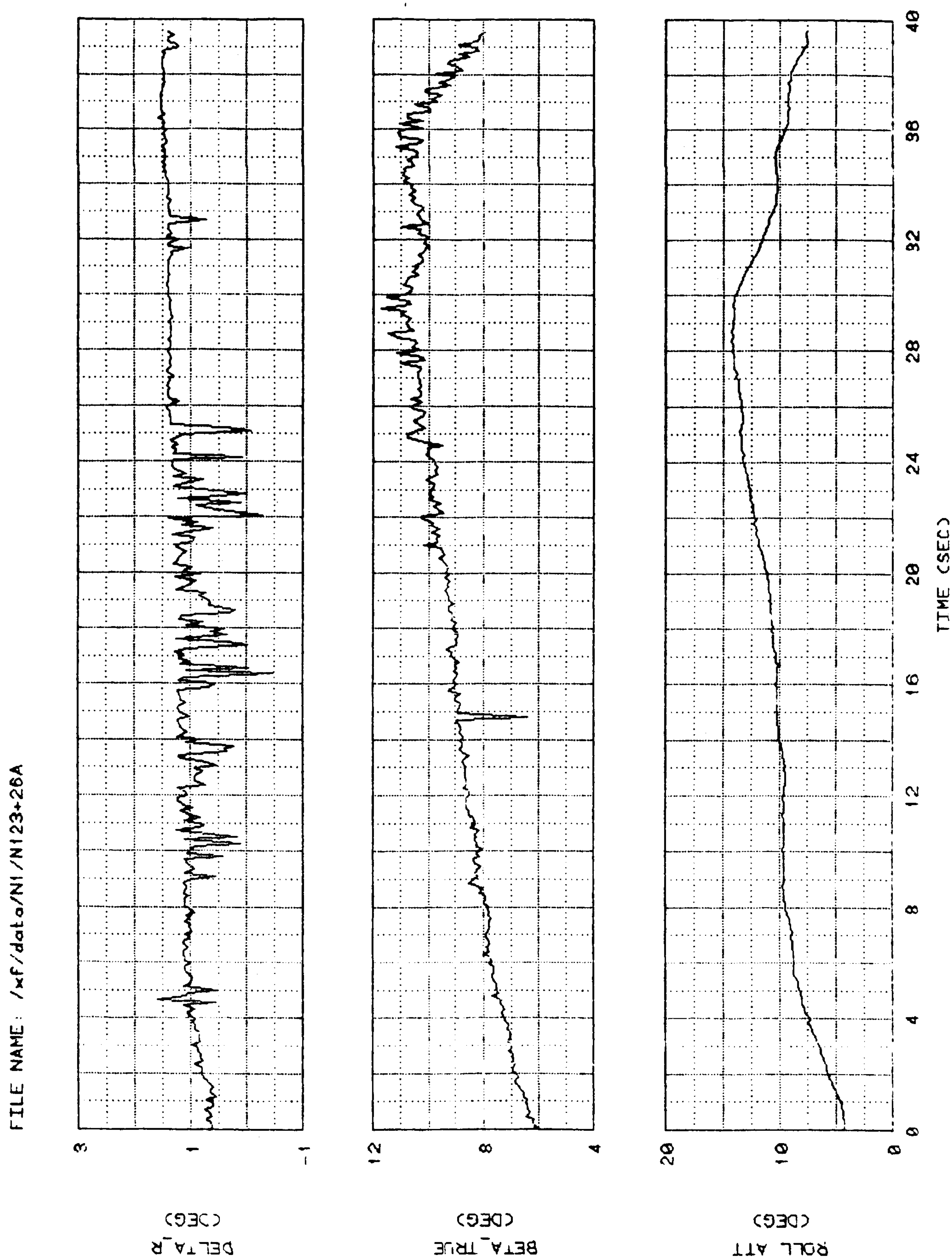

IV		02/10/86	REVISED	DATE
CHECK				
CHECK	J.Y.J.	3/14/86		
APPD				
DRAWN	21:12:28	03/06/86		

SIDELSLIP VERT. FIN DE-ICED

FLT# 23 RUN 26

KOHLMAN SYSTEMS RESEARCH

DHC-6-004

Fig. 8.1.13b

8.1.67

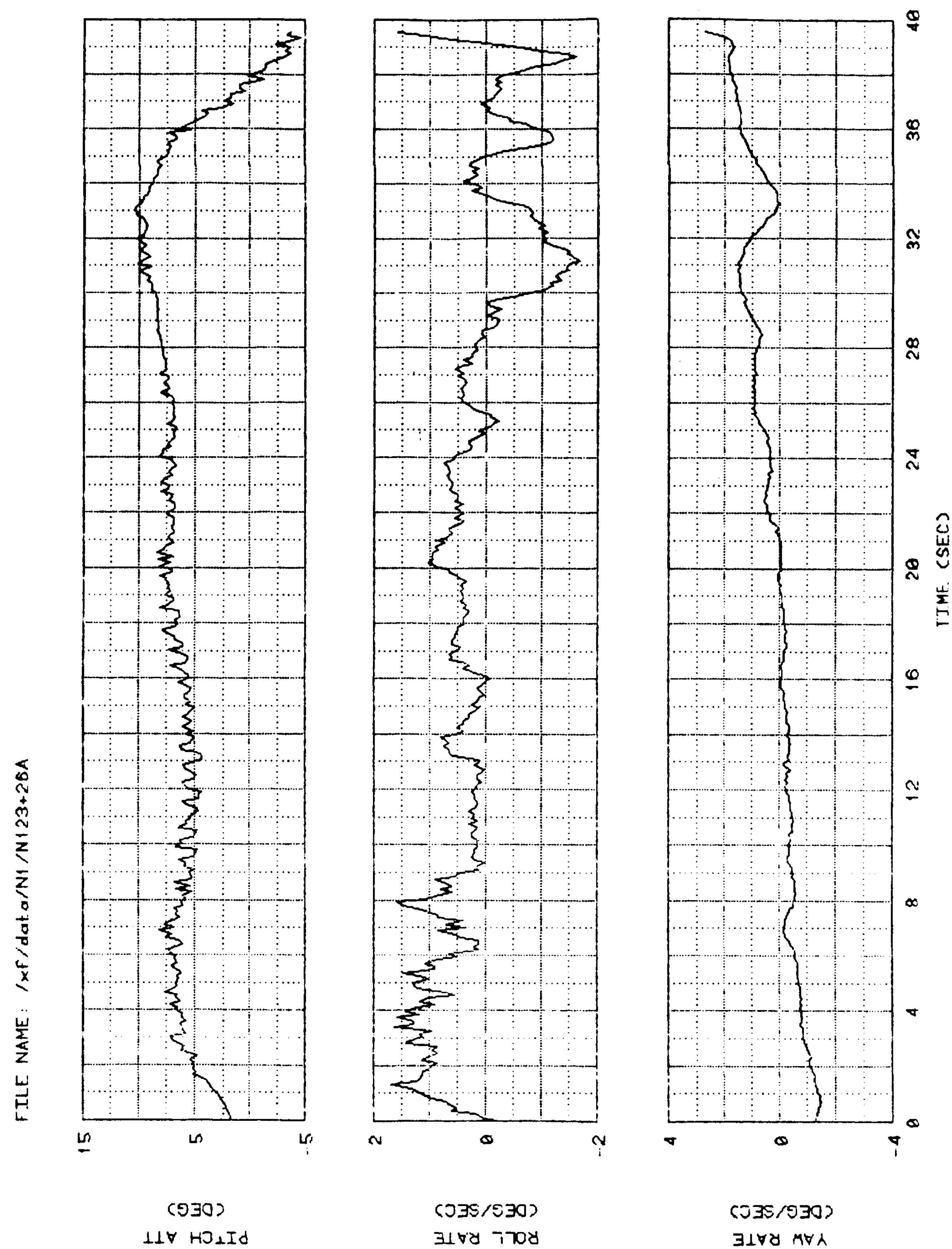

CONV		02/10/86	REVISED	DATE
CHECK				
CHECK	J.D.J.	3/14/86		
APPD				
DRAWN	21:14 14	03/06/86		

SIDELSLIP VERT. FIN DE-ICED

FLT# 23 RUN 26

KOHLMAN SYSTEMS RESEARCH

DHC-6-004

Fig. 8.1.13c

8.1.68

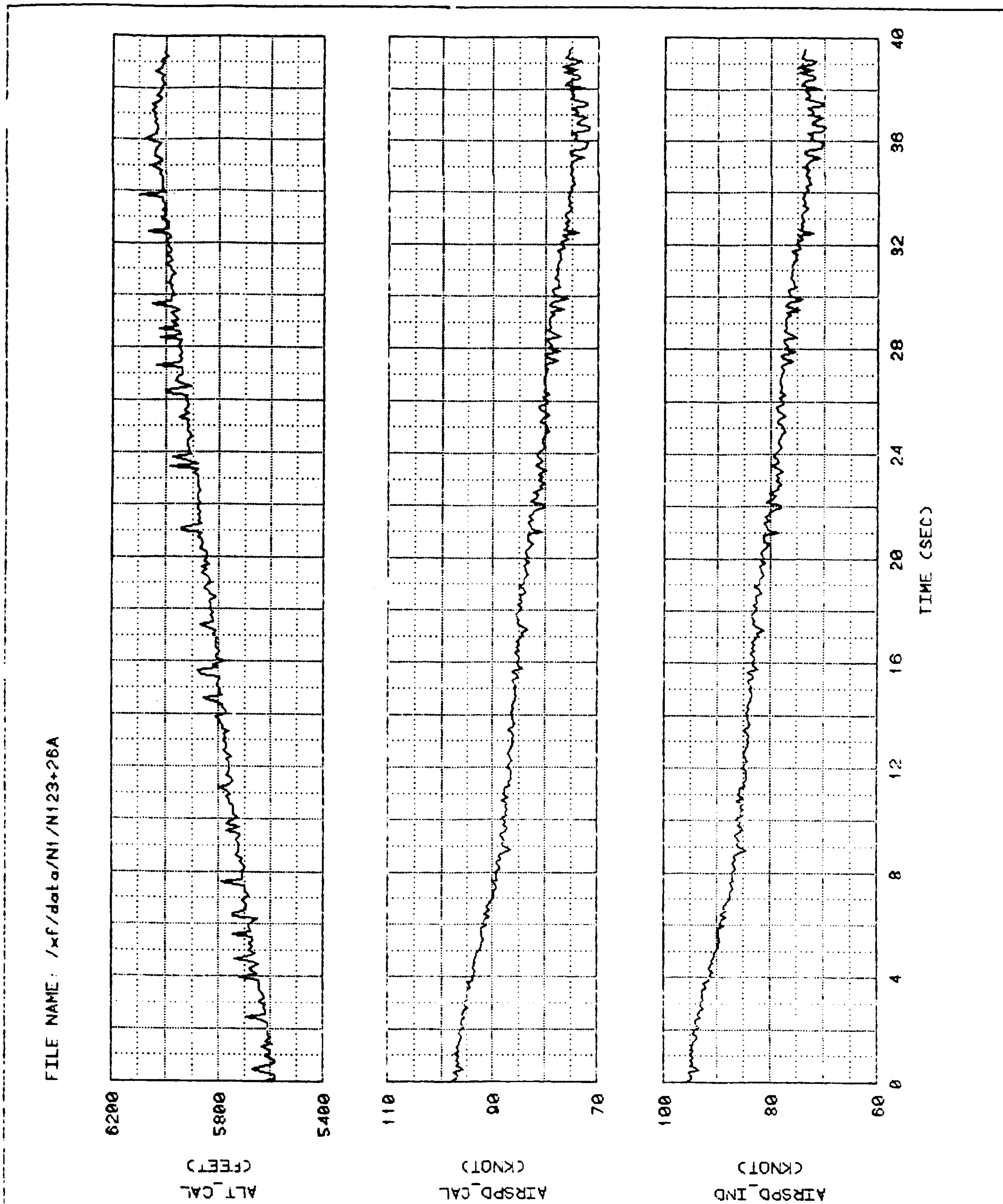

V		02/10/86	REVISED	DATE	SIDELSLIP VERT. FIN DE-ICED	DHC-6-004
CHECK					FLT# 23 RUN 26	
CHECK	J.J.G.	3/14/86				Fig. 8.1.13d
APPD					KOHLMAN SYSTEMS RESEARCH	8.1.69
DRAWN	21:16:01	03/06/86				

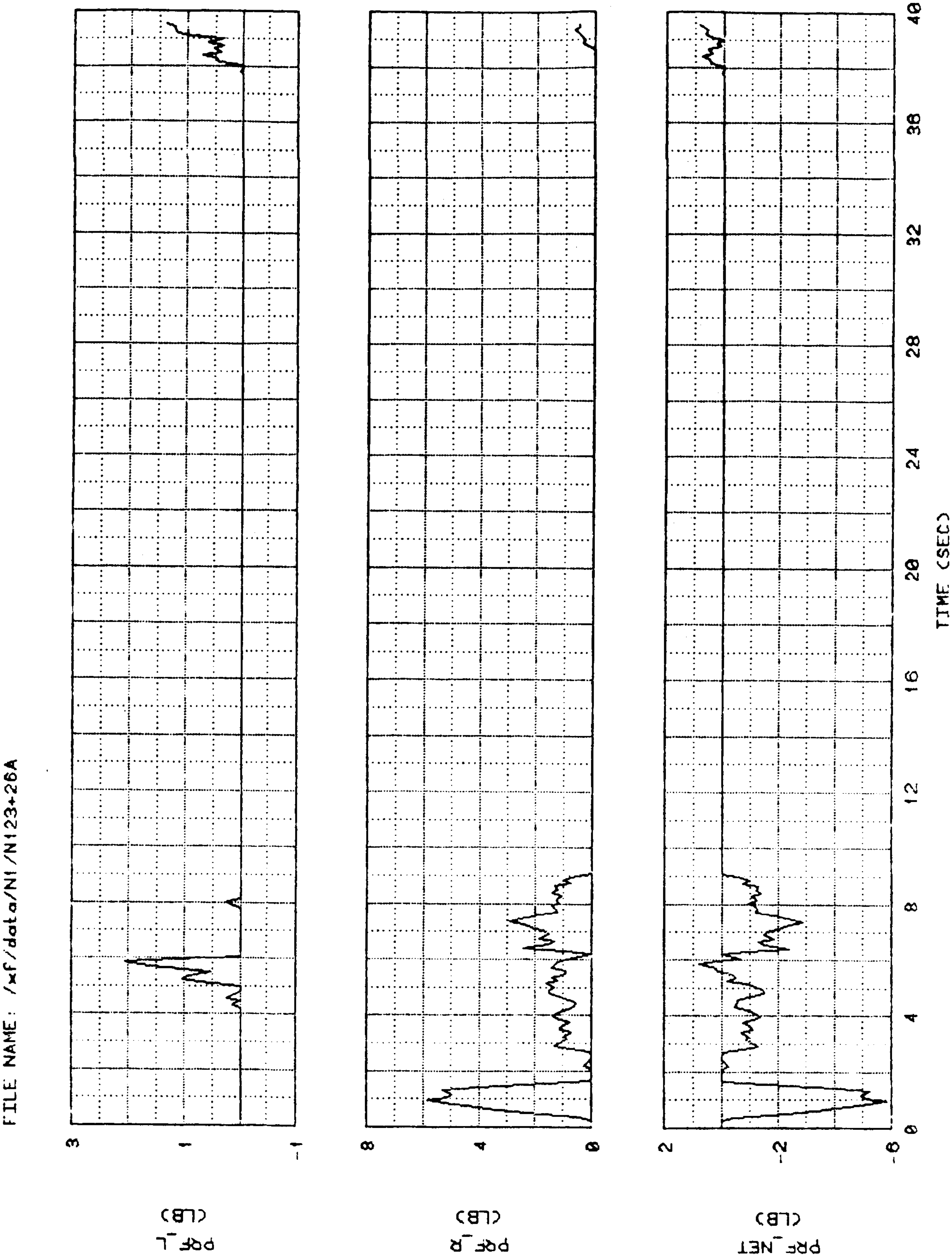

CONV		02/10/86	REVISED	DATE
CHECK				
CHECK	J.Y.J.	3/14/86		
APPD				
DRAWN	21:17:44	03/06/86		

SIDELSLIP VERT. FIN DE-ICED

FLT# 23 RUN 26

KOHLMAN SYSTEMS RESEARCH

DHC-6-004

Fig. 8.1.13c

8.1.70

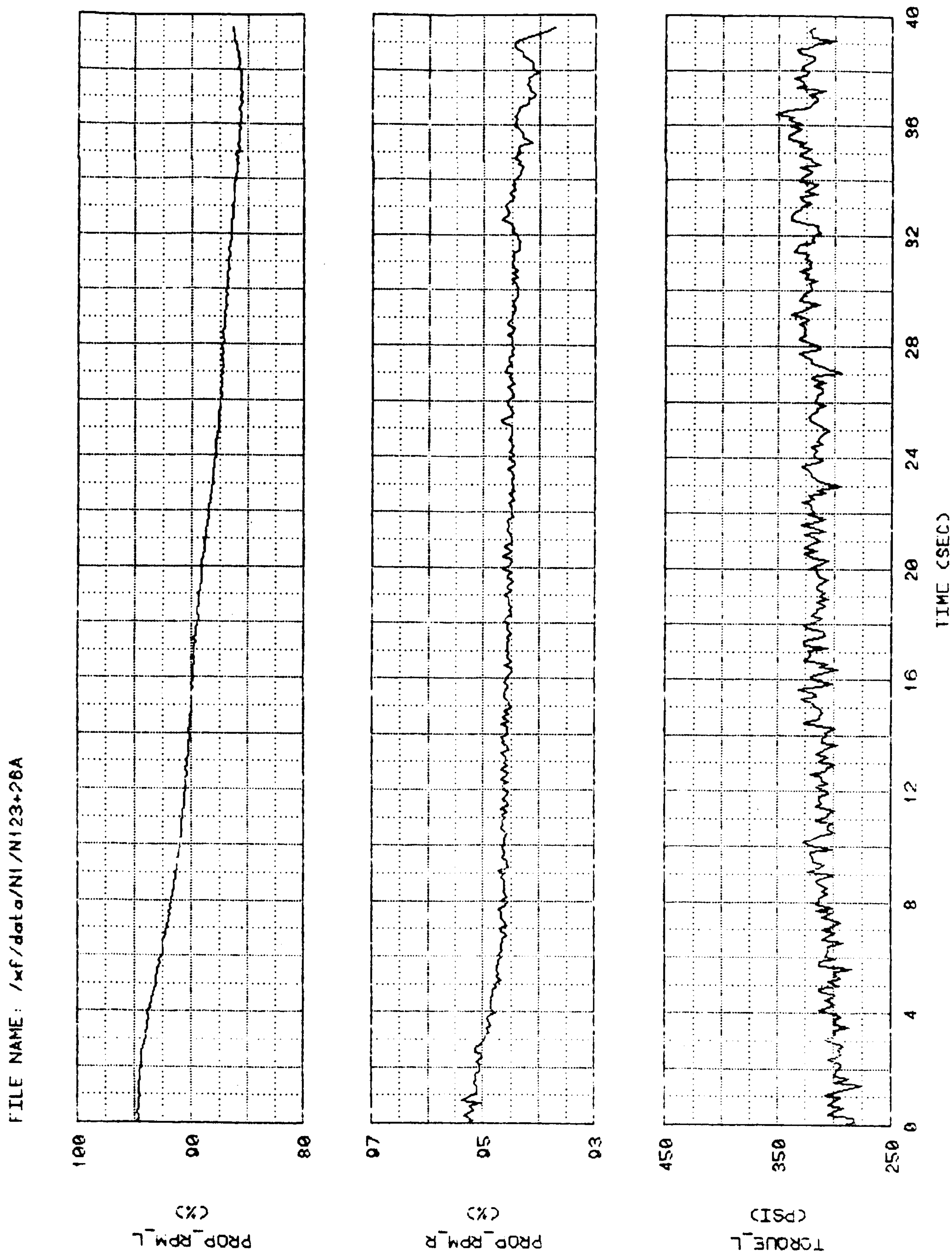

/		02/10/86	REVISED	DATE	SIDELSLIP VERT FIN DE-ICED	DHC-6-004
CHECK						
CHECK	J.J.J.	3/14/86			FLT# 23 RUN 26	
APPD						Fig. 8.1.131
DRAWN	21:19:29	03/06/86			KOHLMAN SYSTEMS RESEARCH	8.1.71

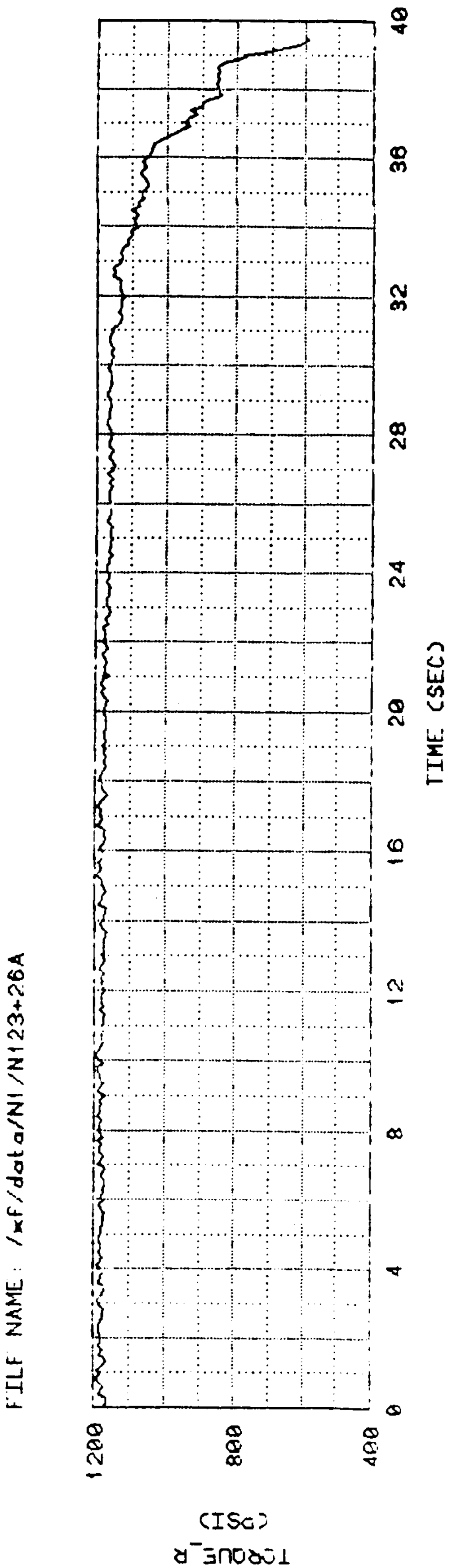

CNV		02/10/86	REVISED	DATE	SIDELSLIP VERT. FIN DE-ICED FLT# 23 RUN 26	DHC-6-004
HECK						
HECK	J.Y.J.	3/14/86				Fig. 8.1.13g
PPD					KOHLMAN SYSTEMS RESEARCH	8.1.72
RAWN	21 21 00	03/06/86				

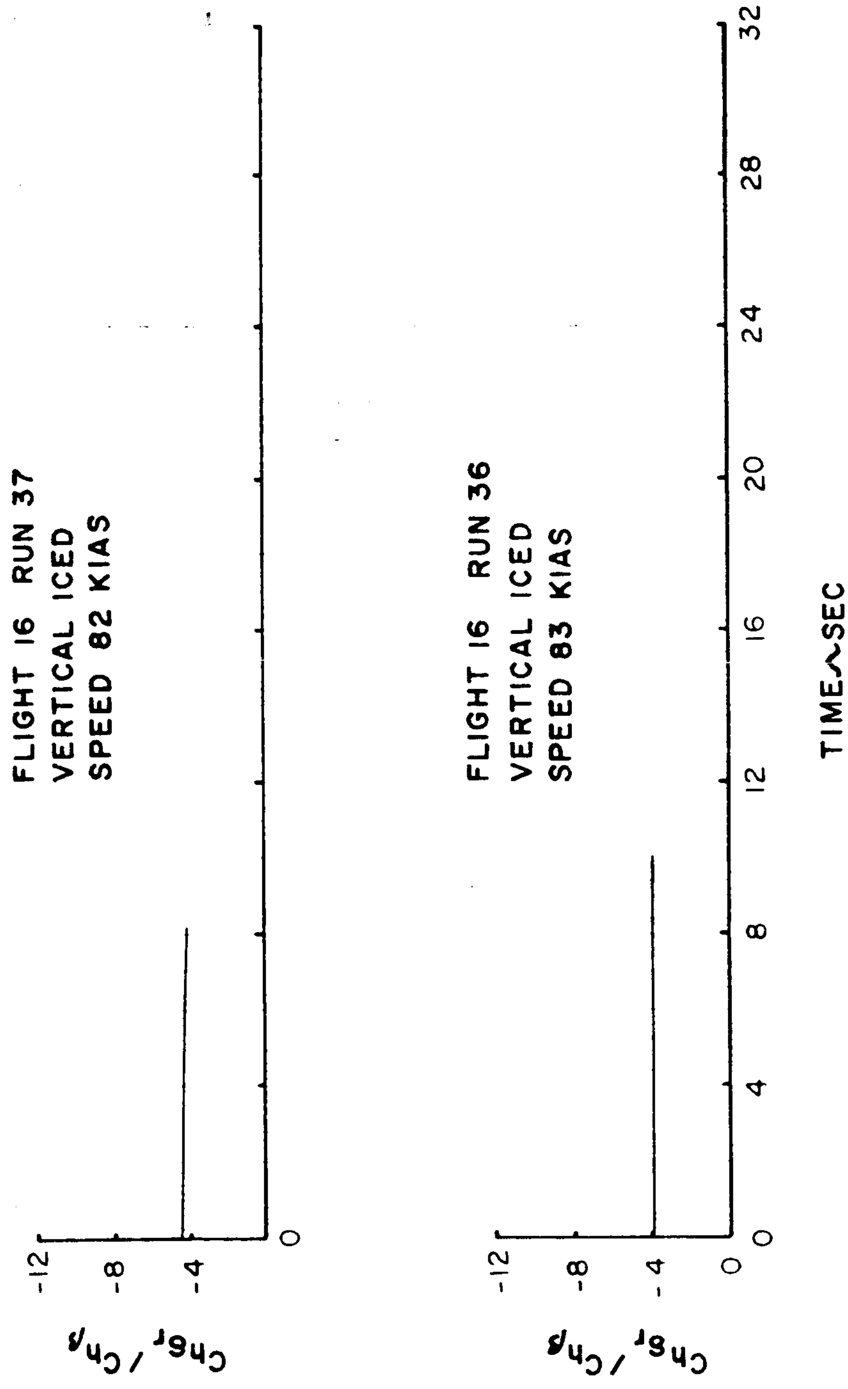

CALC			REVISED	DATE	RATIO OF $C_{h_{\delta_r}}$ TO C_{h_β}, FLIGHT 16	Fig. 8.1.14
CHECK	J.J.J.	3/14/86				DHC-6-004
APPD						
APPD					KOHLMAN SYSTEMS RESEARCH LAWRENCE KANSAS	8.1.73
DRAWN	21 feb	KEB				

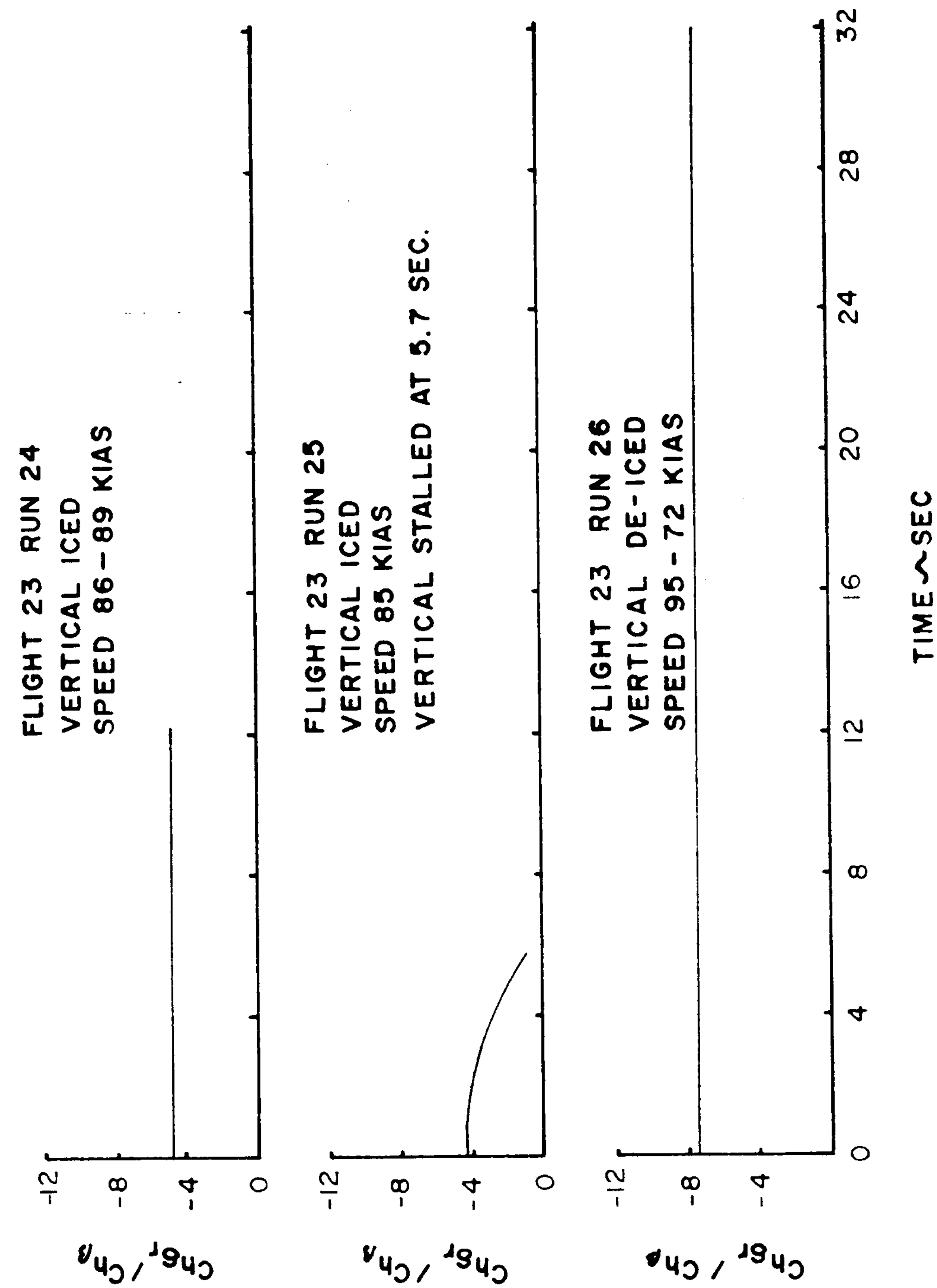

			REVISED	DATE
CALC				
CHECK	J.A.J.	3/14/86		
APPD				
APPD				
DRAWN	21 Feb 86	KEB		

RATIO OF $C_{h_{\delta_r}}$ TO C_{h_β}, FLIGHT 23

Fig. 8.1.15

DHC-6-004

KOHLMAN SYSTEMS RESEARCH
LAWRENCE KANSAS

8.1.74

9. REFERENCES

1. Flight Manual DHC-6 Twin Otter Series 200 (PSM 1-62-1A)

2. Schweikhard, W.G. "A Method of In-Flight Measurement of Ground Effects on a Fixed-Wing Aircraft," Journal of Aircraft, April 1967.

3. Schweikhard, W.G. and Kohlman, D.L., "Flight Test Principles and Practices," University of Kansas Extension Division, 1982.

4. Hoak, D.E. et al: USAF Stability and Control DATCOM, Wright Patterson Air Force Base, Ohio, September 1970.

5. Larson, T.J. and Flechner, S.A., "Wind Tunnel Investigation of an All Flush Orifice Air Data System for a Large Subsonic Aircraft," NASA TN 1642, 1980.

6. Gilyard, G.B. and Belte, D., "Flight Determined Lag of Angle of Attack and Angle of Sideslip Sensors in the YF-12A Airplane from Analysis of Dynamic Maneuvers," NASA TN D-7819, 1974.

THIS PAGE INTENTIONALLY LEFT BLANK

APPENDIX A: FLIGHT TEST DATA BASE FORMAT

This Appendix contains a table of the flight test data base (Table A.1) used in KSR flight test analysis. The table contains the pertinent variables with their corresponding computer names and units.

The flight test data base is saved on MAG TAPE in the following format. The data are stored as 5 records per physical block. Each record of 200 words (32 bit floating point) represents one time slice of flight test data. Table A.2 defines the floating representation used on the Cadmus 9000. The number of each variable indicates the corresponding word in each block where the value is stored. The tape is partioned into files separated by one EOF mark with the final file ending with two EOF marks.

For each file, valid data begins with the first block after the block when BLKCNT equals -300. It ends when BLKCNT equals -600. In the block when BLKCNT equals -300, variable #4 contains the approximate size of the file in blocks of 200 words.

Normally, data are sampled continuously, however, the KSR DAS has the capability to "pause". A pause of arbitrary length is signified by Engineering Status Byte equal to 100 for the first block after the pause. The DAS also can sample in a "burst" mode, where, it will alternately record eight samples at 8.5 Hz and then pause for one to 15 seconds. For these cases ESB1 = 101 to 115 for the first sample after the pause. The last two digits of ESB1 are approximately equal to the length of the pause in seconds.

TABLE A.1

N1 FTDB VARIABLE LIST
LeRC Twin Otter Icing Flts
Twin Otter
DHC-6-004

Date: 03Mar86
Time: 15:40

FTDB NUMBER	VARIABLE NAME		CHANNEL
1	FILCNT	(DIGITAL)	1
2	BLKCNT	(DIGITAL)	2
3	ESB	(DIGITAL)	3
4	ASB	(DIGITAL)	4
5	TIME	(SEC)	5
6	AX	(G)	6
7	AY	(G)	7
8	AZ	(G)	8
9	PITCH RATE	(DEG/SEC)	9
10	ROLL RATE	(DEG/SEC)	10
11	YAW RATE	(DEG/SEC)	11
12	PITCH ATT	(DEG)	12
13	ROLL ATT	(DEG)	13
14	DELP_ALPHA	(PSF)	14
15	DELP_BETA	(PSF)	15
16	DELP_REF	(PSF)	16
17	DELTA_A_L	(DEG)	17
18	-----		0
19	DELTA_E	(DEG)	19
20	DELTA_R	(DEG)	20
21	FLAP	(DEG)	21
22	-----		0
23	-----		0
24	-----		0
25	RPN01		25

TABLE A.1, CONT'D

26	RPN02		26
27	-----		0
28	-----		0
29	-----		0
30	-----		0
31	-----		0
32	DIFF_PRESS	(PSF)	32
33	AIR_TEMP	(DEG_K)	33
34	INERT_VREF	(VOLT)	34
35	STAT_PRESS	(PSF)	35
36	CPT_VREF	(VOLT)	36
37	BATTERY_A	(VOLT)	37
38	-----		0
39	FUEL_USED	(LB)	39
40	PAF	(LB)	40
41	PEF	(LB)	41
42	PRF_L	(LB)	42
43	PRF_R	(LB)	43
44	PRF_NET	(LB)	173
45	-----		0
46	-----		0
47	-----		0
48	-----		0
49	N1_L	(%)	49
50	N1_R	(%)	50
51	PROP_RPM_L	(%)	51
52	PROP_RPM_R	(%)	52
53	TORQUE_L	(PSI)	53
54	TORQUE_R	(PSI)	54
55	FUEL_FLO_L	(LB/HR)	55

TABLE A.1, CONT'D

56	FUEL_FLO_R (LB/HR)	56
57	FUELTEMP_L (DEG_K)	57
58	FUELTEMP_R (DEG_K)	58
59	-----	0
60	-----	0
61	-----	0
62	-----	0
63	-----	0
64	JOHNS_WILL (VOLT)	64
65	LEIGH (VOLT)	65
66	ROSEMOUNT (VOLT)	66
67	GEN_EAST (VOLT)	67
68	-----	0
69	-----	0
70	-----	0
71	BATTERY_B (VOLT)	71
72	PAUSE_EVNT (0 = NO)	72
73	PIRAM_HEAT (0 = OFF)	73
74	ROSEM_HEAT (0 = OFF)	74
75	-----	0
76	GEAR_POS (0 = UP)	76
77	GYRO_ERECT (0 = YES)	77
78	PILOT_EVNT (0 = NO)	78
79	-----	0
80	-----	0
81	P_CORRECTD (DEG/SEC)	81
82	Q_CORRECTD (DEG/SEC)	82
83	R_CORRECTD (DEG/SEC)	83
84	ROLL_ACCEL (DEG/S/S)	84
85	PITCH_ACCL (DEG/S/S)	85

TABLE A.1, CONT'D

86	YAW_ACCEL	(DEG/S/S)	86
87	AX_CORRCTD	(G)	87
88	AY_CORRCTD	(G)	88
89	AZ_CORRCTD	(G)	89
90	EULER_ROLL	(DEG)	90
91	EULR_PITCH	(DEG)	91
92	EULER_YAW	(DEG)	92
93	EULER_P	(DEG/SEC)	93
94	EULER_Q	(DEG/SEC)	94
95	EULER_R	(DEG/SEC)	95
96	ALT_INDCID	(FEET)	96
97	AIRSPD_IND	(KNOT)	97
98	MACH_IND		98
99	DYN_PRS_IN	(PSF)	99
100	CLIC		100
101	NCLIC		101
102	POS_COR_P	(PSF)	102
103	TOTL_PRESS	(PSF)	103
104	AMB_PRESS	(PSF)	104
105	QC	(PSF)	105
106	PRES_RATIO		106
107	PRES_RAT_T		107
108	ALT_CAL	(FEET)	108
109	AIRSPD_CAL	(KNOT)	109
110	MACH_CAL		110
111	DYN_PRS_CA	(PSF)	111
112	CLT		112
113	NCLT		113
114	POS_COR_V	(KNOT)	114
115	POS_COR_H	(FEET)	115

TABLE A.1, CONT'D

116	POS_COR_M		116
117	AIRSPD_EQ	(KNOT)	117
118	TEMP_AMB	(DEGK)	118
119	TEMP_TOTAL	(DEGK)	119
120	THETA		120
121	THETA_TOTL		121
122	AIRSPD_TRU	(KNOT)	122
123	DENSITY	(SLG/CUFT)	123
124	DENS_RATIO		124
125	ALT_DENS	(FEET)	125
126	TTL_PRS_ST	(PSF)	126
127	AMB_PRS_ST	(PSF)	127
128	QC_STD	(PSF)	128
129	PRS_RAT_ST		129
130	PS_RT_T_ST		130
131	PROP_THR_L	(LB)	131
132	PROP_THR_R	(LB)	132
133	FGJ_L	(LB)	133
134	FGJ_R	(LB)	134
135	WA_L	(LB/SEC)	135
136	WA_R	(LB/SEC)	136
137	RAM_DRAG_L	(LB)	137
138	RAM_DRAG_R	(LB)	138
139	THR_COEF_L		139
140	THR_COEF_R		140
141	CT_CALC_L		141
142	CT_CALC_R		142
143	PWR_COEF_L		143
144	PWR_COEF_R		144
145	ADV_RAT_L		145

146	ADV_RAT_R		146
147	PRP_BETA_L	(DEG)	147
148	PRP_BETA_R	(DEG)	148
149	DEL_VE	(KNOT)	149
150	DEL_T_AMB	(DEGK)	150
151	DEL_VT	(KNOT)	151
152	DEL_DENS	(SLG/CUFT)	152
153	ALPHA_CAL1	(DEG)	153
154	-----		0
155	-----		0
156	BETA_CAL	(DEG)	156
157	ALPHA_TRU1	(DEG)	157
158	-----		0
159	-----		0
160	BETA_TRUE	(DEG)	160
161	NLOAD	(G)	161
162	CG_LONG	(FEET)	162
163	CG_LATERAL	(FEET)	163
164	CG_VERT	(FEET)	164
165	IXX_BODY	(SLG-SQFT)	165
166	IYY_BODY	(SLG-SQFT)	166
167	IZZ_BODY	(SLG-SQFT)	167
168	IXZ_BODY	(SLG-SQFT)	168
169	CG_PCT_MAC	(%)	169
170	FUEL_USED	(LB)	170
171	AC_WEIGHT	(LB)	171
172	FUEL_WT	(LB)	172
173	-----		0
174	ALPHA_ROS1	(DEG)	174
175	ALPHA_ROS2	(DEG)	175

TABLE A.1, CONT'D

176	BETA_ROS1	(DEG)	176
177	BETA_ROS2	(DEG)	177
178	TEMP		178
179	DPAOQ		179
180	ATAN_AXAZ	(DEG)	180
181	TORQUE_P_L	(PSI)	181
182	TORQUE_P_R	(PSI)	182
183	TEMP_AIR	(())	183
184	-----		0
185	-----		0
186	-----		0
187	-----		0
188	-----		0
189	-----		0
190	-----		0
191	-----		0
192	-----		0
193	-----		0
194	-----		0
195	-----		0
196	-----		0
197	-----		0
198	-----		0
199	-----		0
200	-----		0

TABLE A.2

Cadmus Floating Pointing Format

Real*4:

```
s eeee eeee mmmm mmmm mmmm mmmm mmmm mmm

where   s = sign (0=pos, 1=neg)

        e = exponent (unsigned binary integer, excess 127 code)

        m = mantissa (binary fraction, normalized with leftmost
                      bit implied)
```

Example:

$$\pm 2^{exp-127} * 1.mantissa$$

THIS PAGE INTENTIONALLY LEFT BLANK

1. Report No.	2. Government Accession No.	3. Recipient's Catalog No.
NASA CR-179515		

4. Title and Subtitle

Flight Test Report of the NASA Icing Research Air-Plane. Performance, Stability, and Control After Flight Through Natural Icing Conditions

5. Report Date

October 1986

6. Performing Organization Code

7. Author(s)

Jerry L. Jordan, Stewart J. Platz, and William C. Schinstock

8. Performing Organization Report No.

KSR 86-01

10. Work Unit No.

505-68-11

9. Performing Organization Name and Address

Kohlman Systems Research, Inc.
319 Perry Street
Lawrence, Kansas 66044

11. Contract or Grant No.

NAS3-24547

13. Type of Report and Period Covered

Contractor Report
Final

12. Sponsoring Agency Name and Address

National Aeronautics and Space Administration
Lewis Research Center
Cleveland, Ohio 44135

14. Sponsoring Agency Code

15. Supplementary Notes

Project Manager, Kevin L. Mikkelsen, Propulsion Systems Division, NASA Lewis Research Center.

16. Abstract

Flight test results are presented documenting the effect of airframe icing on performance and stability and control of a NASA DHC-6 icing research aircraft. Kohlman Systems Research, Inc., provided the data acquisition system and data analysis under contract to NASA. Performance modeling methods and MMLE Techniques were used to determine the effects of natural ice on the aircraft. Results showed that ice had a significant effect on the drag coefficient of the aircraft and a modest effect on the MMLE derived longitudinal stability coefficients (code version "MMLE"). Data is also presented on asymmetric power side-slip maneuvers showing rudder floating characteristics with and without ice on the vertical stabilizer.

17. Key Words (Suggested by Author(s))

Aircraft icing
Aircraft performance
Stability and control

18. Distribution Statement

Unclassified - unlimited
STAR Category 08

19. Security Classif. (of this report)	20. Security Classif. (of this page)	21. No. of pages	22. Price*
Unclassified	Unclassified	159	A08

*For sale by the National Technical Information Service, Springfield, Virginia 22161